Research Paper

GEOSPHERE

GEOSPHERE, v. 17, no. 4

https://doi.org/10.1130/GES02288.1

15 figures; 3 tables; 2 supplemental files

CORRESPONDENCE: geowat@uky.edu

CITATION: Thomas, W.A., Gehrels, G.E., Sundell, K.E., and Romero, M.C., 2021, Detrital-zircon analyses, provenance, and late Paleozoic sediment dispersal in the context of tectonic evolution of the Ouachita orogen: Geosphere, v. 17, no. 4, p. 1214–1247, https://doi.org/10.1130/GES02288.1.

Science Editor: David E. Fastovsky
Associate Editor: Todd LaMaskin

Received 22 May 2020
Revision received 21 October 2020
Accepted 17 February 2021

Published online 14 May 2020

Detrital-zircon analyses, provenance, and late Paleozoic sediment dispersal in the context of tectonic evolution of the Ouachita orogen

William A. Thomas[1], George E. Gehrels[2], Kurt E. Sundell[2], and Mariah C. Romero[3]

[1]Emeritus, University of Kentucky, and Geological Survey of Alabama, P.O. Box 869999, Tuscaloosa, Alabama 35486-9999, USA
[2]Department of Geosciences, University of Arizona, Tucson, Arizona 85721, USA
[3]Department of Earth Sciences, Montana State University, Bozeman, Montana 59717-3480, USA

ABSTRACT

New analyses for U-Pb ages and εHf_t values, along with previously published U-Pb ages, from Mississippian–Permian sandstones in synorogenic clastic wedges of the Ouachita foreland and nearby intracratonic basins support new interpretations of provenance and sediment dispersal along the southern Midcontinent of North America. Recently published U-Pb and Hf data from the Marathon foreland confirm a provenance in the accreted Coahuila terrane, which has distinctive Amazonia/Gondwana characteristics. Data from Pennsylvanian–Permian sandstones in the Fort Worth basin, along the southern arm of the Ouachita thrust belt, are nearly identical to those from the Marathon foreland, strongly indicating the same or a similar provenance. The accreted Sabine terrane, which is documented by geophysical data, is in close proximity to the Coahuila terrane, suggesting the two are parts of an originally larger Gondwanan terrane. The available data suggest that the Sabine terrane is a Gondwanan terrane that was the provenance of the detritus in the Fort Worth basin. Detrital-zircon data from Permian sandstones in the intracratonic Anadarko basin are very similar to those from the Fort Worth basin and Marathon foreland, indicating sediment dispersal from the Coahuila and/or Sabine terranes within the Ouachita orogen cratonward from the immediate forelands onto the southern craton. Similar, previously published data from the Permian basin suggest widespread distribution from the Ouachita orogen. In contrast to the other basins along the Ouachita-Marathon foreland, the Mississippian–Pennsylvanian sandstones in the Arkoma basin contain a more diverse distribution of detrital-zircon ages, indicating mixed dispersal pathways of sediment from multiple provenances. Some of the Arkoma sandstones have U-Pb age distributions like those of the Fort Worth and Marathon forelands. In contrast, other sandstones, especially those with paleocurrent and paleogeographic indicators of southward progradation of depositional systems onto the northern distal shelf of the Arkoma basin, have U-Pb age distributions and εHf_t values like those of the "Appalachian signature." The combined data suggest a mixture of detritus from the proximal Sabine terrane/Ouachita orogenic belt with detritus routed through the Appalachian basin via the southern Illinois basin to the distal Arkoma basin. The Arkoma basin evidently marks the southwestern extent of Appalachian-derived detritus along the Ouachita-Marathon foreland and the transition southwestward to overfilled basins that spread detritus onto the southern craton from the Ouachita-Marathon orogen, including accreted Gondwanan terranes.

William A. Thomas https://orcid.org/0000-0003-0550-258X

INTRODUCTION

The very thick (~15 km) accumulation of Upper Mississippian–Middle Pennsylvanian siliciclastic turbidites in the Ouachita Mountains of Arkansas and Oklahoma (Figs. 1 and 2) (e.g., Arbenz, 1989a) has long challenged understanding of sediment provenance and dispersal. Early interpretations envisioned a continental borderland, "Llanoria," which supplied sediment to the Ouachita geosyncline (e.g., Schuchert, 1923). More recently, Ouachita orogenesis, along with subsidence and filling of a synorogenic basin, is understood in the context of southward subduction of the margin of Laurentian continental crust beneath a volcanic arc and accreted continental terrane during assembly of supercontinent Pangaea (e.g., summary in Viele and Thomas, 1989). Interpretations of late Paleozoic sediment provenance and dispersal in the Arkoma and Fort Worth basins in the foreland of the Ouachita salient of the late Paleozoic thrust belt (Fig. 1) range from proximal Ouachita orogenic sources (e.g., Brown et al., 1973; Sutherland, *in* Johnson et al., 1988; Thompson, *in* Johnson et al., 1988) to distant sources in the Appalachian orogen (Graham et al., 1976), as well as Appalachian sources with other contributions from the Laurentian craton (Xie et al., 2016, 2018a). Other interpretations include a mixture of proximal orogenic sources in the Ouachita orogen, including the accreted Sabine terrane, and more distally supplied sediment from the Appalachians (e.g., Sharrah, 2006; Alsalem et al., 2018), perhaps passing through the Illinois basin. Detrital-zircon data from the Marathon foreland, which is southwest along the orogen from the Ouachita salient (Fig. 1A), document sediment supply from a temporally diverse assemblage of rocks in the accreted Coahuila terrane (Thomas et al., 2019). Paleocurrents in turbidite fans in the Arkoma basin indicate significant slope-parallel flow with sediment input from both the cratonic side and the orogen (e.g., Houseknecht,

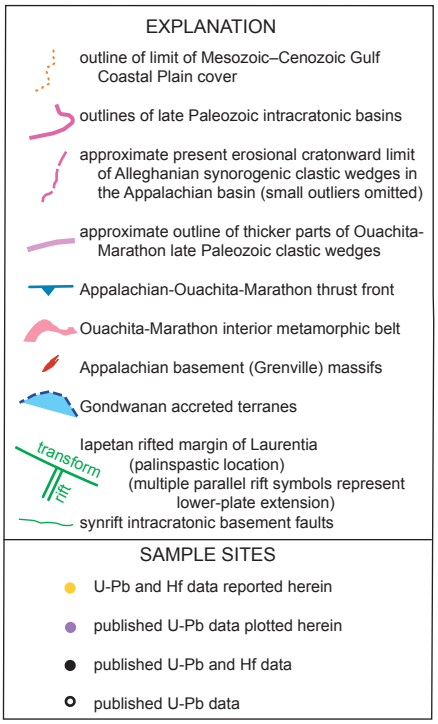

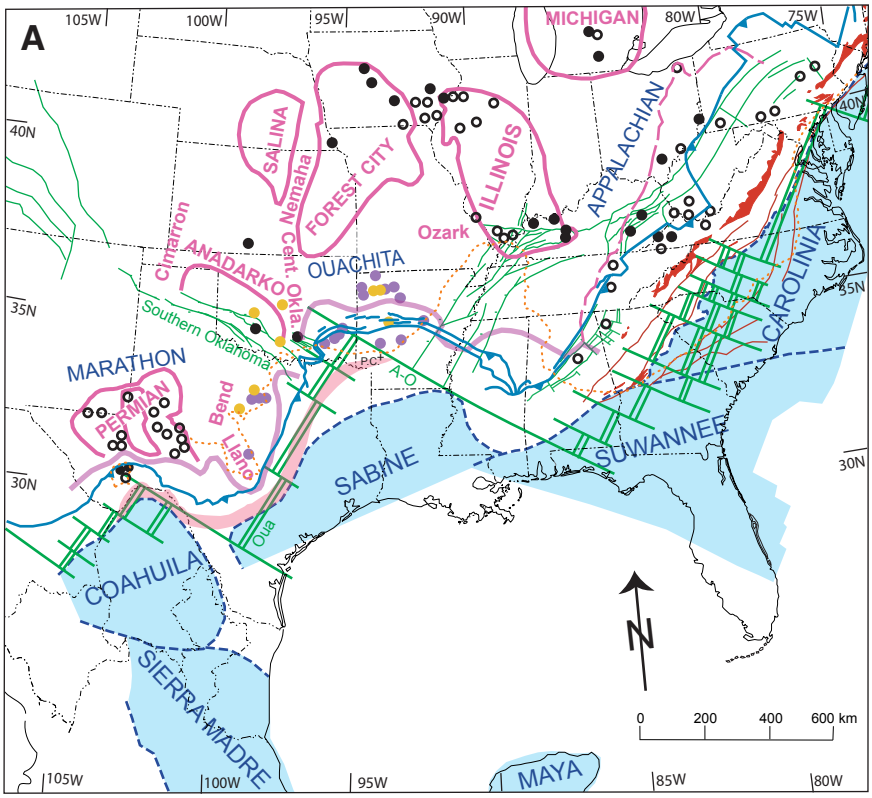

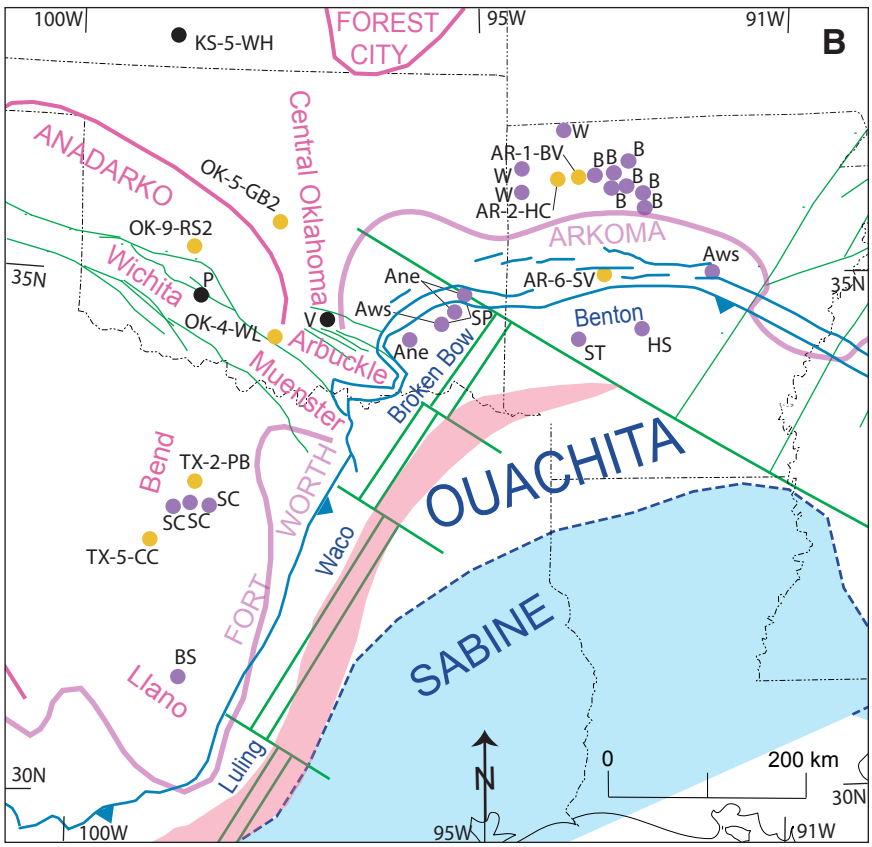

Figure 1. Regional map of the structural setting of the Arkoma and Fort Worth basins in the foreland of the Ouachita orogen, and the Anadarko and other intracratonic basins (names of intracratonic basins in all-capital letters; names of intracratonic arches and uplifts in capital and lowercase letters: Cent. Okla.—Central Oklahoma arch). (A) Map of the lapetan rift margin (A-O—Alabama-Oklahoma transform fault; Oua—Ouachita rift) and synrift intracratonic faults of Laurentia (from Thomas, 2014); locations of Gondwanan accreted terranes (from Krogh et al., 1993; Steiner and Walker, 1996; Stewart et al., 1999; Dickinson and Lawton, 2001; Centeno-García, 2005; Poole et al., 2005; Hibbard et al., 2007; Hatcher, 2010; Martens et al., 2010; Mueller et al., 2014; Thomas, 2014); trace of the Appalachian-Ouachita thrust front, and locations of the Ouachita interior metamorphic belt and Appalachian basement massifs of Grenville-age rocks (compiled from Thomas et al., 1989; Hatcher, 2010); outlines of late Paleozoic clastic wedges along the Ouachita and Appalachian orogens (from Thomas, 2006); and location of the Prairie Creek lamproite pipe (P.C.) (from Clift et al., 2018). Locations of sample sites discussed in the text; some symbols represent multiple closely spaced samples. (B) Map enlarged from Figure 1A with labels for samples. Map shows locations of late Paleozoic basement uplifts (Wichita, Arbuckle, and Muenster) along the Southern Oklahoma fault system and subsurface basement uplifts (Benton, Broken Bow, Waco, and Luling) beneath the Ouachita thrust belt. Identifications of the samples reported herein are listed in Table 1; previously reported samples not listed in Table 1 are: Ane—Atoka Formation northeastward dispersal (Sharrah, 2006); Aws—Atoka Formation westward and southward dispersal (Sharrah, 2006); SP—Spiro (Atoka) Sandstone (Sharrah, 2006); B—Bloyd Formation (Xie et al., 2018a); BS—Big Saline Formation (Alsalem et al., 2018); HS—Hot Springs Sandstone (McGuire, 2017); KS-5-WH—Whitehorse Group (Thomas et al., 2020); P—Post Oak Conglomerate (Thomas et al., 2016); SC—Strawn Group and Canyon Group (Alsalem et al., 2018); ST—Stanley Shale (McGuire, 2017); V—Vanoss Conglomerate (Thomas et al., 2016); W—Wedington Sandstone (Xie et al., 2016); some symbols represent multiple closely spaced samples.

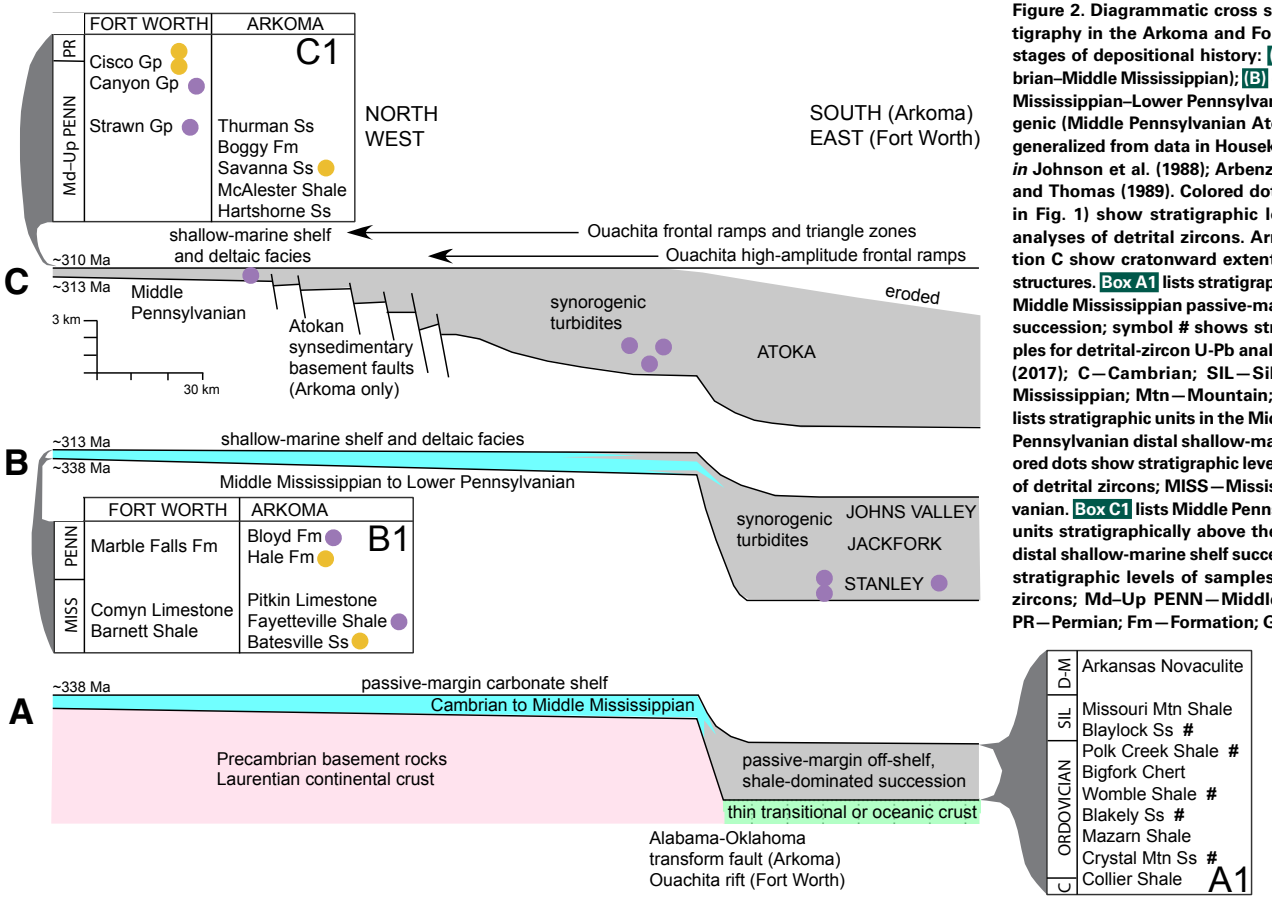

Figure 2. Diagrammatic cross sections of Ouachita stratigraphy in the Arkoma and Fort Worth basins at three stages of depositional history: (A) passive margin (Cambrian–Middle Mississippian); (B) early synorogenic (Middle Mississippian–Lower Pennsylvanian); and (C) late synorogenic (Middle Pennsylvanian Atoka Formation). Figure is generalized from data in Houseknecht (1986); Sutherland, *in* Johnson et al. (1988); Arbenz (1989a, 2008); and Viele and Thomas (1989). Colored dots (symbols as explained in Fig. 1) show stratigraphic locations of samples for analyses of detrital zircons. Arrows at top of cross section C show cratonward extent of Ouachita thrust-belt structures. Box A1 lists stratigraphic units in the Cambrian–Middle Mississippian passive-margin off-shelf deep-water succession; symbol # shows stratigraphic levels of samples for detrital-zircon U-Pb analyses reported in McGuire (2017); C—Cambrian; SIL—Silurian; D-M—Devonian–Mississippian; Mtn—Mountain; Ss—Sandstone. Box B1 lists stratigraphic units in the Middle Mississippian–Lower Pennsylvanian distal shallow-marine shelf succession; colored dots show stratigraphic levels of samples for analyses of detrital zircons; MISS—Mississippian; PENN—Pennsylvanian. Box C1 lists Middle Pennsylvanian–Lower Permian units stratigraphically above the Atoka Formation in the distal shallow-marine shelf succession; colored dots show stratigraphic levels of samples for analyses of detrital zircons; Md–Up PENN—Middle–Upper Pennsylvanian; PR—Permian; Fm—Formation; Gp—Group.

1986; Sutherland, 1988; Sutherland, *in* Johnson et al., 1988; Morris, 1989). Thus, the Arkoma and Fort Worth basins have become the center of controversy, as well as the potential key, regarding regional-scale alternatives to sediment dispersal.

This article reports new U-Pb age data and Hf isotopic data from detrital zircons and summarizes previously published data from the Upper Mississippian to Permian detritus in the Arkoma and Fort Worth foreland basins. The primary objective of this research is to use the detrital-zircon geochronologic and Hf isotopic data to characterize and possibly identify the provenance or provenances of the clastic sediment, especially to distinguish between proximal synorogenic sources and more distant sources in the Laurentian craton or Appalachians. Comparisons with detrital-zircon data from nearby intracratonic basins (both new data from the Anadarko basin and previously published data from other intracratonic basins), as well as possible distant sources of sediment, provide tests of possible dispersal pathways in the context of stratigraphy and sedimentology, including both into and out of the Arkoma and Fort Worth basins.

EVOLUTION OF THE OUACHITA OROGEN AND FORELAND: TECTONICS AND SEDIMENTATION

Ouachita Orogen

The late Paleozoic Appalachian-Ouachita-Marathon orogen rims the eastern and southern margins of the North American craton (Fig. 1A). Postorogenic Mesozoic–Cenozoic strata of the Gulf Coastal Plain cover much of the orogenic belt in southern North America (Fig. 1A), and geologic

interpretations rely on drill holes and geophysical data to supplement observations from the limited exposures (e.g., Thomas et al., 1989). The orogen is part of the continent-scale system that resulted from closure of the oceans that rimmed the Laurentian continent and the late Paleozoic assembly of supercontinent Pangaea (Thomas, 2019).

The Ouachita salient of the orogen forms a large-scale cratonward convex curve with a bend of ~90° in strike, reflecting inheritance of the trace of the pre-orogenic lapetan rifted margin of Laurentia (Fig. 1A) (Thomas, 1977, 2006; Thomas et al., 2012). The Arkoma foreland basin borders the apex and northern arm of the Ouachita salient, and the Fort Worth foreland basin borders the southern arm (Fig. 1B). Thick (as much as 15 km) Mississippian–Pennsylvanian synorogenic clastic wedges fill the proximal parts of the foreland basins and thin dramatically into the distal parts of the basins (Fig. 2) (Arbenz, 1989a). The two foreland basins are separated by the Arbuckle basement uplift along the west-northwest–trending Southern Oklahoma basement fault system, which intersects and is overlain directly by the frontal Ouachita thrust sheets (Fig. 1B). West of the apex of the Ouachita salient and the Arkoma basin, the Anadarko basin extends on the craton along the northern side of the Southern Oklahoma basement fault system (Fig. 1).

The outcrops in the Ouachita Mountains of Arkansas and Oklahoma, along with deep drill holes and geophysical data in the subsurface beneath the Gulf Coastal Plain, provide a profile of the Ouachita orogen (Fig. 3) (Thomas et al., 1989; Viele and Thomas, 1989). Thick continental crust of the Laurentian craton extends southward beneath the Ouachita sedimentary thrust belt, where gravity and seismic-velocity models depict an abrupt edge of the continental crust at the Alabama-Oklahoma transform fault (Figs. 1–4) (Keller et al., 1989; Mickus and Keller, 1992; Harry et al., 2003).

South of the Ouachita thrust belt and the underlying abrupt transform margin of Laurentian crust, seismic-velocity and gravity crustal models display a thick mass of deformed sedimentary rocks overlying thin transitional or oceanic crust (Keller et al., 1989; Mickus and Keller, 1992). Deep drill holes document depositional ages of Middle Pennsylvanian to Middle Permian (Flawn et al., 1961; Nicholas and Waddell, 1989).

Approximately 100 km south of the abrupt southern margin of Laurentian continental crust, the geophysical models show a separate mass of continental crust identified as the Sabine accreted terrane (Figs. 1 and 3) (Keller et al., 1989; Mickus and Keller, 1992), which is inferred to have been a source of synorogenic clastic sediment to the Ouachita foreland (e.g., Sharrah, 2006; Alsalem et al., 2018). No drill holes have penetrated continental basement rocks within the Sabine terrane, leaving the composition and affinities of the terrane unconfirmed. Xenoliths from the Prairie Creek lamproite pipe (Fig. 1A), which is near the edge of the Gulf Coastal Plain and within the subsurface

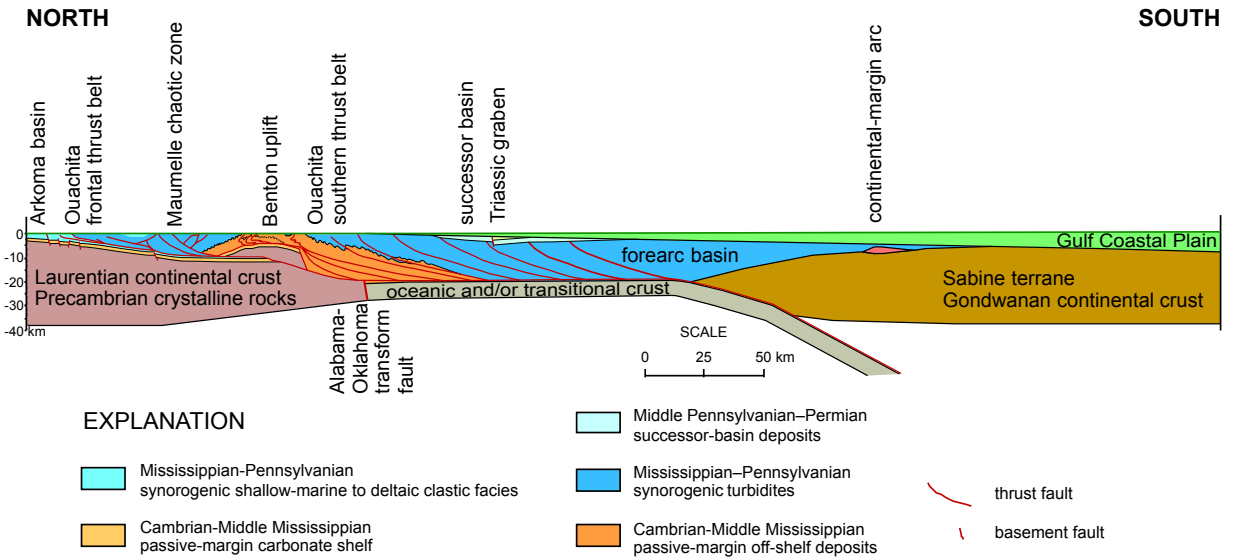

Figure 3. Generalized structural cross section illustrating the components of the Ouachita orogen and the Sabine accreted terrane (compiled from data and interpretations in Nelson et al., 1982; Lillie et al., 1983; Arbenz, 1989b, 2008; Keller et al., 1989; Thomas et al., 1989; Viele and Thomas, 1989; Mickus and Keller, 1992). These structural elements constitute the possible proximal orogenic provenance of sediment in the Arkoma basin, the most proximal part of which is imbricated in the Ouachita thrust belt.

southern part of the Ouachita thrust belt, have U-Pb zircon ages of 1800–1600 Ma (Clift et al., 2018). The xenolith ages have been interpreted to represent the Sabine basement (Clift et al., 2018); however, the lamproite pipe is near (within ~10 km) the projected trace of the transform margin of Laurentian crust (e.g., Dunn, 2009) and is ~100 km north of the northern edge of continental crust of the Sabine terrane as defined in the geophysical models (Fig. 1A) (Keller et al., 1989; Mickus and Keller, 1992). The area inferred by Clift et al. (2018) to be Sabine crust is exactly the same as the area shown to be thin transitional or oceanic crust overlain by sedimentary rocks in the seismic-velocity and gravity crustal models (Keller et al., 1989; Mickus and Keller, 1992). Thus, the data from the lamproite pipe are most likely applicable to Laurentian crust along the Alabama-Oklahoma transform rather than to the Sabine terrane (Van Avendonk and Dalziel, 2018). Granite boulders with ages of 1407–1284 Ma (Bowring, 1984) in Ordovician passive-margin debris flows in the Ouachita thrust belt (Stone and Haley, 1977) indicate that the upper crust along the Laurentian transform margin is within the Granite-Rhyolite province, consistent with K-Ar dates (1471–1323 Ma) from the Prairie Creek xenoliths (Dunn, 2009). The deeper and older crust represented by the xenoliths may be equivalent to Yavapai-Mazatzal (or Central Plains) components of Laurentian crust (Clift et al., 2018).

Following the geophysical models (Keller et al., 1989; Mickus and Keller, 1992), the Sabine terrane is isolated along the Laurentian margin, similar to other accreted terranes (Fig. 1A). The accreted Coahuila terrane within the Marathon salient of the orogenic belt (Fig. 1A) has basement rocks with ages of 1232–1214 Ma (Sunsás) and of 580 Ma (Pan-African/Brasiliano); rocks of Las Delicias volcanic arc have late Paleozoic ages between 331 and 270 Ma (Lopez, 1997; Lopez et al., 2001). Detrital zircons in Jurassic–Cretaceous proximal sedimentary deposits in local fault-bounded basins within the Coahuila terrane have distinctive modes of 1485 Ma (Rondonia–San Ignacio), 1254 Ma (Sunsás), 1040 Ma (Sunsás), 562 Ma (Pan-African/Brasiliano), 414 Ma (early–middle Paleozoic), and 282 Ma (late Paleozoic) (Lawton and Molina-Garza, 2014;

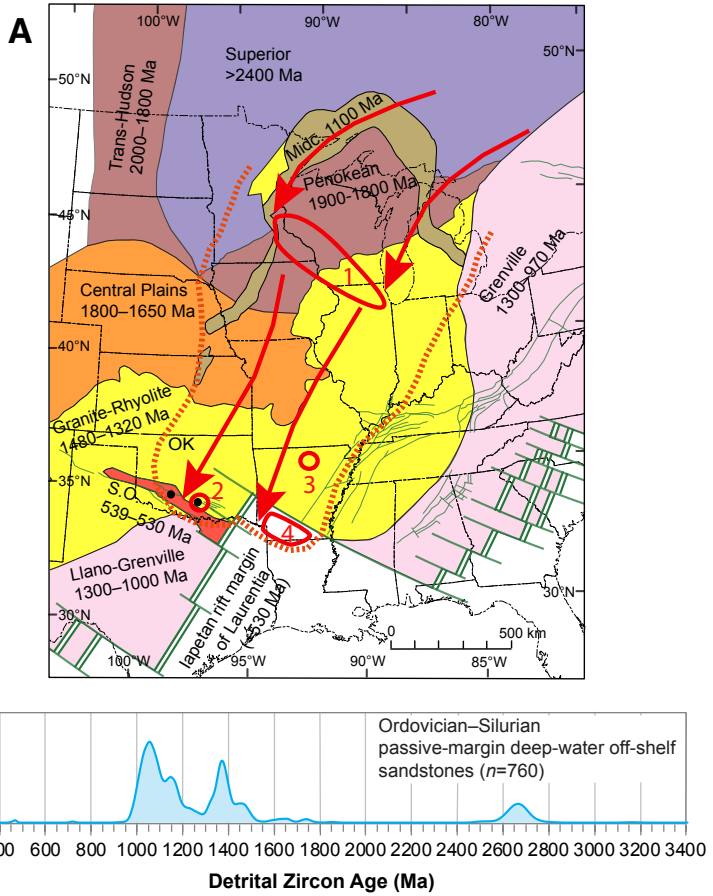

Figure 4. Map of Middle Ordovician sandstones on the Laurentian shelf and detrital-zircon age data from pre-orogenic off-shelf sandstones adjacent to the passive margin of Laurentia. (A) Map of extent and dispersal patterns of Middle Ordovician sandstones in relation to Precambrian basement provinces (from Van Schmus et al., 1993) and the lapetan rift margin of Laurentia (from Thomas, 2014). Red dashed line shows approximate extent of Middle Ordovician sandstone units; red arrows show inferred dispersal patterns. Red bold ovals show: (1) locations of detrital-zircon U-Pb age data from Konstantinou et al. (2014); (2 and 3) locations of detrital-zircon U-Pb age data from Pickell (2012); (4) approximate palinspastic locations to restore Ouachita thrusting of samples for data shown in Figure 4B. Midc.—Midcontinent rift; OK—Oklahoma; S.O.—Southern Oklahoma fault system. (B) Composite U-Pb age-probability density plot of data (*N* = 5, *n* = 717, from McGuire, 2017; *N* = 2, *n* = 43, from Gleason et al., 2002) from stratigraphic units now displaced in the Ouachita thrust belt from pre-orogenic passive-margin off-shelf sites along the rift margin (stratigraphic and tectonic setting shown in Fig. 2, box A1).

Thomas et al., 2019). The Pan-African/Brasiliano ages indicate that the Coahuila terrane is one of several Gondwanan terranes, including Sierra Madre and Maya (Fig. 1A), that may be parts of an originally larger Oaxaquia terrane (Ortega-Gutierrez et al., 1995; Lawlor et al., 1999). The Sierra Madre terrane includes basement rocks with ages of 1235–978 Ma (Sunsás) and volcanic rocks with ages of 334 Ma (late Paleozoic) (Lawlor et al., 1999; Stewart et al., 1999; Cameron et al., 2004). The Maya terrane includes rocks with ages of 554 Ma (Pan-African/Brasiliano) and of 418–404 Ma (middle Paleozoic) (Krogh et al., 1993; Steiner and Walker, 1996; Martens et al., 2010). The Sabine terrane (Fig. 1A) may be either part of Coahuila or Oaxaquia or a separate, but similar, terrane now inside the Ouachita salient of the orogenic belt. Palinspastic reconstruction to restore Triassic rifting and subsequent opening of the Gulf of Mexico places the Maya terrane (now in Yucatan; Fig. 1A) between and contiguous to Coahuila on the southwest and Sabine on the northeast (Pindell and Kennan, 2009). Placing the Sabine terrane within the assembly of Gondwanan terranes suggests that the presently undocumented composition of the Sabine terrane may be generally similar to the well-documented composition of Coahuila and the compositions of the Maya and Sierra Madre terranes.

Another possible indicator of the composition of the Sabine basement is in five successive volcanic tuff units in the Mississippian–Pennsylvanian Stanley Shale in the Ouachita thrust belt. The distribution of the tuffs indicates dispersal from an arc complex on the south, consistent with continental-margin arc magmatism associated with southward subduction beneath a continental terrane (Niem, 1977; Loomis et al., 1994; Shaulis et al., 2012). The pyroclastic units are pumiceous vitric-crystal tuff and "hammer-ringing hard" siliceous vitric tuff; the tuffs include a minor component of shale rip-up clasts, as well as rounded pebbles of quartzite and basalt (Niem, 1977). U-Pb zircon ages from the five successive tuff beds are dominantly 328.5 ± 2.7 to 320.7 ± 2.5 Ma, indicating the ages of tuff crystallization; however, the samples also include a range of older zircon grains (Shaulis et al., 2012). In light of the shale rip-up clasts, the older ages have been interpreted to be from detrital grains (Shaulis et al., 2012), suggesting that they represent ages of the provenance of the muddy turbidites, which was inferred to be Appalachian. The rounded pebbles of quartzite and basalt, however, imply a more proximal source, probably from shallow-marine reworking of clasts along the arc terrane. Alternatively, the lithology and the depositional setting of the ash-flow or ash-fall tuffs (Niem, 1977), particularly the general paucity of lithic clasts and the very hard vitric-crystal tuffs, suggest that the prevolcanic zircons may be xenocrysts from the magma source at the leading edge of the Sabine terrane. Even if some of the grains are detrital, the source of the muddy sediment may have been the proximal Sabine terrane, as suggested by the rounded pebbles of quartzite and basalt. A future focused study to evaluate the alternatives of detrital or xenocrystic zircon grains, as well as the provenance of the quartzite and basalt pebbles, is critical to resolving the provenance of this part of the clastic wedge and the composition of the Sabine basement.

Drill holes have penetrated rhyolite porphyry incorporated in the thick mass of Pennsylvanian sedimentary rocks along the northern leading edge of the Sabine terrane, further suggesting a continental-margin arc (Nicholas and Waddell, 1989). Although the Sabine rhyolites are geochemically distinct from the Stanley tuffs, both have geochemical characteristics of subduction-related magmas (Loomis et al., 1994).

Pre-Orogenic Tectonic Framework and Sedimentation

The intersection of the Alabama-Oklahoma transform fault with the Ouachita rift frames the Ouachita embayment in the Iapetan rifted margin of southern Laurentia (Figs. 1 and 4), reflecting the late stages of continental rifting and breakup of supercontinent Rodinia (e.g., Thomas, 1977, 2019). Juvenile synrift igneous rocks along the transform-parallel Southern Oklahoma fault system, inboard from the rifted margin, indicate the time of rifting at 539–530 Ma (Wright et al., 1996; Hogan and Gilbert, 1998; Thomas et al., 2012; Hanson et al., 2013); coeval early Cambrian synrift clastic and evaporite deposits in the Argentine Precordillera terrane, the conjugate to the Ouachita embayment, confirm the time of rifting (Thomas and Astini, 1996, 1999). Although most of the length of the Laurentian rift margin (as well as most of the Precordillera) is within the Grenville province, synrift boulders and detrital zircons in the Precordillera have ages of the Granite-Rhyolite province, indicating that Iapetan rifting cut across the Grenville Front and excised part of the Laurentian Granite-Rhyolite province in the Ouachita embayment (Fig. 4) (Thomas et al., 2012).

On the passive-margin shelf of southern Laurentia, Cambrian–Mississippian deposits are dominantly shallow-marine carbonates (Fig. 2). The carbonate succession includes quartzose sandstone beds, mostly in the Middle Ordovician, that extend from the onlap limit on the Canadian Shield (Konstantinou et al., 2014) southward to the shelf margin around the Ouachita foreland (Fig. 4) (Pickell, 2012; Thomas et al., 2016). Ages of detrital zircons in the sandstones represent various provinces of the Laurentian craton, dominantly the Superior province (Pickell, 2012; Konstantinou et al., 2014).

Cambrian–Mississippian strata in the Ouachita thrust belt constitute an off-shelf deep-water mud-dominated facies that is the counterpart of the passive-margin shelf carbonates (Fig. 2). The muddy succession includes carbonate mudstone, carbonate-clast conglomerate, and quartzose sandstone, all indicating detritus from the shelf (summaries in Arbenz, 1989a; Viele and Thomas, 1989). The Middle Ordovician Blakely Sandstone (Fig. 2, box A1) contains boulders of granite and meta-arkose from basement rocks along scarps at the rifted continental margin (Stone and Haley, 1977). The granite boulders have U-Pb ages of 1407 ± 13, 1350 ± 30, and 1284 ± 12 Ma; ages of detrital zircons from the sandstones range from 1350 to 1300 Ma (Bowring, 1984). The range of ages corresponds to the Granite-Rhyolite and Grenville provinces of Laurentia (Fig. 4). Samples from five Ordovician–Silurian sandstones (Fig. 2, box A1) have dominant distributions of detrital-zircon ages (Fig. 4) that correspond to the Superior,

Granite-Rhyolite, and Grenville provinces of the Laurentian craton (McGuire, 2017). The range of available ages indicates that the Superior grains are in grain-flow deposits from the quartzose sands on the shelf and that the Granite-Rhyolite and Grenville grains are from the shelf-edge scarps cut into Laurentian basement rocks. The off-shelf passive-margin succession includes two prominent chert units (Fig. 2, box A1)—the Ordovician Bigfork Chert and the Devonian–Mississippian Arkansas Novaculite (Arbenz, 1989a)—that indicate low sedimentation rates along the passive margin (Viele and Thomas, 1989).

Late Paleozoic Orogenesis and Sedimentation—Arkoma Basin

In the proximal Arkoma basin now imbricated in the Ouachita thrust belt (Fig. 1B), a thick succession of muddy turbidites (Stanley Shale, 3350 m thick; Figs. 2B and 5) directly overlies the Arkansas Novaculite, indicating an abrupt increase in the rate of deposition of siliciclastic sediment in the off-shelf deep-water setting and signaling approach to the trench and initiation of orogeny in Middle Mississippian (Meramecian) time (Viele and Thomas, 1989). The five successive volcanic tuff units with ages of 328–320 Ma in the Stanley Shale (Fig. 6) indicate continental-margin arc magmatism on the leading edge of the Sabine terrane (Niem, 1977; Shaulis et al., 2012). Very rapid deposition of synorogenic sandy turbidites (Jackfork and Johns Valley Formations, 2300 m thick; Fig. 2B) continued through the Early Pennsylvanian in a forearc deep-water off-shelf setting (Morris, 1989).

The Middle Mississippian–Lower Pennsylvanian succession thins dramatically toward the craton and consists of shallow-marine and deltaic facies in the distal foreland (Fig. 2B) (Arbenz, 1989a; Viele and Thomas, 1989). The shallow-marine carbonates and sandstones generally intertongue with and pinch out southward into a shale succession that thickens gradually southward toward the continental margin (Ogren, 1968; Handford, 1986, 1995; Sutherland, 1988; Sutherland, *in* Johnson et al., 1988). Distributions of sandstones, as well as paleocurrent data, suggest that most of the sandstones represent southward prograding depositional systems with regional sediment dispersal across the craton on the north (Sutherland, 1988; Xie et al., 2016); some shale units suggest localized partly starved basins, e.g., the Mississippian Fayetteville Shale (Fig. 2, box B1).

In contrast to the pre-Atoka shallow-marine facies in the distal Arkoma basin, the Middle Pennsylvanian Atoka Formation is a much thicker succession (9000 m thick; Fig. 2C) of sandy turbidites, indicating a rapid increase in subsidence rate and sediment-accumulation rate in response to advance of the accretionary prism (Ouachita allochthon) and tectonic loading of continental crust (Houseknecht, 1986). Paleocurrent indicators in the turbidites show northeast-directed currents in the western part of the deep basin and west-directed currents in the eastern part (Sharrah, 2006). The deep-water facies grade upward toward the top of the Atoka Formation and toward the foreland into shallow-marine to deltaic facies, indicating filling of the late stages of the peripheral foreland basin (Houseknecht, 1986). The Atoka Formation thins cratonward to <400 m at the distal northern margin of the Arkoma foreland basin (Fig. 2C) (Sutherland, 1988; Sutherland, *in* Johnson et al., 1988; Arbenz, 1989a; Morris, 1989).

Post-Atokan Middle Pennsylvanian stratigraphic units (Fig. 2, box C1) are preserved only in the distal foreland (not in the proximal basin) and record deposition in the latest stages of subsidence of the Arkoma basin (Sutherland, *in* Johnson et al., 1988). The succession of sandstones and shales includes deltaic facies prograding southward into the basin, as well as some sediment from the orogen on the south. The Middle Pennsylvanian (middle Desmoinesian) Thurman Sandstone (Fig. 2, box C1) contains chert-pebble conglomerate derived from the Ordovician and Devonian cherts in the Ouachita thrust belt (Sutherland, *in* Johnson et al., 1988).

Late Paleozoic Orogenesis and Sedimentation—Fort Worth Basin

The Fort Worth basin (Fig. 1B) is a broad homocline that dips gently eastward from the Bend arch, an intracratonic uplift that separates the orogenic foreland basin from the intracratonic Permian basin (Brown et al., 1973; Kier et al., 1979). The Fort Worth basin dips more steeply eastward beneath the east-dipping Ouachita frontal thrust faults (Fig. 1), and the eastern proximal fill of the basin is imbricated in the Ouachita thrust belt (Nicholas, *in* Arbenz et al., 1989). Along strike, the Fort Worth basin ends northward at the Muenster uplift and southward at the intracratonic Llano uplift (Fig. 1B) (Crosby and Mapel, 1975).

The initial synorogenic deposits along the southern arm of the Ouachita salient are muddy turbidites of the Mississippian–Lower Pennsylvanian Stanley Shale (Fig. 2B), now deep in the subsurface in the Ouachita thrust belt in east Texas (Mapel et al., 1979). The Stanley Shale directly overlies the Arkansas Novaculite at the top of the off-shelf passive-margin succession in the Ouachita thrust belt in east Texas (Fig. 2), as it does in the outcrops in the Ouachita Mountains (Arbenz, 1989a; Viele and Thomas, 1989). A very thick succession of sandy turbidites in the Lower Pennsylvanian Jackfork Formation overlies the Stanley Shale in the Ouachita thrust belt. Equivalent shelf-facies rocks west of the Ouachita thrust belt (Fig. 2, box B1) include relatively thin Upper Mississippian shale and overlying limestones that grade eastward to muddy facies (Crosby and Mapel, 1975; Mapel et al., 1979).

The thick (>1800 m) Middle Pennsylvanian Atoka Formation (Fig. 2C), consisting of muddy and sandy turbidites, records initial rapid subsidence of the Fort Worth foreland basin, now imbricated in the Ouachita thrust belt. Fan-delta and deeper water deposits prograded into the subsiding basin, which bordered the shelf east of the Bend arch, where a relatively thin Smithwick Shale was deposited during Atokan time (Kier et al., 1979). Near the northern end of the Fort Worth basin, coarse fan-delta deposits prograded across the subsiding basin and onto the western shelf from sources in the fault-bounded Muenster uplift and along the northern part of the Ouachita thrust belt, near where it impinges on the eastern part of the basement uplifts associated with the Southern Oklahoma fault system (including the Muenster uplift; Fig. 1B) (Thompson, 1982).

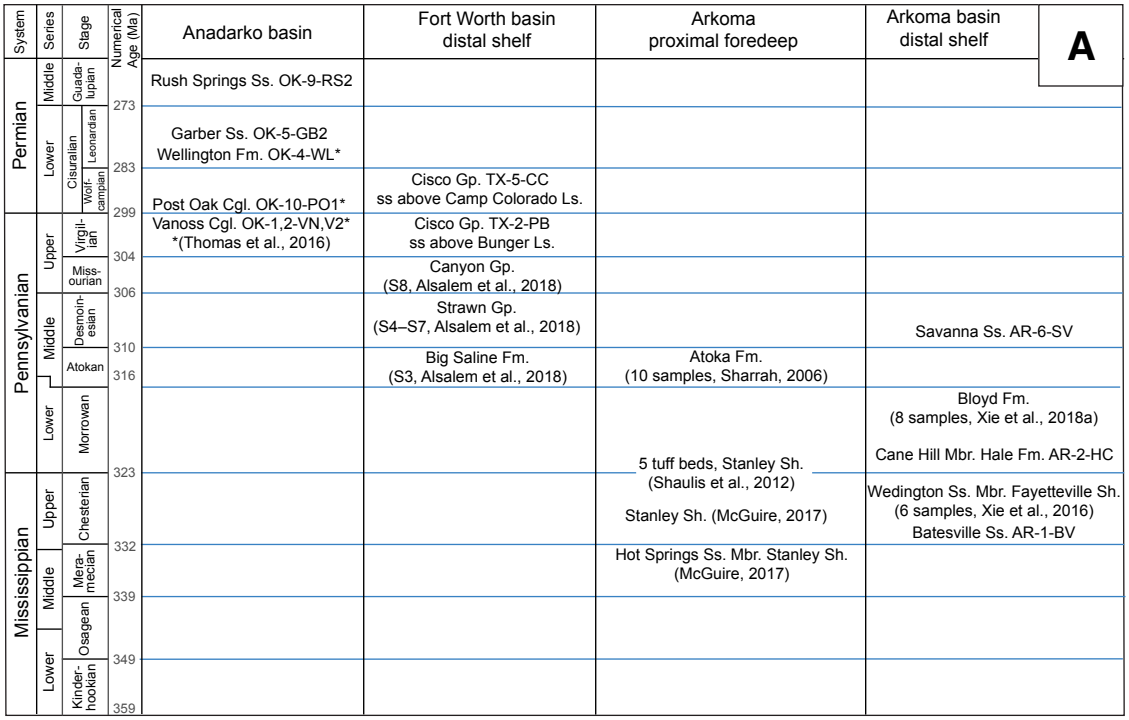

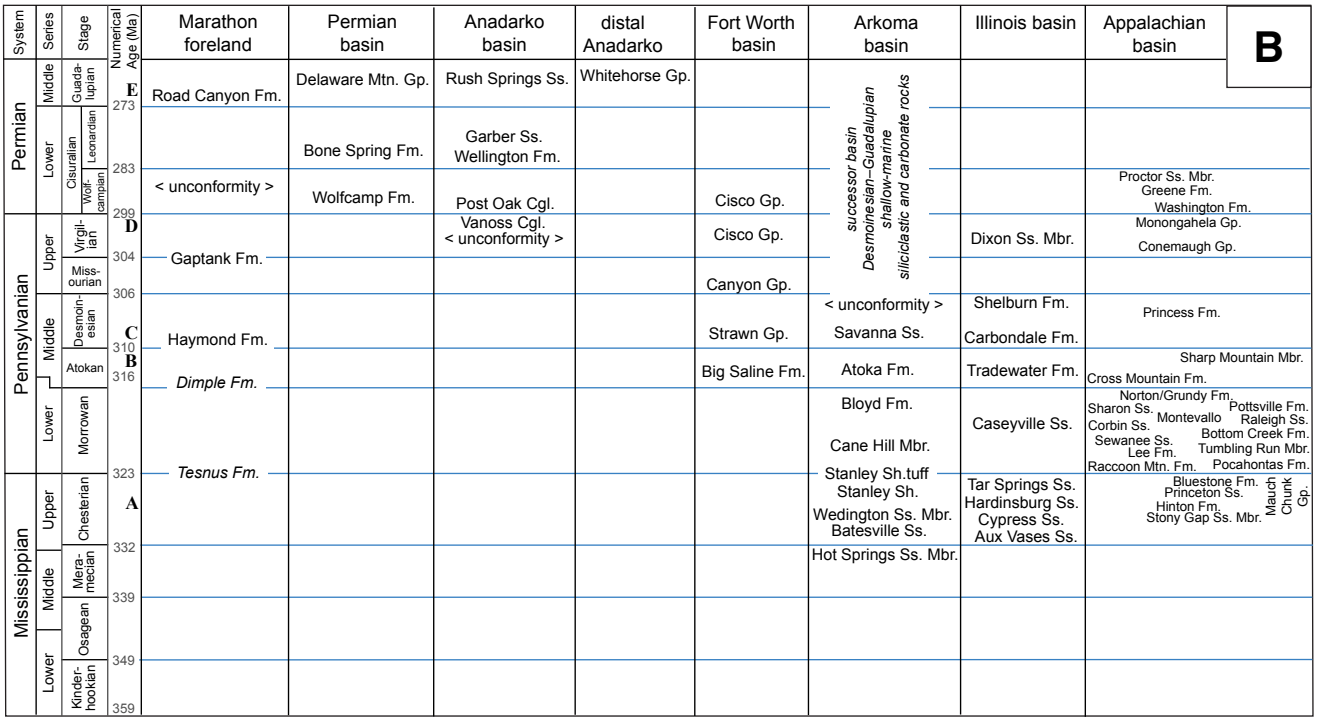

Figure 5. Stratigraphic columns of upper Paleozoic units in the Arkoma, Fort Worth, and Anadarko basins and surrounding regions. (A) Stratigraphic columns showing units sampled for analyses of detrital zircons from the Arkoma, Fort Worth, and Anadarko basins. Cgl.—Conglomerate; Fm.—Formation; Gp.—Group; Ls.—Limestone; Mbr.—Member; Ss.—Sandstone; Sh.—Shale. (B) Regional stratigraphic columns showing units sampled for analyses of detrital zircons from localities that are relevant to discussion of regional relations of U-Pb age distributions and Hf isotopic data for the Arkoma, Fort Worth, and Anadarko basins. Units with names in italics are shown for correlation but are not represented by U-Pb age data. Stratigraphic levels of angular unconformities are shown for the Arkoma basin, Anadarko basin, and Marathon foreland. The Desmoinesian–Guadalupian successor basin deposits overlie Atokan beds at an angular unconformity in the interior of the Ouachita thrust belt; the Savanna Sandstone is near the top of the preserved succession in the distal foreland of the Arkoma basin. Mtn.—Mountain. The time scale is International Commission on Stratigraphy (ICS) *International Chronostratigraphic Chart 2019* (Cohen et al., 2013, updated), using correlations from Gradstein et al. (2004). The letters A–E in the Numerical Age column indicate the approximate stratigraphic levels of the maps in Figure 12.

The Strawn Group (Desmoinesian) includes fluvial-deltaic systems that prograded westward, filling the Fort Worth basin and lapping over the Bend arch (Kier et al., 1979). The overlying Canyon and Cisco Groups (Upper Pennsylvanian, Missourian and Virgilian, to Lower Permian; Fig. 2, box C1; Fig. 5) include numerous cycles of westward prograding deltaic sandstones and mudstones and eastwardly transgressive limestones (Galloway and Brown, 1973; Kier et al., 1979). The vertical succession of sediment-dispersal systems and thickness distribution of clastic facies suggest that post-Atokan sediment was eroded from the Ouachita orogen and transported westward as the postorogenic fill of the Fort Worth basin. Chert-clast conglomerates (Brown et al., 1973) indicate sediment dispersal from erosion of the Ordovician and/or Devonian cherts in the Ouachita thrust belt.

Late Paleozoic Tectonics and Sedimentation—Anadarko Basin

The Anadarko basin is a deep intracratonic basin along the north side of the Arbuckle and Wichita basement uplifts, which are bounded by the Southern Oklahoma fault system (Fig. 1B). On the east, the north-striking Ouachita thrust front cuts across the west-northwest–striking uplifts, faults, and basin; the shallow Central Oklahoma arch separates the eastern part of the Anadarko basin from the Arkoma basin in the Ouachita foreland (Rascoe and Johnson, *in* Johnson et al., 1988; Perry, 1989; Jusczuk, 2002).

The structure of the Southern Oklahoma fault system (Fig. 1) includes fractures associated with emplacement of a very large volume of synrift magma between 539 and 530 Ma (Denison, 1982; Hogan and Gilbert, 1998; Thomas et al., 2012; Hanson et al., 2013). A transgressive passive-margin succession of basal sandstone (middle Upper Cambrian) and overlying shallow-marine carbonates (Upper Cambrian–Middle Ordovician) overlaps the Cambrian igneous rocks (Denison, *in* Johnson et al., 1988). The Middle Ordovician part of the carbonate succession includes mature quartzose sandstone. A relatively thin, unconformity-punctuated, heterolithic, Upper Ordovician–Mississippian succession represents deposition on a stable shelf (Amsden, *in* Johnson et al., 1988).

In contrast to the earlier history, a very thick, dominantly clastic succession of Pennsylvanian age reflects the rise of multiple components of the Arbuckle and Wichita basement uplifts along large-magnitude basement faults (Johnson et al., 1988; Denison, 1989; Perry, 1989). Thickness and facies distributions of a relatively thin succession of Upper Mississippian to Lower Pennsylvanian (Morrowan) shale, sandstone, and limestone show no influence of the uplifts along the Southern Oklahoma fault system; however, beginning abruptly during the Morrowan and persisting into the Early Permian, deposition of a coarse proximal facies, called the "Granite Wash," indicates steep fault-bounded uplifts along the southwestern edge of the evolving Anadarko basin (Rascoe and Johnson, *in* Johnson et al., 1988). The "Granite Wash" laps onto an erosion surface, which truncates faulted and folded rocks that range down through the Paleozoic succession to the synrift Cambrian igneous rocks and the Precambrian basement. The onlapping proximal Upper Pennsylvanian Vanoss Conglomerate and Lower Permian Post Oak Conglomerate (Fig. 5)

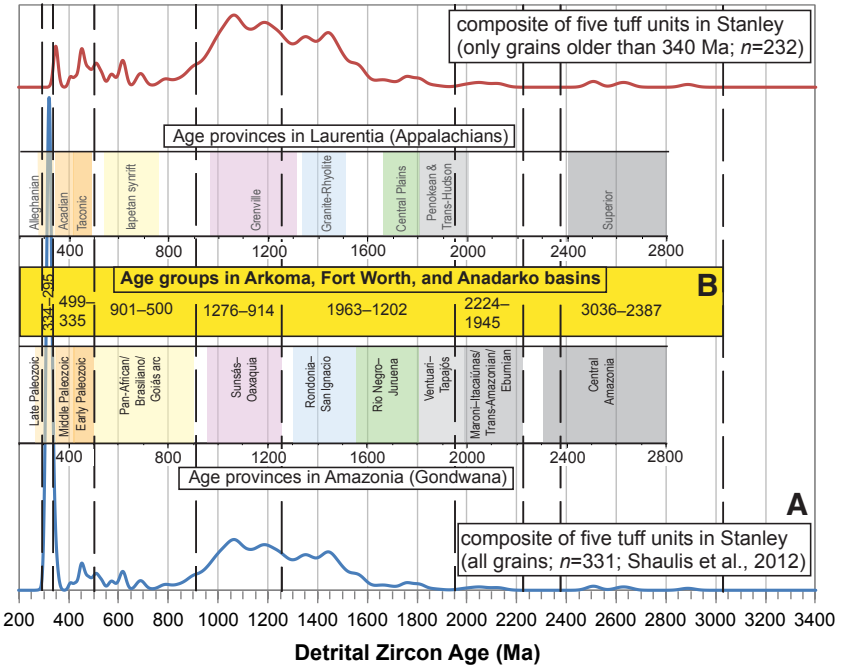

Figure 6. Zircon age data from tuff units in the Stanley Shale and comparison with ages of Laurentian and Gondwanan provinces, as well as age groups of detrital zircons in the Arkoma, Fort Worth, and Anadarko basins. (A) U-Pb age-probability density plots of a composite of five separate tuff units in the Stanley Shale in the Ouachita thrust belt from data published in Shaulis et al. (2012). The lower plot shows all data with a very strong mode of 328–320 Ma, the crystallization age of the tuffs; the upper plot shows only data from prevolcanic (older than 340 Ma) grains. (B) Age-correlation diagram comparing ages of provinces in Laurentia (Appalachians), provinces in Amazonia (Gondwana), and age groups of detrital zircons in the Arkoma, Fort Worth, and Anadarko basins. Boundaries of the age groups are shown by dashed black lines, which are defined in Table 3 and used in Figures 7–10.

have detrital-zircon age distributions from recycling of earlier Paleozoic sedimentary rocks and from local primary sources in synrift Cambrian igneous rocks, respectively (Thomas et al., 2016). The proximal Granite Wash is limited to a relatively narrow area adjacent to the Arbuckle-Wichita uplifts and interfingers basinward into a succession of shale, sandstone, and limestone. A maximum thickness of >4500 m of Atokan through Virgilian beds indicates rapid subsidence of the Anadarko basin (Rascoe and Johnson, *in* Johnson et al., 1988). Subsidence slowed in Permian time, and the supply of coarse clastic sediment from the uplifts diminished. By Middle Permian time, the uplifts were largely covered by a more blanket-like succession of red beds and evaporites (Johnson et al., 1988).

The Anadarko basin is highly asymmetric, with a long, gentle, southwest-dipping limb that bends abruptly upward along the Southern Oklahoma fault system (Fig. 1B), defining a deep trough in the southern part of the basin (Rascoe and Johnson, *in* Johnson et al., 1988). The basin is doubly plunging, up plunge onto the Cimarron arch on the northwest and up plunge onto the southern part of the Nemaha uplift or Central Oklahoma arch on the east (Fig. 1A). The Central Oklahoma arch separates the eastern up-plunge end of the Anadarko basin from the Arkoma foreland basin, which had a distinctly different subsidence history, both mechanically and temporally.

Late Paleozoic Ouachita Orogen

In the Ouachita Mountains, along the northern arm of the Ouachita thrust belt, facing the Arkoma basin, the Cambrian–Mississippian off-shelf passive-margin succession and overlying Mississippian–Pennsylvanian synorogenic muddy to sandy turbidites are imbricated in the Ouachita allochthon and thrust over the Cambrian–Mississippian passive-margin carbonate-shelf facies, which remained in the Ouachita footwall (Fig. 3) (Arbenz, 1989a, 2008; Viele and Thomas, 1989). The Ouachita detachment generally ramps upward toward the foreland from the lower part of the Cambrian–Mississippian off-shelf passive-margin succession into the Middle Pennsylvanian (Atokan) part of the synorogenic succession (Fig. 3). The Maumelle chaotic zone (along the trailing side of the frontal thrust belt; Fig. 3) of broken Mississippian–Pennsylvanian sandstone and shale is interpreted to be the leading edge of the accretionary prism, which was thrust onto the pre-orogenic shelf (Viele and Thomas, 1989). During the later stages of contraction, basement-rooted thrusts inserted the deep subsurface Benton and Broken Bow uplifts (Figs. 1B and 3) beneath the sedimentary thrust belt, raising internally folded, disharmonic thrust sheets of Cambrian–Mississippian off-shelf passive-margin mudstone, chert, and sandstone in large-scale frontal thrust ramps (Viele and Thomas, 1989; Arbenz, 2008). Rare tectonically bounded slivers of ultramafic rocks within the deformed sedimentary rocks along the uplifts are interpreted to be fragments of the oceanic crust of the Laurentian plate that were picked off from the down-going slab (Morris and Stone, 1986; Nielsen et al., 1989; Viele and Thomas, 1989).

South of the intersection of the Ouachita thrust front with basement structures along the Southern Oklahoma fault system, postorogenic Mesozoic–Cenozoic strata of the Gulf Coastal Plain cover the Ouachita orogen and the proximal part of the Fort Worth basin in the footwall of the orogen (Fig. 1) (e.g., Thomas et al., 1989). Drill data and seismic-reflection profiles document Upper Cambrian to Lower Mississippian off-shelf deep-water passive-margin strata and Middle Mississippian to Middle Pennsylvanian synorogenic clastic facies in the Ouachita frontal trust belt (Fig. 2), which have been thrust over the shelf edge onto the Cambrian–Mississippian passive-margin shelf-carbonate facies (e.g., King, *in* Flawn et al., 1961; Nicholas and Rozendal, 1975; Nicholas, *in* Arbenz et al., 1989; Nicholas and Waddell, 1989; Thomas et al., 1989; Viele and Thomas, 1989; Culotta et al., 1992). The frontal structures and stratigraphy in the subsurface east of the Fort Worth basin (southern arm of Ouachita salient; Fig. 1) are like those in the outcrops in the Ouachita Mountains in the eastern arm of the Ouachita salient, except that the detachment does not ramp up stratigraphically at the front of the southern arm. The Waco and Luling basement uplifts (Fig. 1B) underlie tectonically thickened and deformed clastic rocks along the trailing edge of the sedimentary thrust belt (Rozendal and Erskine, 1971; Nicholas and Waddell, 1989; Culotta et al., 1992). Trailing the Ouachita sedimentary thrust belt, the "Ouachita interior metamorphic belt" (Fig. 1) consists of low-grade metasedimentary rocks and extends along strike southwestward around the Texas recess to the Marathon salient (Nicholas and Waddell, 1989; Thomas et al., 1989; Viele and Thomas, 1989). The trailing part of the Ouachita orogen east of the Fort Worth basin may have been impacted by accretion of the Sabine terrane (Fig. 1), the extent of which is better defined south of the Ouachita orogen in Arkansas and Louisiana (Keller et al., 1989; Mickus and Keller, 1992); however, no definitive data are available for the location of the leading edge of the Sabine terrane in east Texas.

The timing of the end of Ouachita thrusting in the accretionary prism is well constrained in the subsurface, where an angular unconformity (Fig. 3) separates deformed "Ouachita facies" rocks as young as early Middle Pennsylvanian (Atokan) from overlying undeformed shallow-marine successor-basin strata of late Middle Pennsylvanian (Desmoinesian) to Middle Permian (Guadalupian) age (Nicholas and Waddell, 1989). In the foreland, rocks as young as middle Desmoinesian (Thurman Sandstone; Fig. 2, box C1) are involved in folds that parallel the Ouachita thrust front (Denison, 1989). These observations bracket the age of the end of Ouachita deformation at approximately 310 Ma (end Atokan) in the interior structures and the end of contraction on the frontal faults at approximately 309 Ma (middle Desmoinesian) in the foreland.

SAMPLES FOR DETRITAL-ZIRCON ANALYSES

Detrital zircons from three samples of Upper Mississippian to Middle Pennsylvanian sandstones in the distal northern fringe of the Arkoma basin were analyzed for U-Pb ages and Hf isotopic compositions (Figs. 1B, 2, and 5; Tables 1 and 2; Supplemental Tables S1[1] and S2[2]). In addition, previously published U-Pb analyses from two other sandstones in the distal Arkoma basin (Xie et al.,

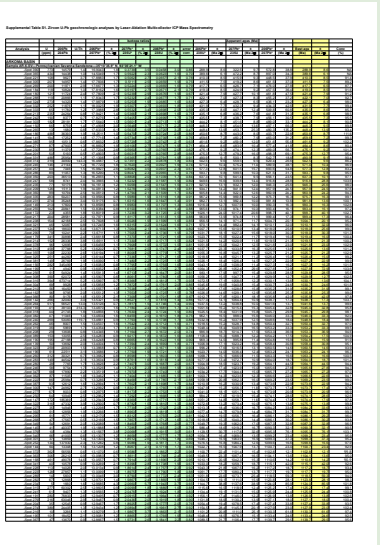

[1]Supplemental Material. Table S1. Zircon U-Pb geochronologic analyses. Please visit https://doi.org/10.1130/GEOS.S.14049965 to access the supplemental material, and contact editing@geosociety.org with any questions.

[2]Supplemental Material. Table S2. Hf isotopic data. Please visit https://doi.org/10.1130/GEOS.S.14049980 to access the supplemental material, and contact editing@geosociety.org with any questions.

TABLE 1. LIST OF SAMPLES WITH DEPOSITIONAL AGES AND ENVIRONMENTS

Sample	Stratigraphic unit	Approximate depositional age* (Ma)	Depositional environment	Reference
Arkoma basin				
AR-6-SV	Savanna Sandstone	309	Fluvial-deltaic	Sutherland (1988)
AR-2-HC	Cane Hill Member of the Hale Formation	322	Fluvial-deltaic	Sutherland (1988)
AR-1-BV	Batesville Sandstone	330	Shallow marine	Sutherland (1988)
Fort Worth basin				
TX-5-CC	Cisco Group, above Camp Colorado Limestone	298	Fluvial-deltaic	Brown et al. (1973)
TX-2-PB	Cisco Group, above Bunger Limestone	302	Fluvial-deltaic	Brown et al. (1973)
Anadarko basin				
OK-9-RS2	Rush Springs Sandstone	265	Eolian	Johnson et al. (1988)
OK-5-GB2	Garber Sandstone	281	Fluvial-deltaic	Johnson et al. (1988)
OK-4-WL	Wellington Formation	282	Fluvial-deltaic	Johnson et al. (1988)

*Approximate depositional age extrapolated by correlation to *International Chronostratigraphic Chart*, version 2019/05 (Cohen et al., 2013, updated).

TABLE 2. SUMMARY OF εHf_t VALUES FOR U-Pb AGE GROUPS

Sampled unit	Sample number	εHf_t values for U-Pb zircon age groups			
		334–295 Ma	499–335 Ma	898–500 Ma	1276–914 Ma
Arkoma basin					
Savanna	AR-6-SV		+8.3 to –15.6	–2.0 to –10.0	+7.5 to –0.7
Cane Hill	AR-2-HC		+10.0 to –19.2	+6.4 to –10.1	+11.2 to –5.0
Batesville	AR-1-BV		+6.1 to –30.5	+7.2 to –4.4	+7.3 to –3.9
Fort Worth basin					
Camp Colorado	TX-5-CC		+4.2 to 0	+9.0 to –14.4	+13.7 to –15.3
Bunger	TX-2-PB		–1.7 to –7.1	+9.1 to –31.7	+7.9 to –16.4
Anadarko basin					
Whitehorse	KS-5-WH	+4.8 to –5.8	+11.4 to –15.4	+7.1 to –10.6	+13.7 to –4.0
Rush Springs	OK-9-RS2	+0.3 to –1.8	+6.2 to –8.1	+6.3 to –5.7	+7.3 to –2.0
Garber	OK-5-GB2		+6.5 to –13.4	+4.2 to –8.5	+9.6 to –3.5
Wellington	OK-4-WL	+1.1	+6.6 to –10.8	+6.5 to –32.2	+12.1 to –6.4
Total range		+4.8 to –5.8	+11.4 to –30.5	+9.1 to –32.2	+13.7 to –16.4

2016, 2018a) are discussed here for comparison with the new data (Figs. 1B, 2, and 5). Previously published U-Pb analyses from the Mississippian–Pennsylvanian Stanley Shale (McGuire, 2017) and from the Pennsylvanian Atoka Formation (Sharrah, 2006) characterize the more proximal basin in the Ouachita thrust belt (Figs. 1B, 2, and 5). Published U-Pb data from tuff beds (Shaulis et al., 2012) in the Mississippian–Pennsylvanian Stanley Shale in the western part of the proximal Arkoma basin in the Ouachita thrust belt provide a summary of ages of volcanism, as well as possible xenocrysts from basement rocks of the Sabine terrane (Figs. 5 and 6).

New analyses for U-Pb ages and Hf isotopic compositions of two samples from Upper Pennsylvanian and Lower Permian sandstones characterize the upper part of the late synorogenic to early postorogenic fill of the Fort Worth basin (Figs. 1B, 2, and 5; Tables 1 and 2; Supplemental Tables S1 and S2). Previously published U-Pb data from Middle to Upper Pennsylvanian sandstones in the Fort Worth basin (Alsalem et al., 2018) are discussed here for comparison (Figs. 1B and 5). The early, proximal deposits in the Fort Worth basin are now deep in the subsurface beneath the thrust belt, and the available samples are from the stratigraphically higher, deltaic to shallow-marine deposits on the distal shelf (Fig. 2C).

Analyses for U-Pb ages and Hf isotopic compositions of three samples (one previously published; Thomas et al., 2016) from the southern part of the intracratonic Anadarko basin (Figs. 1B and 5; Tables 1 and 2; Supplemental Tables S1 and S2) represent the sedimentary cover over the Wichita and Arbuckle uplifts, in contrast to the conglomerates that rest unconformably on the Precambrian–Cambrian crystalline rocks in the uplifts (Thomas et al., 2016). Published U-Pb and Hf data from a Permian sandstone (Thomas et al., 2020) on the divide between the Anadarko basin and the intracratonic Forest City basin on the north (Figs. 1 and 5B) provide a test of regional dispersal systems. Published U-Pb data from the Permian basin (Soreghan and Soreghan, 2013; Xie et al., 2018b; Liu and Stockli, 2019) provide comparison with a more distant intracratonic basin (Figs. 1A and 5B).

ANALYTICAL METHODS

Sample Collection and Processing

Each detrital-zircon sample, consisting of approximately 12 kg of medium- to coarse-grained sandstone, was collected from a restricted stratigraphic interval of a few successive beds and then was processed utilizing methods outlined by Gehrels (2000), Gehrels et al. (2008), Gehrels and Pecha (2014), and Thomas et al. (2017). Zircon grains were extracted using traditional methods of jaw crushing and pulverizing, followed by density separation using a Wilfley table. The resulting heavy-mineral fraction was further purified using a Frantz LB-1 magnetic barrier separator and heavy liquids. A representative split of the zircon yield was incorporated into a 2.54 mm epoxy mount along with multiple fragments of the U-Pb primary standards Sri Lanka SL-F, FC-1, and R33, and Hf standards R33, Mud Tank, FC-1, Plesovice, Temora, and 91500. The mounts were sanded down ~20 µm, polished to 1 µm, and imaged by backscattered electron (BSE) and cathodoluminescence (CL) imaging techniques using a Hitachi 3400N scanning electron microscope (SEM) and a Gatan Chroma CL2 detector system at the Arizona LaserChron SEM Facility (www.laserchron.org). Prior to isotopic analysis, mounts were cleaned in an ultrasonic bath of 1% HNO_3 and 1% HCl in order to remove contaminants and surficial common Pb.

U-Pb Geochronologic Analysis

Uranium-lead (U-Pb) geochronologic analyses of individual zircon crystals were conducted by laser ablation–inductively coupled plasma–mass spectrometry (LA-ICP-MS) at the Arizona LaserChron Center (www.laserchron.org). The isotopic analyses involved ablation of zircon using a Photon Machines Analyte G2 excimer laser coupled to either a Thermo Element2 single-collector ICP-MS or a Nu Instruments multicollector ICP-MS. Ultrapure helium carried the ablated material from the HelEx cell into the plasma source of each ICP-MS instrument.

Analyses conducted with the Nu ICP-MS utilized Faraday collectors for measurement of ^{238}U and ^{232}Th, either Faraday collectors or ion counters for ^{208}Pb, ^{207}Pb, and ^{206}Pb, and ion counters for ^{204}(Pb, Hg) and ^{202}Hg (see Supplemental Table S1 for specific methods used for each sample), depending on grain size. For larger grains, a 30-µm-diameter spot was used, and masses 206, 207, 208, 232, and 238 were measured with Faraday detectors, whereas the smaller 202 and 204 ion beams were measured with ion counters. The acquisition routine included a 15 s integration on peaks with the laser off (for backgrounds), fifteen 1 s integrations with the laser firing, and a 30 s delay to ensure that the previous sample was completely purged from the system. Smaller grains were analyzed with all Pb isotopes in ion counters, using a 20 µm beam diameter, and consisted of a 12 s integration on peaks with the laser off (for backgrounds), twelve 1 s integrations with the laser firing, and a 30 s delay to purge the previous sample.

Analyses conducted with the Element2 ICP-MS utilized a single scanning electron multiplier that sequenced rapidly through U, Th, Pb, and Hg isotopes. Ion intensities were measured in pulse-counting mode for signals less than 50,000 cps, in both pulse-counting and analog mode for signals between 50,000 and 5,000,000 cps, and in analog mode above 5,000,000 cps. The calibration between pulse-counting and analog signals was determined line-by-line for signals between 50,000 and 5,000,000 cps and was applied to signals >5,000,000 cps. Four intensities were determined and averaged for each isotope, with dwell times of 0.0052 s for 202, 0.0075 s for 204, 0.0202 s for 206, 0.0284 s for 207, 0.0026 s for 208, 0.0026 s for 232, and 0.0104 s for 238. With the laser set at an energy density of ~5 J/cm^2, a repetition rate of 8 Hz, and an ablation time of 10 s, ablation pits were ~12 µm in depth. Sensitivity with these settings was ~5000 cps/ppm. Each analysis consisted of 5 s on peaks with the laser off (for backgrounds), 10 s with the laser firing (for peak intensities), and a 20 s delay to purge the previous sample and save files.

Analyses were conducted with one U-Th-Pb measurement per grain (numbers of grains per sample varied and are reported in Supplemental

Table S1). Grains were selected in random fashion; crystals were rejected only if they contained cracks or inclusions or were too small to be analyzed. The use of high-resolution BSE and CL images provided assistance in grain selection and spot placement.

Data reduction was accomplished using AgeCalc (a Microsoft Excel macro), which is the standard Arizona LaserChron Center reduction protocol (Gehrels et al., 2008; Gehrels and Pecha, 2014). Data were filtered for discordance, $^{206}Pb/^{238}U$ precision, and $^{206}Pb/^{207}Pb$ precision as indicated in the notes in Supplemental Table S1. Data are presented on normalized age-probability diagrams, which sum all relevant analyses and uncertainties and divide each curve by the number of analyses such that all curves contain the same area. Age groups are characterized by the ages of modes in age probability and by the range of constituent ages (Fig. 6; Table 3).

Age-probability diagrams were quantitatively compared using multidimensional scaling (MDS; Vermeesch, 2013). MDS facilitates the comparison of detrital age distributions by converting sample dissimilarity into a Cartesian plot where distance is a proxy for dissimilarity (i.e., more dissimilar age-probability diagrams plot farther apart, and similar age-probability diagrams cluster together). Mismatch (Amidon et al., 2005) was used to calculate dissimilarity, and the program DZmds (Saylor et al., 2018) was used to produce MDS plots. Transformation to Cartesian distance was calculated using metric squared stress.

Hf Isotopic Analysis

Hafnium (Hf) isotopic analyses were conducted utilizing the Nu multicollector LA-ICP-MS system at the Arizona LaserChron Center following methods reported by Cecil et al. (2011) and Gehrels and Pecha (2014). An average of 56 Hf analyses was conducted for each sample. Grains were selected to represent each of the main age groups and to avoid crystals with discordant or imprecise ages. CL images were utilized to ensure that all Hf analyses

TABLE 3. AGE GROUPS OF DETRITAL ZIRCONS FROM MISSISSIPPIAN–PERMIAN SANDSTONES IN THE ARKOMA, FORT WORTH, AND ANADARKO BASINS; CHARACTERISTICS OF POSSIBLE APPALACHIAN (LAURENTIAN) OR OUACHITA-MARATHON (GONDWANAN) PROVENANCE*

Age group (Ma)	Appalachian provenance	Ouachita-Marathon provenance
334–295	**Primary:** synorogenic Alleghanian plutons. **Dispersal:** very rare (7 grains of 3564) in synorogenic Alleghanian clastic wedges.	**Primary:** synorogenic magmatic arc rocks in Coahuila and Sabine Gondwanan accreted terranes. **Dispersal:** in Marathon clastic wedge.
499–335	**Primary:** synorogenic Taconic and Acadian plutons. **Recycled:** from Acadian synorogenic clastic wedge. **Dispersal:** abundant in Alleghanian clastic wedges.	**Primary and/or recycled:** early and middle Paleozoic synorogenic plutons and detrital zircons in Coahuila, Maya, and Sierra Madre accreted terranes. **Dispersal:** abundant in Marathon clastic wedge.
901–500	**Primary:** Pan-African/Brasiliano basement rocks in Gondwanan accreted terranes. **Dispersal:** rare in Alleghanian clastic wedges.	**Primary:** Pan-African/Brasiliano basement rocks in Gondwanan accreted terranes. **Dispersal:** generally abundant in Marathon clastic wedge.
1276–914	**Primary:** Grenville rocks in external and internal Appalachian basement massifs. **Recycled:** post-Grenville synrift, passive-margin, and synorogenic clastic rocks. **Dispersal:** abundant in Alleghanian clastic wedges.	**Primary:** Sunsás basement rocks in Gondwanan accreted terranes. **Dispersal:** abundant in Marathon clastic wedge.
1963–1202	**Primary:** scattered enclaves of older rocks within Grenville-age rocks in basement massifs. **Recycled:** synrift and passive-margin deposits, originally supplied to the Laurentian rifted margin and passive-margin shelf from the Penokean–Trans-Hudson, Central Plains–Yavapai–Mazatzal, and Granite-Rhyolite provinces of the Laurentian craton. **Dispersal:** common in Alleghanian clastic wedges.	**Primary:** Ventuari-Tapajós, Rio Negro–Juruena, and Rondonia–San Ignacio provinces of Gondwanan Coahuila accreted terrane. **Recycled:** passive-margin deposits along the Laurentian rifted margin, especially slope deposits from Granite-Rhyolite rocks at the Alabama-Oklahoma transform margin. **Dispersal:** common in Marathon clastic wedge.
2224–1945	**Primary:** Trans-Amazonian/Eburnian basement rocks in Gondwanan accreted terranes. **Dispersal:** rare in Alleghanian clastic wedges.	**Primary:** Maroni-Itacaiúnas and Trans-Amazonian/Eburnian provinces of Gondwanan Coahuila accreted terrane. **Dispersal:** minor in Marathon clastic wedge.
3036–2387	**Recycled:** synrift and passive-margin detritus from the Superior province of the Canadian Shield. **Dispersal:** minor to rare in Alleghanian clastic wedges.	**Primary and/or recycled:** Central Amazonian province of Gondwanan accreted terranes. **Dispersal:** minor in Marathon clastic wedge.

*Compiled from summary and references cited in Thomas et al. (2017, 2019).

were within the same growth domain as the U-Pb pit, although in most analyses, Hf laser pits were located directly on top of the U-Pb analysis pits. Complete Hf isotopic data and Hf evolution plots of individual samples are presented in Supplemental Table S2.

Hafnium data are presented using Hf evolution diagrams, where initial $^{176}Hf/^{177}Hf$ ratios are expressed in εHf_t notation, which represents the Hf isotopic composition at the time of zircon crystallization relative to the chondritic uniform reservoir (CHUR) (Bouvier et al., 2008). Internal precision for $^{176}Hf/^{177}Hf$ and εHf_t is reported for each analysis on Hf evolution plots in Supplemental Table S2 and as the average for all analyses (2.2 epsilon units at 2σ) on εHf_t evolution diagrams. On the basis of the in-run analysis of zircon standards, the external precision was 2–2.5 epsilon units (2σ). Hf isotopic evolution of typical continental crust is shown with arrows on εHf_t evolution diagrams, which are based on a $^{176}Lu/^{177}Hf$ ratio of 0.0115 (Vervoort and Patchett, 1996; Vervoort et al., 1999).

Our Hf isotope data were interpreted within the standard framework of juvenile (positive) values indicating magma consisting mainly of material extracted from the mantle during or immediately prior to magmatism versus more evolved (negative) values recording incorporation of significantly older crust. Vertical arrays on εHf_t diagrams are interpreted to represent magmas that contain both materials derived from the mantle during (or immediately prior to) magmatism and significantly older crustal materials.

Hf isotope data are plotted as bivariate kernel density estimates (KDEs) using HafniumPlotter (Sundell et al., 2019; github.com/kurtsundell/HafniumPlotter). Bivariate KDEs facilitate comparison of two-dimensional (2-D, U-Pb–Hf) data by converting sample density into a color-coded intensity plot, where higher intensity corresponds to higher data density. Density estimation uses a diagonal kernel bandwidth matrix and generates bivariate KDEs by (1) applying a discrete cosine transform to the 2-D data, (2) multiplying the resulting 2-D matrix of points by a Gaussian function generated on the basis of set kernel bandwidths (25 m.y. for U-Pb age and 2 epsilon units for εHf_t), (3) performing an inverse discrete cosine transform of the Gaussian-scaled matrix, and (4) normalizing the three-dimensional (3-D) bivariate KDE volume sum to 1. The bivariate KDE 3-D surface is color-coded to intensity based on *z*-axis height and viewed parallel to the *z* axis to visualize density in 2-D. Results are clipped at the 95% confidence level from relative peak data density.

DETRTIAL-ZIRCON DATA FROM ARKOMA BASIN

Results of U-Pb Analyses

Batesville Sandstone (Sample AR-1-BV)

The stratigraphically lowest sample was collected from the Batesville Sandstone, which is one of two quartzose sandstones within the lower Upper Mississippian succession of shallow-marine sandstones, limestones, and shales in the northern fringe of the Arkoma basin (Figs. 1B, 2, and 5A). The most dominant group of detrital-zircon ages is between 488 and 339 Ma with a dominant mode of 434 Ma (Fig. 7). Another prominent group with ages of 1210–942 Ma has subequal modes of 1161 and 1042 Ma. Secondary modes of 1898, 1788, 1650, 1479, and 1397 Ma are broadly spaced through a distribution from 1907 to 1210 Ma (Fig. 7). A few grains have ages of 2176–1996 and of 762–502 Ma. A subordinate age group of 2909–2634 Ma has a mode of 2723 Ma (Fig. 7).

Cane Hill Member of the Hale Formation (Sample AR-2-HC)

A deltaic to shallow-marine sandstone at the base of the Cane Hill Member of the Lower Pennsylvanian Hale Formation (Sutherland, 1988) overlies truncated Mississippian strata at a regional unconformity in the distal northern part of the Arkoma basin (Figs. 1B, 2, and 5A). The dominant age group of detrital zircons between 1265 and 935 Ma has a mode of 1045 Ma with a secondary shoulder of 1131 Ma (Fig. 7). Another prominent group has ages of 487–380 Ma and subequal modes of 458 and 433 Ma. A group with ages between 1935 and 1295 Ma has a strong mode of 1618 Ma and secondary modes of 1821, 1505, and 1339 Ma (Fig. 7). Five grains have ages between 682 and 532 Ma, and one grain has an age of 2041 Ma. A secondary age group between 2957 and 2550 Ma has a lesser mode of 2820 Ma (Fig. 7).

Savanna Sandstone (Sample AR-6-SV)

The upper Middle Pennsylvanian (lower Desmoinesian) Savanna Sandstone is within a succession of southward prograding fluvial-deltaic systems (Sutherland, 1988) in the distal northern part of the Arkoma basin (Figs. 1B, 2, and 5A); in contrast, the stratigraphically higher middle Desmoinesian Thurman Sandstone (Fig. 2, box C1) contains chert clasts transported northwestward from the Ouachita thrust belt (Sutherland, 1988). A sample from the stratigraphically highest sandstone preserved in the Savanna Sandstone has a dominant detrital-zircon age group between 1208 and 946 Ma with a primary mode of 1055 Ma and a secondary mode of 1183 Ma (Fig. 7). Another important group with ages of 491–390 Ma has a mode of 420 Ma. The youngest grain in the sample is 390 Ma; however, one grain (289 Ma) was omitted from the plot because it is younger than the depositional age. A secondary age group between 1847 and 1606 Ma has modes of 1798, 1742, and 1629 Ma (Fig. 7). A lesser group of ages between 1549 and 1224 Ma has minor modes of 1455, 1334, and 1229 Ma (Fig. 7). A minor age group between 637 and 543 Ma has a mode of 589 Ma, and three grains are scattered between 2098 and 1950 Ma. Ages scattered between 2916 and 2503 Ma have minor modes of 2723 and 2569 Ma (Fig. 7).

Results of Hf Isotopic Analyses

Hf isotopic data are similar through the set of three samples (AR-1-BV, AR-2-HC, and AR-6-SV) from the Arkoma basin (Fig. 7; Table 2). Zircon grains in the age range 1265–935 Ma have εHf_t

values ranging from +11.2 to –5.0, but most values are concentrated between +6.2 and –1.0 (Fig. 7). Zircon grains in the age range of 762–502 Ma have εHf_t values between +7.2 and –10.1. Although zircon grains with ages of 488–390 Ma have εHf_t values spread between +10.0 and –30.5, most are tightly clustered between +6.0 and –11.2 (Fig. 7). The range of εHf_t values indicates mixing of magma sources, including evolved crust and juvenile magmas.

Summary of Previously Published U-Pb Age Data

Hot Springs Sandstone Member of the Stanley Shale (McGuire, 2017)

The Mississippian Hot Springs Sandstone Member in the lowermost part of the Stanley Shale in the more proximal part of the Arkoma basin and now in the Ouachita thrust belt (Figs. 1B, 2, and 5A) has been interpreted to be a marginal turbidite fan from the northern (cratonic) margin of the Ouachita foredeep (Morris, 1989). Previously reported results of U-Pb analyses (McGuire, 2017) of a sample from the Hot Springs Sandstone Member include a dominant age group between 1195 and 994 Ma with a dominant mode of 1050 Ma (Fig. 7). A prominent secondary group with ages of 484–373 Ma has a mode of 420 Ma. A lesser group with ages between 1809 and 1231 Ma has a minor mode of 1457 Ma (Fig. 7). Two grains have ages of 767 and 551 Ma, and two grains have ages of 2287 and 2263 Ma. Three older grains have ages of 2739–2704 Ma.

Wedington Sandstone Member of the Fayetteville Shale (Xie et al., 2016)

Previously published results (Xie et al., 2016) of U-Pb analyses of six samples from southward prograding deltaic deposits of the Upper Mississippian Wedington Sandstone in the distal northern part of the Arkoma basin (Figs. 1B, 2, and 5A) are similar through the sample set and are summarized here in a composite plot (Fig. 7). A strongly dominant group of ages between 1209 and 937 Ma

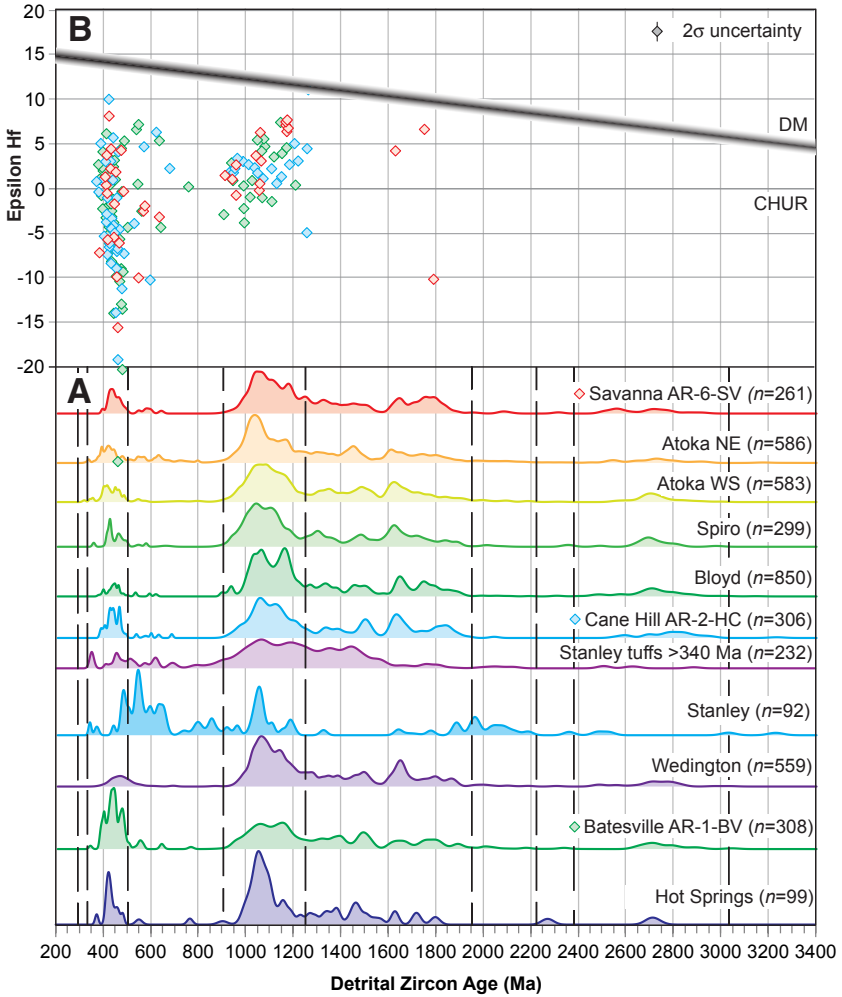

Figure 7. U-Pb age-probability density plots (A) and Hf-evolution diagram (B) showing results from analyses of Mississippian–Pennsylvanian sandstones in the Arkoma basin. (A) U-Pb age-probability density plots for three analyzed samples (data in Supplemental Table S1 [see text footnote 1]) and from published data as follows: Wedington (Xie et al., 2016); Hot Springs and Stanley (McGuire, 2017); Stanley tuffs (Shaulis et al., 2012); Bloyd (Xie et al., 2018a); Spiro, Atoka WS—westward and southward dispersal, and Atoka NE—northeastward dispersal (Sharrah, 2006). Vertical, dashed, black lines mark boundaries of detrital-zircon age groups (Fig. 6; Table 3). (B) εHf_t data for three samples (data in Supplemental Table S2 [see text footnote 2]). Data points are color coded as in panel A. The average uncertainty of Hf isotopic analyses is 2.6 epsilon units at 2σ. The Hf-evolution diagram shows the Hf isotopic composition at the time of zircon crystallization, in epsilon units, relative to the chondritic uniform reservoir (CHUR) (Bouvier et al., 2008) and to the depleted mantle (DM) (Vervoort et al., 1999).

has a primary mode 1051 Ma with a secondary shoulder of 1120 Ma (Fig. 7). The most prominent secondary group with ages of 496–388 Ma has a mode of 471 Ma. A spread of relatively abundant grains between 1883 and 1215 Ma has secondary modes of 1873, 1802, 1637, and 1480 Ma (Fig. 7). Minor numbers of grains are scattered between 2186 and 1945 Ma and between 687 and 501 Ma. Another minor group of ages extends from 3036 to 2466 Ma.

Sandstone in the Stanley Shale (McGuire, 2017)

A sample of a sandstone in the upper part of the succession of mud-dominated turbidites in the Mississippian–Pennsylvanian Stanley Shale in the more proximal part of the Arkoma basin, which is now in the Ouachita southern thrust belt (Figs. 1B, 2, and 5A), was analyzed for U-Pb ages of detrital zircons (McGuire, 2017), and the results are shown in Figure 7. The most dominant group with ages of 874–501 Ma has a dominant mode of 547 Ma and secondary modes of 856 and 622 Ma; this dominant age group contrasts notably with other samples from the Arkoma basin (Fig. 7). Another important group with ages of 1197–1018 Ma has a mode of 1054 Ma. Twelve grains are scattered between 2185 and 1953 Ma and define minor modes of 2053 and 1969 Ma. Another secondary group has ages of 1885–1637 Ma (Fig. 7). The sample has only one grain (1322 Ma) with an age between 1637 and 1197 Ma, an age interval that is well represented in the other samples from the Arkoma basin. A secondary age group between 486 and 336 Ma has a mode of 482 Ma. A few older grains have ages scattered between 3228 and 2358 Ma.

Tuff Beds in the Stanley Shale (Shaulis et al., 2012)

Published U-Pb data from five tuff beds (Shaulis et al., 2012) in the Mississippian–Pennsylvanian Stanley Shale in the western part of the proximal Arkoma basin in the Ouachita thrust belt (Fig. 6) are dominated by grains with ages of the volcanism (328.5 ± 2.7 to 320.7 ± 2.5 Ma). In addition, the samples include a range of older grains (Figs. 6 and 7) that have been interpreted as detrital (Shaulis et al., 2012), but the depositional setting of the ash-flow or ash-fall tuffs (Niem, 1977) within a succession of deep-water muddy turbidites suggests that the zircons may be xenocrysts from the magma source in the Sabine terrane. A plot of the ages of prevolcanic zircons (Figs. 6 and 7) is included here to evaluate the possible xenocrystic grains by comparison with detrital-zircon age distributions and to illustrate the composition of the possible Sabine magma chamber as a component of the provenance for synorogenic clastic sediment. The dominant zircon age group of 1276–928 Ma has modes of 1177 and 1068 Ma, and a strong secondary age group extends between 1577 and 1283 Ma with modes of 1440 and 1353 Ma (Figs. 6 and 7). A secondary age group of 787–506 Ma has a mode of 613 Ma, and three grains are scattered between 2129 and 1997 Ma. Another secondary group with ages of 483–409 Ma has a mode of 451 Ma, but the age-probability plot of the young boundary of that distribution is obscured by the strongly dominant mode of the volcanic crystallization ages (Fig. 6). A few older grains have ages between 2889 and 2503 Ma.

Middle Sandstone Unit in the Bloyd Formation (Xie et al., 2018a)

Previously published results (Xie et al., 2018a) of U-Pb analyses of eight samples from the middle sandstone unit in the Lower Pennsylvanian (upper Morrowan) Bloyd Formation in the distal northern part of the Arkoma basin (Figs. 1B, 2, and 5A) are summarized here in a composite plot (Fig. 7). The dominant detrital-zircon age group of 1200–972 Ma is bimodal with modes of 1165 and 1052 Ma (Fig. 7). A group of ages spread between 1923 and 1202 Ma has a secondary mode of 1635 Ma (Fig. 7). Another secondary age group of 495–374 Ma has a mode of 434 Ma. Seven grains have ages between 618 and 528 Ma, and six grains have ages between 2190 and 1979 Ma. A secondary age group between 3146 and 2636 Ma has a mode of 2713 Ma (Fig. 7).

Spiro Sandstone in Lower Atoka Formation (Sharrah, 2006)

The Spiro and related sandstones in the lower Atoka Formation (Figs. 1B, 2, and 5A) include southward trending channel sands that grade southward into deltaic facies and marine-reworked facies along the northern (cratonic) side of the Ouachita foredeep (Sutherland, *in* Johnson et al., 1988). A composite plot (Fig. 7) of two samples ($N = 2$, $n = 299$) of Spiro sandstone (Sharrah, 2006) shows a dominant age group between 1203 and 933 Ma with a prominent mode of 1026 Ma and a minor shoulder mode of 1082 Ma (Fig. 7). A secondary group with ages of 492–353 Ma has a mode of 418 Ma. The youngest grain in the two samples is 353 Ma; however, one grain with an age of 295 Ma was omitted from the age-probability plot because it is younger than the depositional age of the sandstone. A scatter of ages between 1894 and 1221 Ma has a strong secondary mode of 1609 Ma and a minor mode of 1308 Ma. Three grains have ages of 656–541 Ma, and three ages are scattered between 2060 and 1956 Ma (Fig. 7). Older grains between 2978 and 2342 Ma have a minor mode of 2699 Ma.

Sandstones with Westward and Southward Dispersal in the Atoka Formation (Sharrah, 2006)

Sandstones in a thick succession of turbidites in the Atoka Formation (Figs. 1B, 2, and 5A) with paleocurrent indicators of westward and southward sediment dispersal are now mostly in the more easterly part of the frontal Ouachita thrust belt in Arkansas but extend farther west (Sharrah, 2006). A composite plot (Fig. 7) of data from four samples ($N = 4$, $n = 583$) has a dominant group of detrital-zircon ages of 1205–934 Ma and two prominent modes of 1062 and 1031 Ma (Fig. 7). A secondary age group of 481–336 Ma has modes of 441 and 412 Ma. The single youngest grain in the four samples is 313 Ma; however, three grains with ages (309–248 Ma) that are younger than the depositional age of the sandstone were omitted from the age-probability plot. A scatter of ages between 1935 and 1214 Ma has a secondary mode of 1607 Ma.

Nine grains have ages scattered between 799 and 534 Ma, and 10 ages are scattered between 2197 and 1968 Ma (Fig. 7). Older grains between 2999 and 2546 Ma have a minor mode of 2711 Ma.

Sandstones with Northeastward Dispersal in the Atoka Formation (Sharrah, 2006)

Sandstones in a thick succession of turbidites in the Atoka Formation (Figs. 1B, 2, and 5A) with paleocurrent indicators of northeastward sediment dispersal are now in the more westerly part of the frontal Ouachita thrust belt in Oklahoma (Sharrah, 2006). A composite plot of data from four samples ($N = 4$, $n = 586$) has a dominant age group of 1195–937 Ma with a prominent mode of 1040 Ma (Fig. 7). A secondary group with ages of 492–354 Ma has modes of 408 and 384 Ma. A minor but distinct younger group has two grains with ages of 331–327 Ma, but two other grains with ages of 295 and 293 Ma were omitted from the age-probability plot because they are younger than the depositional age. A scatter of ages between 1947 and 1210 Ma has secondary modes of 1613 and 1455 Ma. An important group of 34 grains has ages between 799 and 505 Ma with a minor mode of 632 Ma, and 15 ages are scattered between 2218 and 1962 Ma (Fig. 7). Older grains between 2932 and 2523 Ma have a minor mode of 2735 Ma.

DETRITAL-ZIRCON DATA FROM FORT WORTH BASIN

Results of U-Pb Analyses

Sandstone above the Bunger Limestone, Cisco Group (Sample TX-2-PB)

The Pennsylvanian–Permian Cisco Group includes numerous cyclic westward prograding fluvial-deltaic systems and transgressive shallow-marine limestones in the distal shelf of the Fort Worth basin (Brown et al., 1973). A sample was collected from a road-cut exposure of the sandstone above the Bunger Limestone in the Upper Pennsylvanian (Virgilian) Cisco Group (Figs. 1B, 2, and 5A). The sandstone includes beds of conglomerate with subrounded clasts of white to light-gray chert as much as 4 cm in diameter in channel-fill deposits (Brown et al., 1973). The sample has two dominant age groups of detrital zircons: one between 898 and 501 Ma with modes of 644 and 532 Ma, and the other between 1255 and 919 Ma with two modes of 1051 and 1009 Ma and a secondary shoulder mode of 1161 Ma (Fig. 8). Another prominent group has ages of 491–339 Ma and modes of 421 and 344 Ma (Fig. 8); three grains with ages of 334–325 Ma document a distinctively young age range. A group of detrital-zircon ages extends from 1963 to 1280 Ma and has a prominent mode of 1466 Ma along with several minor modes (Fig. 8). A group of ages between 2121 and 1981 Ma has modes of 2073 and 1984 Ma. An older minor group with ages of 2856–2519 Ma has a minor mode of 2712 Ma.

Sandstone above Camp Colorado Limestone, Cisco Group (Sample TX-5-CC)

A sample of the sandstone stratigraphically above the Camp Colorado Limestone (Figs. 1B, 2, and 5A) is from part of the cyclic succession of westward prograding fluvial-deltaic sandstones and transgressive limestones in the Lower Permian part of the Cisco Group (Brown et al., 1973). The most prominent group of detrital-zircon ages is between 861 and 511 Ma and has modes of 731, 657, 588, and 531 Ma (Fig. 8). The second most prominent group has ages of 1256–935 Ma and modes of 1213 and 1034 Ma. Notably, the mode of 588 Ma exceeds the Mesoproterozoic-age modes in this sample (Fig. 8). Another prominent group has ages of 498–362 Ma and a mode of 419 Ma. The youngest grain in the sample has an age of 327 Ma; however, one grain with an age of 274 Ma was omitted from the age-probability plot because it is younger than the depositional age of the sandstone. A group with detrital-zircon ages of 1959–1279 Ma has modes of 1668 and 1503 Ma. A secondary group with ages of 2224–1997 Ma has a mode of 2092 Ma. A minor age group of 2859–2395 Ma has a mode of 2750 Ma.

Results of Hf Isotopic Analyses

Hf isotopic data from the Fort Worth basin are generally similar in the two samples TX-5-CC and TX-2-PB (Fig. 8; Table 2). The older Precambrian grains generally conform to crustal evolution trends with some exceptions toward more positive εHf_t values (Fig. 8). Zircon grains with ages of 1252–969 Ma have εHf_t values between +13.7 and –16.4 (Fig. 8). Zircon grains in the age range of 871–524 Ma have εHf_t values between +9.1 and –31.7, although grains with ages older than 600 Ma are mostly between +9.0 and –4.9, whereas those with ages younger than 600 Ma are mostly between +4.9 and –5.6, indicating heterogeneous sources. Zircon grains in the age range of 474–348 Ma have εHf_t values tightly clustered between +4.2 and –7.1 (Fig. 8).

Summary of Previously Published U-Pb Age Data

Sample from Middle Pennsylvanian Big Saline Formation (Alsalem et al., 2018)

A sample of a sandstone in the Big Saline Formation (Figs. 1B, 2, and 5A) of the Bend Group is from the lower part of the Middle Pennsylvanian (Atokan) succession in the southwestern part of the Fort Worth basin (Alsalem et al., 2018). A group of ages between 1214 and 914 Ma has a dominant mode of 1029 Ma (Fig. 8). The sample includes two prominent secondary age groups: 795–514 Ma with modes of 616 and 538 Ma, and 498–354 Ma with a mode of 421 Ma (Fig. 8). Ages are scattered between 1885 and 1228 Ma with modes of 1728 and 1668 Ma. A minor age group of 2188–1952 Ma has a mode of 1976 Ma. A group of older grains ranges from 2801 to 2440 Ma and has a mode of 2687 Ma (Fig. 8).

Samples from Upper Middle to Lower Upper Pennsylvanian Formations (Alsalem et al., 2018)

Analytical data from five samples from multiple formations in the upper Middle (Desmoinesian) to

lower Upper Pennsylvanian (Missourian) succession are from closely spaced sites in a relatively small area in the northwestern part of the Fort Worth basin (Figs. 1B, 2, and 5A) and have very similar age distributions (Alsalem et al., 2018); the data from all five samples are shown in a composite plot (Fig. 8). The most prominent age group of 1237–920 Ma has a dominant mode of 1047 Ma (Fig. 8). Another age group, nearly as strong, of 828–500 Ma has modes of 616 and 548 Ma; a minor group with ages of 2188–1981 Ma has a mode of 2066 Ma. A secondary group has ages of 499–335 Ma; a younger group of three grains has ages of 329–318 Ma. Ages are scattered between 1913 and 1258 Ma with modes of 1745, 1637, 1509, and 1369 Ma. An older group between 2893 and 2460 Ma has a mode of 2706 Ma (Fig. 8).

DETRITAL-ZIRCON DATA FROM ANADARKO BASIN

Results of U-Pb Analyses

Wellington Formation (Sample OK-4-WL)

The Lower Permian Wellington Formation (Figs. 1B and 5A) is the lowermost part of a widespread succession of alluvial to deltaic red sandstones and mudstones covering the proximal conglomerates and angular unconformity over the Arbuckle and Wichita uplifts at the southern margin of the Anadarko basin (Johnson et al., 1988). Detrital-zircon grains of the Wellington Formation (previously reported; Thomas et al., 2016) have three dominant age groups: 1210–924 Ma with modes of 1145 and 1032 Ma, 857–504 Ma with a mode of 558 Ma, and 499–339 Ma with a mode of 435 Ma (Fig. 9). Two grains have distinctively young ages of 334–329 Ma. A secondary group with ages of 2156–1960 Ma has a secondary mode of 1976 Ma (Fig. 9). Age groups of 1922–1602 Ma and 1532–1223 Ma have multiple secondary modes of 1852, 1744, and 1648 Ma and of 1453, 1326, and 1253 Ma, respectively (Fig. 9). An older secondary group has ages of 2905–2305 Ma and a secondary mode of 2721 Ma.

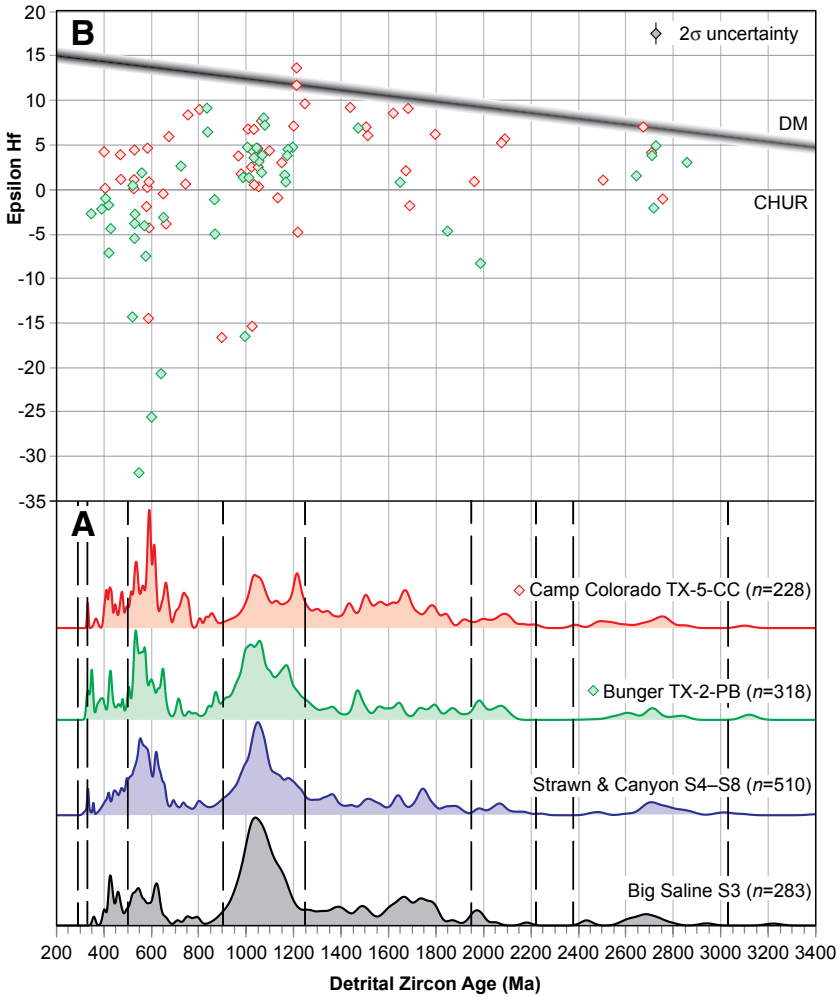

Figure 8. U-Pb age-probability density plots (A) and Hf-evolution diagram (B) showing results from analyses of Pennsylvanian–Permian sandstones in the Fort Worth basin. (A) U-Pb age-probability density plots for two analyzed samples (data in Supplemental Table S1 [see text footnote 1]) and from published data for Big Saline and composite Strawn–Canyon (Alsalem et al., 2018). Vertical, dashed, black lines mark boundaries of detrital-zircon age groups (Fig. 6; Table 3). (B) εHf_t data for two samples (data in Supplemental Table S2 [see text footnote 2]). Data points are color coded as in panel A. Specifications for the Hf-evolution diagram are described in the caption for Figure 7. CHUR—chondritic uniform reservoir; DM—depleted mantle.

Garber Sandstone (Sample OK-5-GB2)

A sample from a sandstone in the Lower Permian Garber Sandstone (Figs. 1B and 5A) is part of a succession of fluvial to deltaic red beds (Johnson et al., 1988). The sample has a dominant group with ages of 1228–932 Ma and a prominent mode of 1035 Ma and a lesser mode of 1141 Ma (Fig. 9). The sample includes three strong secondary age groups: 1794–1621 Ma with modes of 1745 and 1645 Ma; 1520–1240 Ma with modes of 1490, 1384, and 1347 Ma; and 499–354 Ma with modes of 454 and 415 Ma (Fig. 9). A lesser group has ages between 820 and 510 Ma and multiple minor modes; four grains are scattered between 2137 and 1976 Ma. A minor age group of 2992–2401 Ma has a minor mode of 2715 Ma (Fig. 9).

Rush Springs Sandstone (Sample OK-9-RS2)

A sample of the Middle Permian Rush Springs Sandstone (Figs. 1B and 5A) was collected from a southwest-directed eolian sandstone within an erg system (Poland and Simms, 2012). Two age groups of detrital zircons dominate the sample age distribution: ages of 1200–940 Ma with modes of 1138, 1070, and 1023 Ma; and ages of 496–337 Ma with modes of 420 and 343 Ma (Fig. 9). A distinctive younger group has ages of 327–295 Ma. The next most prominent group with ages of 897–502 Ma (mostly between 649 and 502 Ma) has modes of 630 and 590 Ma, and a secondary age group of 2182–1981 Ma has a minor mode of 2079 Ma (Fig. 9). Other strong secondary groups have ages of 1913–1626 Ma with modes of 1737 and 1637 Ma, and ages of 1524–1221 Ma with modes of 1490, 1377, and 1339 Ma. Older zircons with ages between 2925 and 2438 Ma have a minor mode of 2645 Ma (Fig. 9).

Results of Hf Isotopic Analyses

Hf isotopic data for older Precambrian grains in samples OK-4-WL, OK-5-GB2, and OK-9-RS2 generally conform to crustal evolution trends (Fig. 9). Zircon grains with ages of 1162–932 Ma have εHf_t

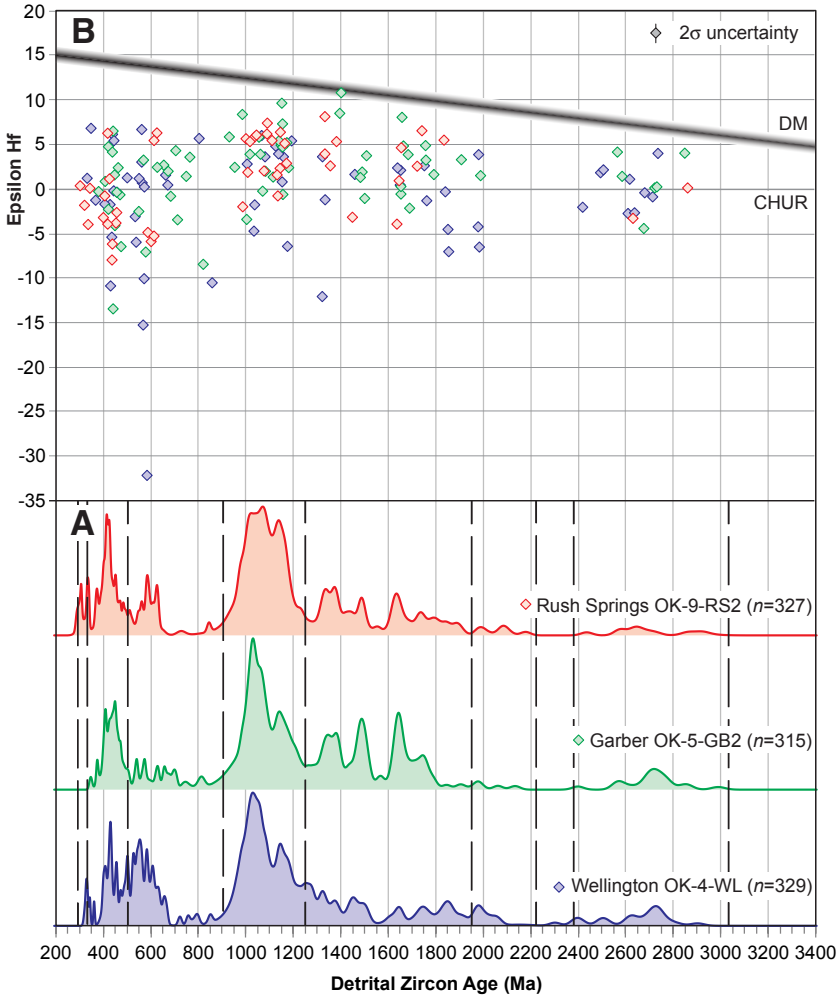

Figure 9. U-Pb age-probability density plots (A) and Hf-evolution diagram (B) showing results from analyses of Permian sandstones in the Anadarko basin. (A) U-Pb age-probability density plots for two analyzed samples (data in Supplemental Table S1 [see text footnote 1]) and from published data for Wellington (Thomas et al., 2016). Vertical, dashed, black lines mark boundaries of detrital-zircon age groups (Fig. 6; Table 3). (B) εHf_t data for two samples (data in Supplemental Table S2 [see text footnote 2]) and for published data for Wellington (Thomas et al., 2016). Data points are color coded as in panel A. Specifications for the Hf-evolution diagram are described in the caption for Figure 7. CHUR—chondritic uniform reservoir; DM—depleted mantle.

values between +12.1 and –6.4 (Fig. 9; Table 2). For zircon grains in the age range 857–504 Ma, εHf_t values range from +6.5 to –32.2 and cluster around +3.2 to –0.9, consistent with involvement of older crust in the source of the magmas. Zircon grains in the age range of 464–337 Ma have εHf_t values between +6.6 and –13.4 (Fig. 9), indicating variable sources. The few young grains in the age range of 327–308 Ma have εHf_t values of +1.1 to –1.8.

DISCUSSION

Age Groups of Detrital Zircons and Implications for Sediment Provenance

The U-Pb age distributions of detrital zircons from sandstones in the Arkoma, Fort Worth, and Anadarko basins define several general groups (Figs. 6 and 10; Table 3). The distributions within each age group (Figs. 6 and 10; Table 3), along with corresponding ranges of εHf_t values (Fig. 11; Table 2), can be used to characterize the provenance(s). The primary alternatives for provenance are either the Appalachian orogen, generally with dispersal through the southern Illinois basin, or the Ouachita orogen, including accreted Gondwanan terranes (Table 3). Lesser alternatives for provenance include synrift igneous rocks in the Arbuckle-Wichita uplifts, other intracratonic uplifts, or the Canadian Shield. Variability between samples suggests variations in provenance.

334–295 Ma

This age group (Table 3) is sparsely represented or lacking in most of the samples but is a distinctive minor component in some (e.g., samples OK-9-RS2 and OK-4-WL; Fig. 9). The age range corresponds to the age of the Alleghanian orogeny, including the ages of plutons (330–270 Ma) in the Appalachians and tonsteins in coal beds (316–311 Ma) in the Appalachian basin (summary in Thomas et al., 2017, and references therein). Grains of this age range, however, are nearly lacking among detrital zircons (7 grains of 3564) from synorogenic Alleghanian sandstones of the Appalachian basin (Fig. 10A) (Thomas et al., 2004, 2017), indicating that Appalachian dispersal systems are not the likely source of these grains. This age group is well represented in magmatic arc rocks of the accreted Coahuila (Gondwanan) terrane within the Marathon orogen (Lopez, 1997; Lopez et al., 2001) and brackets the ages of tuff beds in the Ouachita synorogenic clastic wedge (Fig. 6). These ages are represented also in detrital zircons from sandstones in the Marathon foreland (Fig. 10E). The small numbers of grains of this age group in multiple samples favor a provenance in the Coahuila terrane or another accreted Gondwanan terrane in the interior of the Ouachita-Marathon orogen.

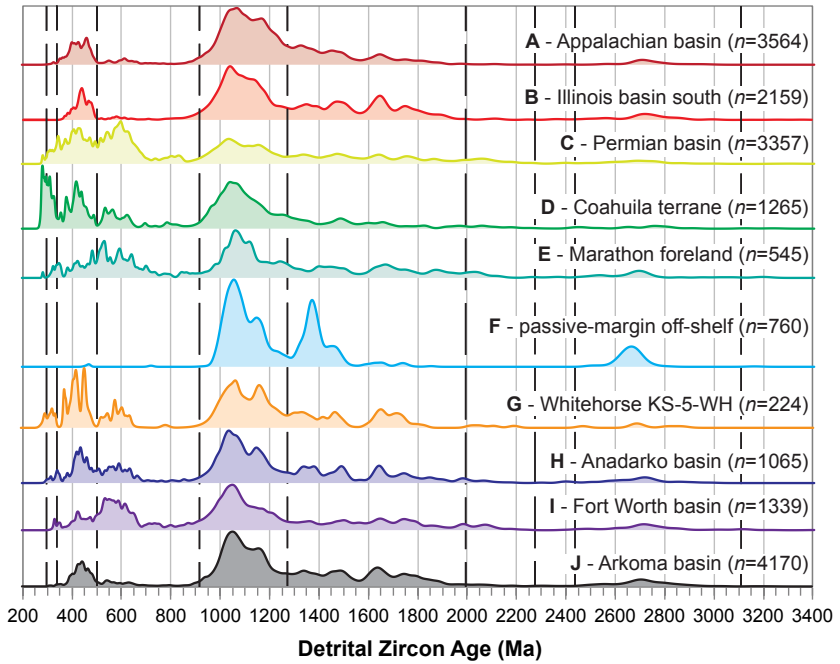

Figure 10. U-Pb age-probability density plots of composites of data from selected basins, including those along potential dispersal pathways, as well as some potential provenances. Data sources are as follows: (A) Appalachian basin (composite plot from Thomas et al., 2017, which includes original analytical data from seven samples plus previously published data from Gray and Zeitler, 1997; Eriksson et al., 2004; Thomas et al., 2004; Becker et al., 2005, 2006; Dodson, 2008; Park et al., 2010; Grimm et al., 2013); (B) southern Illinois basin (composite of original analytical data from Thomas et al., 2020); (C) Permian basin (composite of published data from Soreghan and Soreghan, 2013; Xie et al., 2018b; Liu and Stockli, 2019); (D) Coahuila terrane (composite plot from Thomas et al., 2019, which includes original analytical data from 10 samples plus previously published data from Lawton and Molina-Garza, 2014); (E) Marathon foreland (composite plot from Thomas et al., 2019, which includes original analytical data from two samples plus previously published data from Gleason et al., 2007); (F) Ordovician–Silurian of Ouachita passive-margin off-shelf deep-water sandstones (composite of data from McGuire, 2017; Gleason et al., 2002); (G) Whitehorse Group KS-5-WH, distal Anadarko basin (from Thomas et al., 2020); (H) Anadarko basin (composite from Fig. 9); (I) Fort Worth basin (composite from Fig. 8); (J) Arkoma basin (composite from Fig. 7).

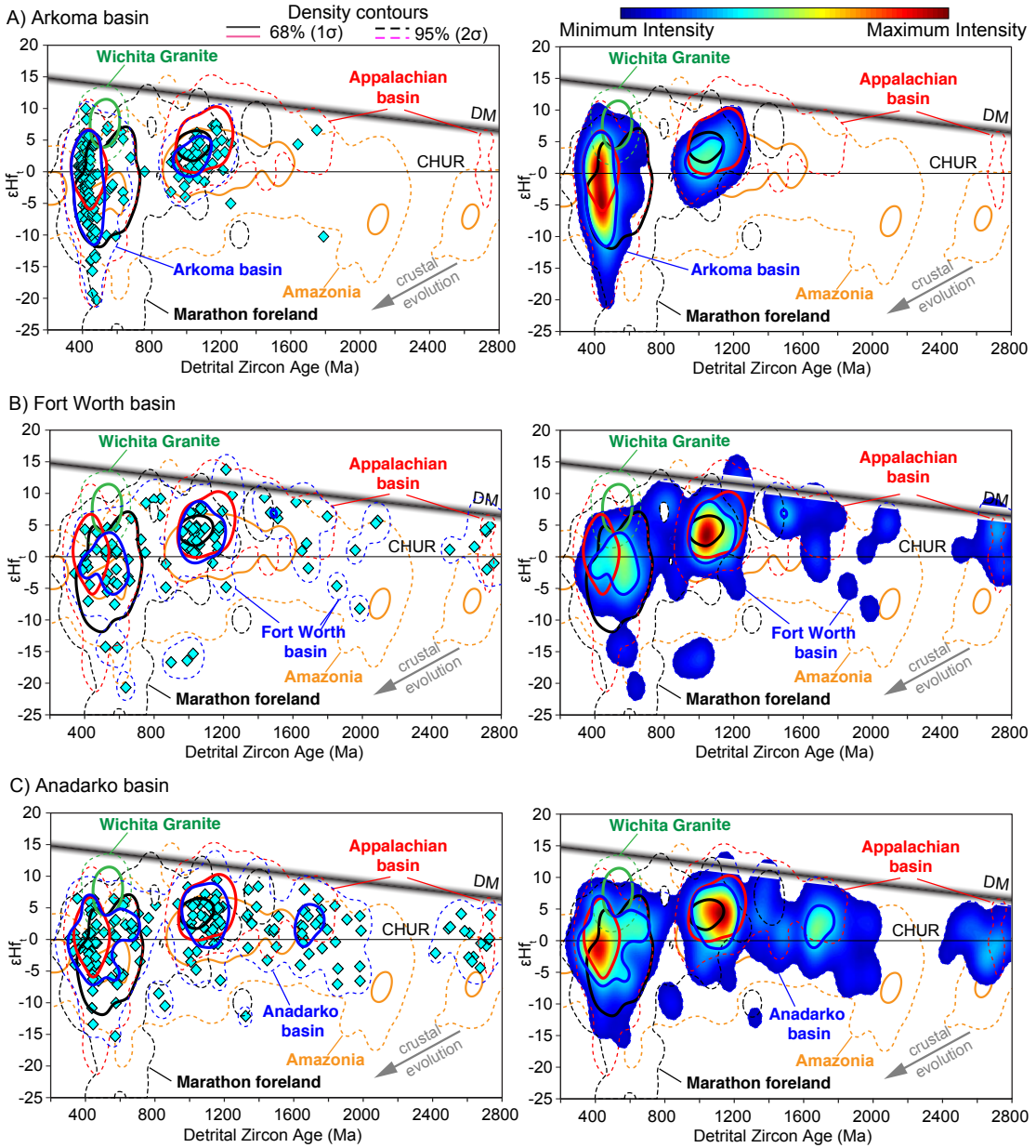

Figure 11. Comparisons of εHf$_t$ data for the (A) Arkoma (Fig. 7), (B) Fort Worth (Fig. 8), and (C) Anadarko (Fig. 9) basins with respect to the Appalachian basin, Marathon foreland, and Amazonia (from Thomas et al., 2017, 2019). Age-εHf$_t$ data are plotted as bivariate kernel density estimates (KDEs), using HafniumPlotter version 1.5 (github.com/kurtsundell/HafniumPlotter; Sundell et al., 2019). This construction of bivariate KDEs follows a similar formulation as standard one-dimensional KDEs (Silverman, 1986) and incorporates set kernel bandwidths of 25 m.y. along the *x* axis (U-Pb age) and 2 epsilon units along the *y* axis (εHf$_t$ value). The bivariate KDEs were constructed on a two-dimensional *x*-*y* grid of 512 × 512 cells, in which each cell had a corresponding density value on the *z* axis. When viewed parallel to the *z* axis, bivariate KDEs produce a density map that is contoured to specified intervals. Contours are plotted at 68% (solid lines) and 95% (dashed lines) (1σ and 2σ, respectively) of peak density; density is the height of the *z* axis and is shown by a color gradient, in which hotter colors represent larger (higher) *z*-axis values. See text for discussion of interpretations. CHUR—chondritic uniform reservoir; DM—depleted mantle.

499–335 Ma

This age group (Table 3) is represented in all of the samples and is prominent in many. These ages, corresponding to the ages of the Taconic and Acadian orogenies, are generally abundant in sandstones of the Appalachian basin (Fig. 10A) (Thomas et al., 2017, and references therein). Likewise, these ages are common in Gondwanan accreted terranes adjacent to the southern margin of Laurentia, and the ages are generally abundant among detrital zircons in the Marathon foreland (Fig. 10E) (Thomas et al., 2019). This age group offers no clear distinction between an Appalachian or Gondwanan provenance.

901–500 Ma

This age group (Table 3) is one of the most distinctive, in that it is a dominant group in many samples but is only sparsely represented in others. The age range corresponds to the Pan-African/Brasiliano components of accreted terranes of Gondwanan origin, along both the Appalachians and the Ouachita-Marathon orogen (Thomas et al., 2017, 2019). Alleghanian synorogenic sandstones in the Appalachian basin have persistent but only minor numbers of detrital-zircon grains of this age group (Fig. 10A), indicating limited dispersal of grains of this age through the Appalachian basin (Thomas et al., 2017). The Coahuila and other Gondwanan accreted terranes along the Ouachita-Marathon orogen include Pan-African/Brasiliano rocks, and this age group is represented in dominant modes of detrital-zircon ages in the Marathon foreland (Fig. 10E) (Thomas et al., 2019). The possibility that Iapetan synrift volcanic-magmatic rocks (539–530 Ma; e.g., Wichita Granite Group) along the Southern Oklahoma fault system might have contributed to this age group (e.g., Sharrah, 2006) is eliminated by the contrast between the εHf_t values of detritus from the Wichita Granite Group (+10.1 to +4.7; Thomas et al., 2016) and those of the detrital zircons in the Ouachita foreland (+8.3 to –30.5, mostly +4.9 to –5.6 in grains <600 Ma; Figs. 7–9 and 11). Abundant grains in this age group along the Ouachita foreland favor a provenance in the accreted Gondwanan terranes, including Sabine, along the Ouachita-Marathon orogen.

1276–914 Ma

This age group (Table 3) is represented in all of the samples and is the dominant age group in many. This is the age range of the Grenville orogen in the Appalachians, and Grenville-age detrital zircons are abundant in late Paleozoic sandstones in the Appalachian basin (Fig. 10A) (Thomas et al., 2017). The same age range is similarly abundant in the Gondwanan Coahuila accreted terrane (Fig. 10D) along the Marathon orogen, representing the Sunsás province of Amazonia. Detrital grains of this age group are abundant in synorogenic sandstones in the Marathon foreland (Fig. 10E) (Thomas et al., 2019). This age group does not provide a clear distinction between an Appalachian Grenville or a Gondwanan Sunsás provenance.

1963–1202 Ma

This multimodal (generally four to six modes) age group (Table 3) is represented in all of the samples. With some variations, the abundance of grains generally decreases with increasing age. The complete range of ages spans the Penokean, Trans-Hudson, Central Plains, Yavapai, Mazatzal, and Granite-Rhyolite provinces of the Laurentian craton and also includes the Ventuari-Tapajós, Rio Negro–Juruena, and Rondonia–San Ignacio provinces of Amazonia (Fig. 6). The Central Plains–Yavapai–Mazatzal subgroup (1800–1600 Ma) is represented by intermediate modes in the detrital zircons, suggesting a possible source in the Nemaha basement uplift (Xie et al., 2016, 2018a); however, Appalachian samples have similar modes in this age range (Fig. 10A), interpreted to be recycled from synrift sedimentary rocks along the Iapetan margin (Thomas et al., 2017). Ages of the Granite-Rhyolite province are particularly abundant in the passive-margin off-shelf sandstones that were deposited around the Ouachita embayment and subsequently imbricated in the Ouachita thrust belt (McGuire, 2017), providing a potential source for recycling from the Ouachita thrust belt to the synorogenic sandstones (Fig. 10F). Because of the matches of ages with both Laurentian and Amazonian/Gondwanan provinces, as well as the incorporation of Laurentian detritus in the Ouachita thrust belt, these detrital zircons provide no clear distinction of the provenance.

2224–1945 Ma

Most samples have small numbers of grains in this age group (Table 3). The age group, which has no counterpart in Laurentia, is distinctive of the Moroni-Itacaiúnas province and the Trans-Amazonian belt of Amazonia and the Eburnian province of West Africa (Fig. 6). Sandstones in the Appalachian basin have small numbers of grains of these ages, indicating a provenance in Gondwanan accreted terranes in the Appalachian orogen (Fig. 10A) (Thomas et al., 2017). This age group is clearly linked to Gondwana, but the numbers of detrital zircons are less than those of the Pan-African/Brasiliano age group (Fig. 10).

3036–2387 Ma

Most samples have a minor mode in this age group (Table 3), which overlaps the ages of the Superior province of Laurentia and the Central Amazonia province of Amazonia/Gondwana (Cordani and Teixeira, 2007; Cardona et al., 2010). Grains with ages of the Superior province of Laurentia are relatively abundant in Ordovician passive-margin off-shelf sandstones, which were deposited along the rifted margin of Laurentia (Fig. 2, box A1; Figs. 4 and 10F) (Gleason et al., 2002; McGuire, 2017). The Ordovician sandstones are in the Ouachita thrust belt and were available for recycling of Laurentian Superior detritus from sources in the Ouachita orogen.

Provenance and Dispersal of Late Paleozoic Detritus in the Ouachita Foreland

Fort Worth Basin

Similarities through all the analyzed samples from the Fort Worth basin (Fig. 8) indicate a consistent ultimate provenance through Middle Pennsylvanian to Early Permian time. Most of the age groups of detrital zircons in the Fort Worth basin are equally available from Gondwanan and Appalachian sources, making identity of the provenance problematic and leaving only a few age groups that are clear discriminants (Table 3). One of the most dominant modes (616–532 Ma) in the Fort Worth basin (Fig. 8) matches Gondwanan Pan-African/Brasiliano ages, which are not abundant in samples from Mississippian–Permian sandstones of the Alleghanian Appalachian basin (Fig. 10A). In some of the Fort Worth samples (TX-2-PB and TX-5-CC; Fig. 8), grains with Neoproterozoic ages (898–500 Ma) are especially abundant in proportion to grains with Mesoproterozoic ages (1256–914 Ma) (ratios of 0.570 and 0.983, respectively). Minor modes between 2092 and 1984 Ma match the ages of the Moroni-Itacaiúnas province and Trans-Amazonian belt of Amazonia/Gondwana (Table 3); this age group is rare in Mississippian–Permian sandstones of the Alleghanian Appalachian basin (Fig. 10A). The mix of inferred Laurentian and Gondwanan ages in the Fort Worth basin has been used to support an interpretation that detritus from sources in the Appalachian orogen of eastern Laurentia was mixed with clearly non-Appalachian, more proximal detritus from the accreted Sabine terrane in the Ouachita orogen (Alsalem et al., 2018). The detrital-zircon ages that correspond to Appalachian age groups, however, are also available from Gondwanan accreted terranes (Table 3) along the Ouachita-Marathon orogen, which could have supplied all of the detritus in the Fort Worth basin (Fig. 12). Chert-clast conglomerates in Middle Pennsylvanian sandstones in the Fort Worth basin have been interpreted to record dispersal from exposures of Ordovician Bigfork Chert and/or Devonian Arkansas Novaculite in the Ouachita sedimentary thrust belt (Brown et al., 1973), further indicating sediment dispersal from the Ouachita orogen to the foreland (Fig. 12C). In summary, the consistent age distributions throughout the stratigraphic succession and into the distal Fort Worth basin indicate persistent dispersal of clastic sediment from the orogenic source, as well as no mixing of sediment from cratonic or more distal sources into the distal foreland (Fig. 12).

The detrital-zircon age distributions in Pennsylvanian–Permian sandstones of the Fort Worth basin are remarkably similar to those in the Marathon foreland (cf. Figs. 10I and 10E). In an MDS plot, the sandstones in the Fort Worth basin are near the coeval sandstones in the Marathon foreland (Fig. 13), indicating that detritus along the Ouachita-Marathon foreland in the Fort Worth basin and Marathon foreland came from the same or similar sources. In the MDS plot, the separation between the Middle Pennsylvanian Haymond Formation and the Upper Pennsylvanian Gaptank Formation and Middle Permian Road Canyon Formation in the Marathon foreland (Fig. 13) suggests a change through time in the provenance, possibly because of erosional unroofing. The distributions of ages of detrital zircons in Middle Pennsylvanian to Middle Permian sandstones in the Marathon foreland are similar to those in the Coahuila terrane (Figs. 10D and 10E), and the age groups in the Marathon foreland have potential sources in the Coahuila terrane (Thomas et al., 2019). The MDS plot shows that the Fort Worth samples are closer to the Marathon and Coahuila data and are more distant from the Appalachian data (Fig. 13B). The Hf data have substantial overlap; however, the distribution of values from the Fort Worth basin in the age range of 850–350 Ma is nearly identical to that of the Marathon samples but only partially overlaps with the more restricted range of Appalachian values (Fig. 11B). If the Sabine terrane is similar in composition to the other components (Coahuila, Sierra Madre, and Maya) of the Oaxaquia assemblage, the Sabine terrane could have supplied all of the age groups of detrital zircons in the sandstones of the Fort Worth basin (Table 3), similar to the supply from Coahuila to the Marathon foreland (Fig. 12) (Thomas et al., 2019).

Anadarko Basin and Other Intracratonic Basins

Along the southern margin of the Anadarko basin, the Lower Permian Post Oak Conglomerate unconformably overlies the Cambrian synrift Wichita Granite Group in the Wichita uplift (Figs. 1B, 5B, and 12D). The Post Oak Conglomerate has detrital zircons almost exclusively near the crystallization age (539–530 Ma) of the Wichita Granite Group, and distinctively positive εHf_t values between +10.1 and +4.7 (Fig. 11C) indicate juvenile magmas (Thomas et al., 2016).

Farther east, the sandstone matrix of the Upper Pennsylvanian Vanoss Conglomerate, which overlies an angular unconformity on lower Paleozoic strata above the Precambrian basement in the Arbuckle uplift (Figs. 1B, 5B, and 12D), is dominated by Superior-age (2860–2620 Ma) zircons (Thomas et al., 2016). The Ordovician limestone succession beneath the unconformity includes units of quartzose sandstone that contain Superior-age detrital zircons (Pickell, 2012). The combination of limestone clasts from proximal strata beneath the unconformity and the lack of Superior-age basement rocks in the region strongly argues that the detrital zircons in the Vanoss Conglomerate were recycled from the sandstones within the Ordovician limestone succession (Thomas et al., 2016).

Stratigraphically above the Post Oak and Vanoss Conglomerates, the Lower Permian Wellington Formation (Fig. 5A) in the lower part of a succession of widespread Lower–Middle Permian red beds and evaporites (Johnson et al., 1988) has detrital-zircon age distributions distinctly different from those of the conglomerates (Thomas et al., 2016). A subset (673–504 Ma) of a dominant age group (857–504 Ma) in the Wellington Formation (Fig. 9) overlaps the age of detrital zircons from the Cambrian synrift igneous rocks in the Post Oak Conglomerate. Although some grains in the Wellington have εHf_t values (+6.5) similar to those in the Post Oak Conglomerate, most Wellington grains (+6.5 to –32.2) are significantly more negative (Figs. 9 and 11C), indicating that the Wellington sands are from different, more evolved sources than the juvenile sources of the detritus in the Post Oak Conglomerate (Thomas et al., 2016). The abundance

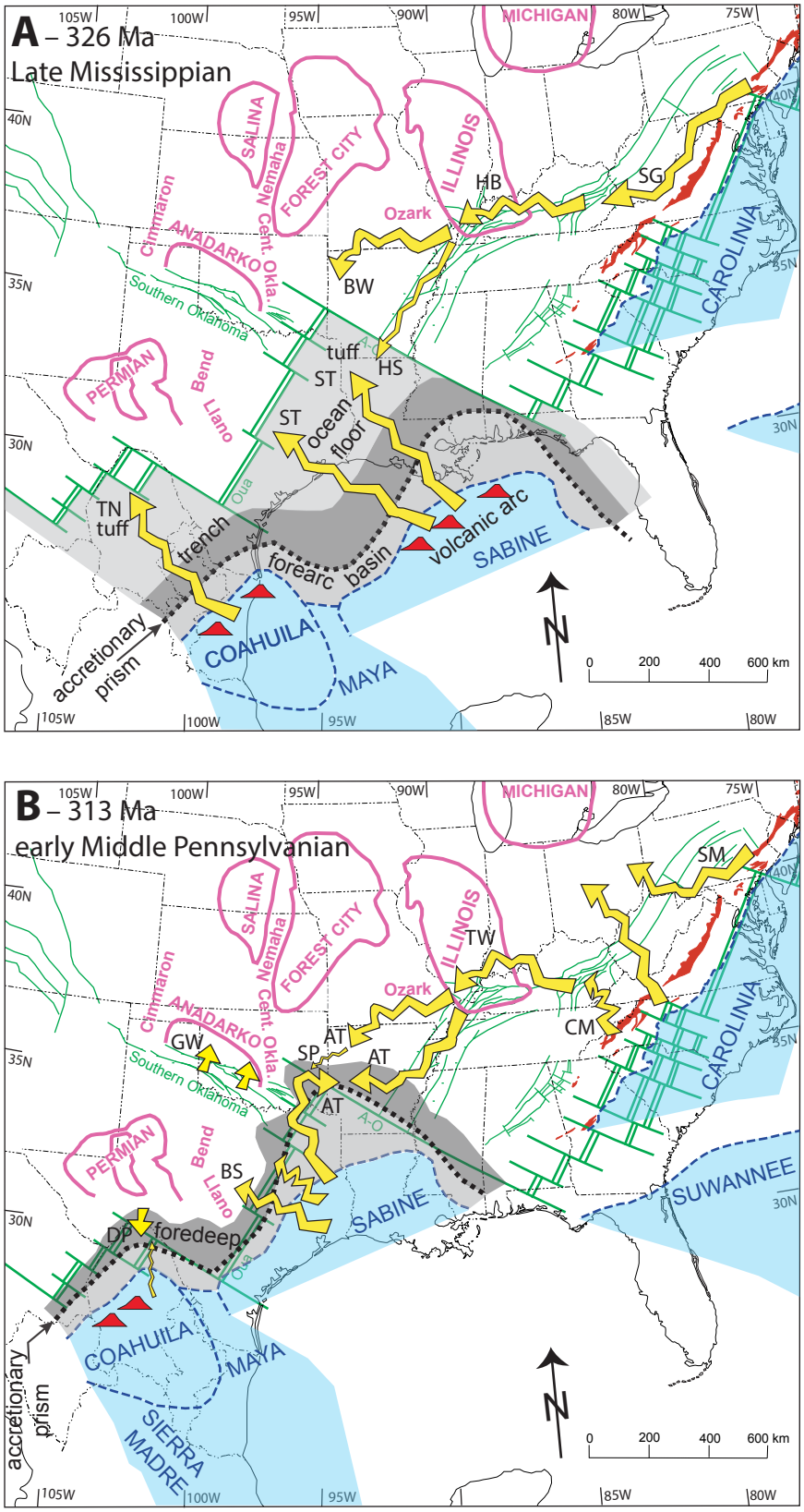

Figure 12. Sequence of regional maps showing interpreted sediment dispersal pathways (yellow lines and arrows) into and across the Ouachita foreland and southern Midcontinent. lapetan rifted margin of Laurentia and intracratonic basins are from Figure 1. Tectonic evolution through the sequence of maps is adapted from Mack et al. (1983), Houseknecht (1986), Ross (1986), Thomas (1989, 2011), Viele and Thomas (1989), and Mueller et al. (2014). Correlations of all named stratigraphic units and approximate stratigraphic level of each map are shown in Figure 5B. A-O—Alabama-Oklahoma transform fault; Oua—Ouachita rift. (A) Late Mississippian, 326 Ma. Southward subduction beneath continental-margin volcanic arcs on the leading edges of the accreted Coahuila (subduction initiated 355 Ma) and Sabine (subduction initiated 338 Ma) terranes, and rapid accumulation of deep-water muddy turbidites along with eruptions of ash-flow tuffs (ST—Stanley, including tuffs with ages of 328–320 Ma; TN—Tesnus). Fluvial dispersal of synorogenic detritus through the Appalachian basin (SG—Stony Gap, Mauch Chunk–Pottsville clastic wedge) via the southern Illinois basin (HB—Hardinsburg) to the northern shelf of the Arkoma basin (BW—Batesville and Wedington) and over the shelf margin into deep water (HS—Hot Springs). (B) Early Middle Pennsylvanian, 313 Ma. Fort Worth basin: filling of the foredeep and progradation of synorogenic clastic sediment onto the distal shelf (BS—Big Saline). Marathon foreland: restricted clastic sediment from the Coahuila terrane and deposition of carbonate detritus from the shelf (DP—Dimple). Arkoma basin: rapid and deep flexural subsidence in response to emplacement of the tectonic load of the accretionary prism onto the edge of continental crust and deposition of very thick synorogenic turbidites (AT—Atoka), dispersal from the Appalachian basin (CM—Cross Mountain, for example) via the southern Illinois basin (TW—Tradewater) to the northern shelf of the Arkoma basin (AT—Atoka) and over the shelf margin (SP—Spiro) into deep water (AT—Atoka) to mix with proximal sediment from the Sabine terrane. Appalachian basin: Pennington-Lee clastic wedge (CM—Cross Mountain) and Mauch Chunk–Pottsville clastic wedge (SM—Sharp Mountain) prograde to distal foreland. Anadarko basin: deposition of proximal detritus (GW—Granite Wash) eroded from Arbuckle and Wichita basement uplifts. (*Continued on following two pages.*)

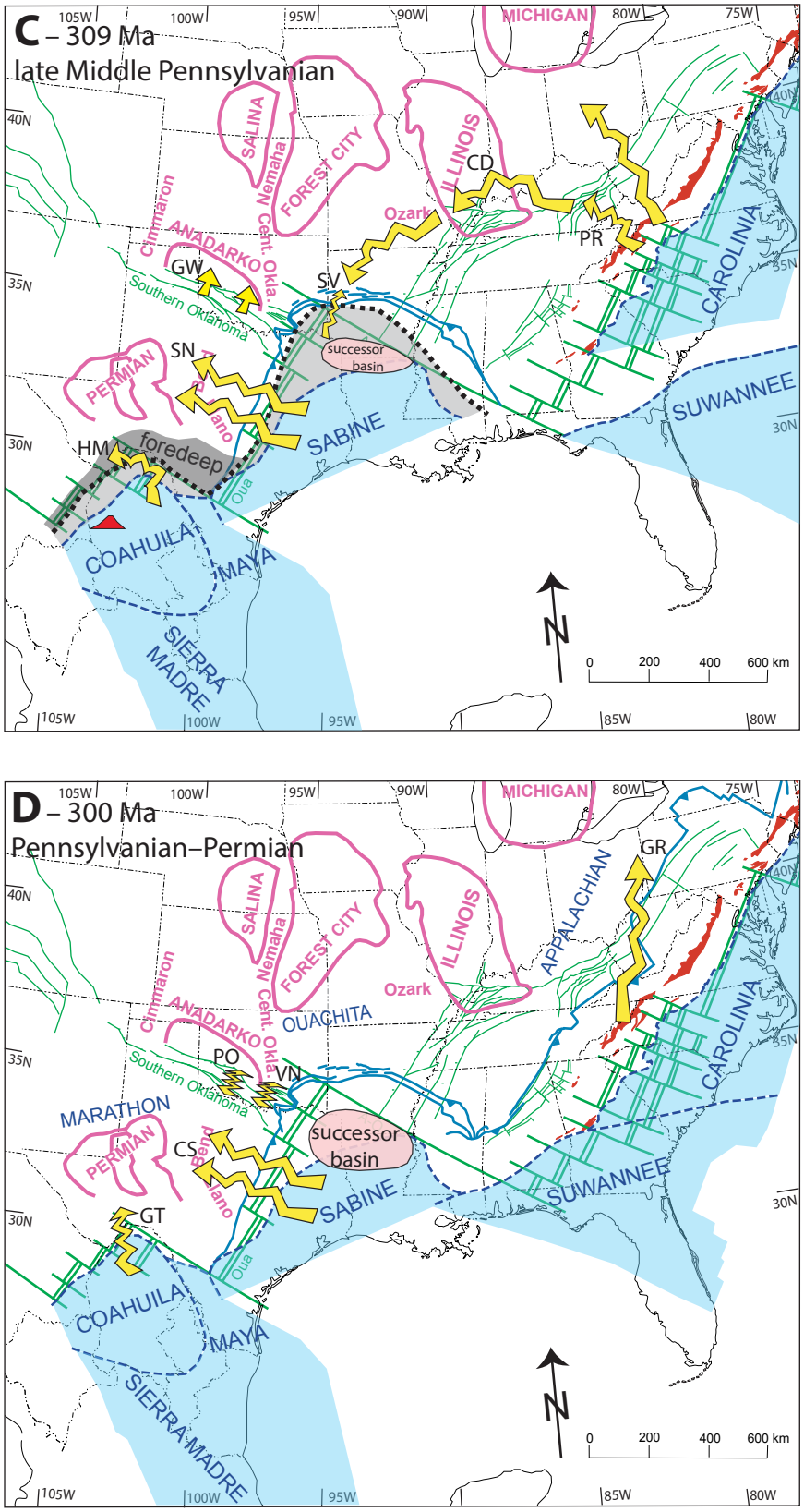

Figure 12 (*continued*). (C) Late Middle Pennsylvanian, 309 Ma. Final accretion of Sabine terrane and last stage of Ouachita thrusting (blue lines from Fig. 1). Marathon foreland: filling of the foredeep with turbidites (HM—Haymond). Fort Worth basin: progradation of deltaic deposits from the overfilled foredeep to the distal shelf (SN—Strawn). Arkoma basin: progradation of fluvial to deltaic deposits from the Appalachian basin (PR—Princess, Pennington-Lee clastic wedge) via the southern Illinois basin (CD—Carbondale) to southward prograding deltaic deposits on the northern Arkoma shelf to mix with minor deltaic deposits (SV—Savanna, for example) from the overfilled Arkoma foredeep; initial shallow-marine deposits unconformably overlie deformed Atokan strata in a successor basin in the Ouachita orogenic belt. Anadarko basin: deposition of proximal detritus (GW—Granite Wash) eroded from Arbuckle and Wichita basement uplifts. (D) Pennsylvanian–Permian, 300 Ma. Final transpressional accretion of Suwannee terrane and latest stages of Appalachian thrusting (blue lines from Fig. 1). Marathon foreland: filling of foredeep and progradation of deltaic to shallow-marine deposits onto the distal shelf (GT—Gaptank). Fort Worth basin: progradation of deltaic deposits to the distal shelf (CS—Cisco). Arkoma basin: successor-basin deposits of Desmoinesian–Guadalupian age cover deformed Ouachita sedimentary rocks (Atoka) at an angular unconformity. Anadarko basin: Wichita and Arbuckle basement uplifts at southern edge of basin; onlap of conglomerates (PO—Post Oak, VN—Vanoss) above angular unconformity on the basement uplifts. Appalachian basin: northward dispersal of clastic sediment of Pennington-Lee clastic wedge (GR—Greene, for example).

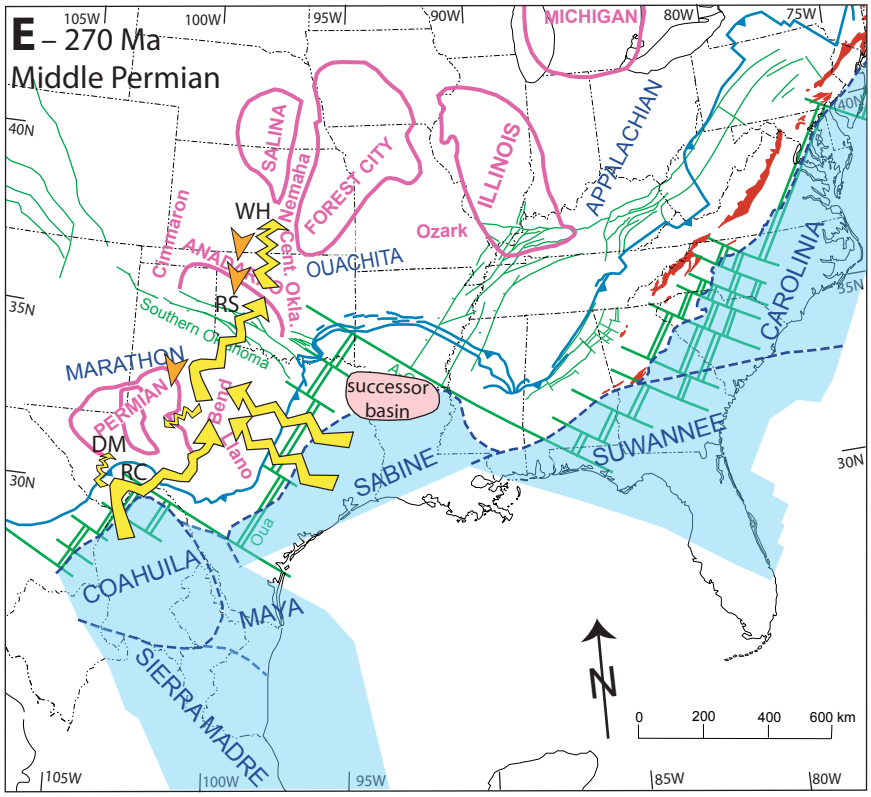

Figure 12 (*continued*). (E) Middle Permian, 270 Ma. Final accretion of Coahuila terrane and last stage of Marathon thrusting at 295 Ma (blue lines from Fig. 1). Marathon foreland: above multiple unconformities, progradation of deltaic to shallow-marine deposits (RC—Road Canyon) onto southern craton, to merge with detritus from the overfilled Fort Worth basin, and possibly continuing to the Permian basin (DM—Delaware Mountain). Anadarko basin: progradation of detritus from Marathon foreland and/or Fort Worth basin to cover eroded Wichita and Arbuckle uplifts and the overfilled Anadarko basin (RS—Rush Springs); dispersal northward on the craton to the southwest of the Forest City basin (WH—Whitehorse); detritus reworked by south-southwest winds (orange arrowheads) over northern part of Anadarko basin and possibly to Permian basin. Arkoma basin: filling of successor basin.

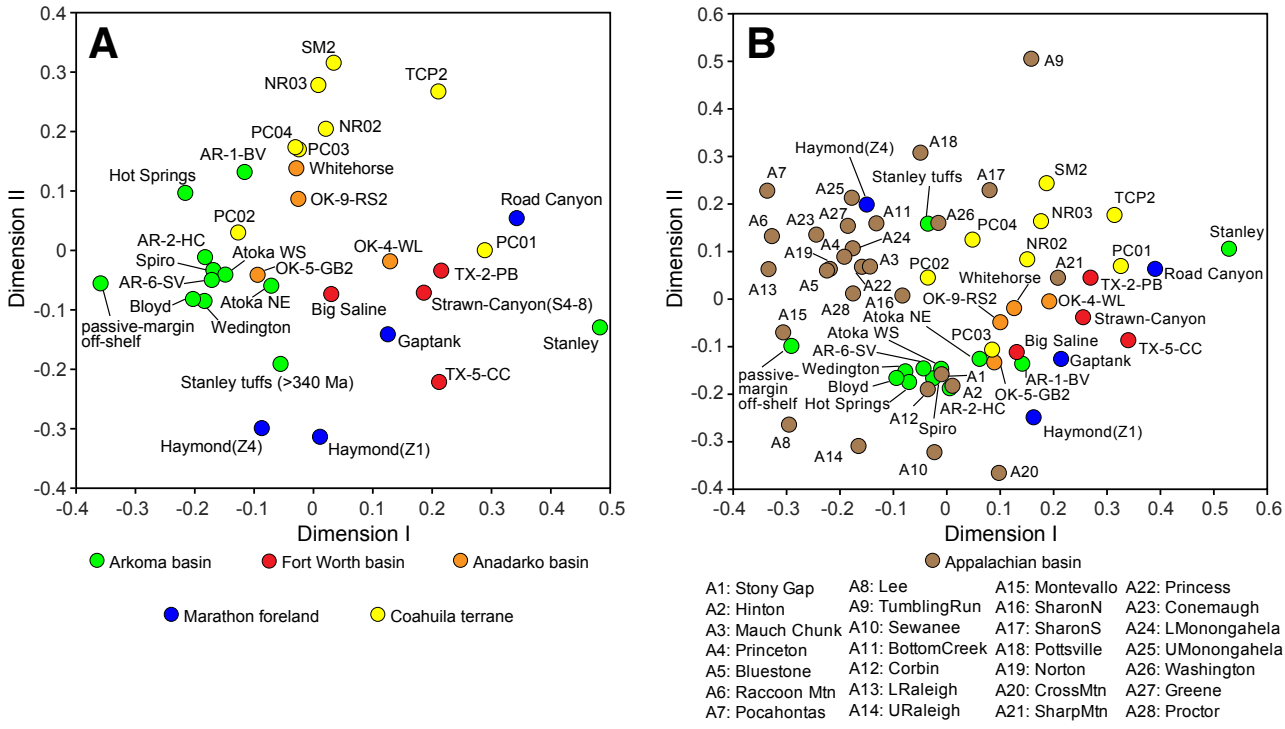

Figure 13. Two-dimensional multidimensional scaling (MDS) plots for detrital-zircon U-Pb age distributions of Mississippian–Permian sandstones in the Arkoma (Fig. 7), Fort Worth (Fig. 8), and Anadarko (Fig. 9) basins in comparison with distributions of samples from the Appalachian basin (from Thomas et al., 2017, and references cited therein; Fig. 10A), from the Whitehorse Group in the distal Anadarko basin (KS-5-WH, from Thomas et al., 2020; Fig. 10G), from the Marathon foreland (from Thomas et al., 2019, and Gleason et al., 2007; Fig. 10E), from the Coahuila terrane (only samples with n >45; from Thomas et al., 2019, and Lawton and Molina-Garza, 2014; Fig. 10D), and in a composite from Ouachita passive-margin off-shelf sandstones (from McGuire, 2017, and Gleason et al., 2002; Fig. 10F). Points that plot closer together have greater correspondence (are more similar) for detrital-zircon ages. The MDS plots (Vermeesch, 2013) were constructed using the program DZmds (github.com/kurtsundell/DZmds) (Saylor et al., 2018) using Mismatch of age-probability density plots (Amidon et al., 2005) to calculate dissimilarity. Axis scales are calculated dissimilarities between samples. (A) Samples from Arkoma, Fort Worth, and Anadarko basins; Marathon foreland; and Coahuila terrane. (B) Comparison of samples plotted in A with samples from Appalachian basin. See text for discussion of interpretations.

of recycled Superior-age zircons (2860–2620 Ma) in the Vanoss Conglomerate is only weakly represented in the detrital zircons in the Wellington Formation (Fig. 9). The mix of zircon ages in the Wellington Formation (Fig. 9), along with the generally more negative εHf_t values, indicates that the sands were derived neither from the local synrift igneous rocks in the Wichita and Arbuckle uplifts nor from recycling from the conglomerates that lap onto the uplifts. Instead, the age distributions suggest a source separate and distal from the Arbuckle and Wichita uplifts. In a broader sense, these data show that the crystalline rocks of the Wichita and Arbuckle uplifts were rapidly covered in the Early Permian and were not available later as a source of regionally dispersed sediment (Soreghan and Soreghan, 2013; Thomas et al., 2016).

Along with the Wellington Formation, the Garber and Rush Springs Sandstones include a distinct Pan-African/Brasiliano component (857–502 Ma), the usual abundance of Mesoproterozoic grains (1228–924 Ma, Sunsás = Grenville age), and moderate abundance of zircons in the age range of 2200–1200 Ma (Fig. 9). Similarities of detrital-zircon distributions in Permian sandstones in and above the Wellington Formation in the intracratonic Anadarko basin (Figs. 9, 10H, 11C, and 13) to those in the Marathon foreland (Figs. 10E, 11C, and 13) and Fort Worth basin (Figs. 8, 10I, 11, and 13) suggest the same or a similar provenance. Dispersal of sediment through either or both the Marathon foreland and Fort Worth foreland basin requires fluvial systems that prograded onto the craton and into the Anadarko basin (Fig. 12E). The Rush Springs Sandstone consists primarily of eolian deposits in an erg system with southwest-directed wind currents (Poland and Simms, 2012), which are compatible with overall north to northwest drainage from the Ouachita-Marathon orogen onto the craton and into the Anadarko intracratonic basin with episodic wind reworking back over the fluvial system (Fig. 12E) (Soreghan and Soreghan, 2013).

A sample from the Middle Permian Whitehorse Group (KS-5-WH; Fig. 10G; Thomas et al., 2020) on the structural divide between the Anadarko basin and the Forest City basin on the north (Fig. 1) suggests distant transport from the Ouachita-Marathon orogen onto the craton (Fig. 12E). The detrital-zircon distributions are generally similar to those in the stratigraphically lower Pennsylvanian and Mississippian sandstones in the Forest City basin, which are characteristic of an Appalachian provenance (Kissock et al., 2018; Chapman and Laskowski, 2019; Thomas et al., 2020). In contrast, the Middle Permian Whitehorse sample includes a secondary group with ages of 638–519 Ma and a minor mode of 576 Ma (Fig. 10G); in addition, four grains have ages of 2196–2021 Ma. These distinctly Pan-African/Brasiliano and Moroni-Itacaiúnas/Trans-Amazonian/Eburnian ages suggest a Gondwanan provenance. Another, distinctively young secondary distribution with ages of 335–287 Ma has a mode of 319 Ma (Fig. 10G), corresponding to the age of the Alleghanian orogeny in the Appalachians, but contrasting with the general lack of Alleghanian-age grains in the synorogenic dispersal systems of the Appalachian basin (Table 3; Thomas et al., 2017). The secondary mode with Alleghanian ages in the Whitehorse sample is similar in age to distributions in coeval sandstones in the Anadarko basin (Fig. 9) and Marathon foreland (Fig. 10E; fig. 4 *in* Thomas et al., 2019), as well as a prominent mode in Jurassic–Cretaceous sandstones in fault-bounded basins in the Coahuila terrane (Fig. 10D). The association of these detrital-zircon age distributions with Permian red beds forms a distinctive assemblage, implying long-distance fluvial transport onto the southern craton from Gondwanan accreted terranes, such as Coahuila (Fig. 12E).

Detrital-zircon data from Lower and Middle Permian sandstones in the Permian (Delaware and Midland basins) basin (Figs. 1A, 5B, and 10C) suggest widespread sediment dispersal from sources like those for the Marathon foreland, as well as the Fort Worth and Anadarko basins (Soreghan and Soreghan, 2013; Xie et al., 2018b; Liu and Stockli, 2019). Most samples from the Permian basin have abundant detrital-zircon ages in the age ranges of 1975–1211, 1208–930, and 500–335 Ma (Fig. 10C), all consistent with either Appalachian or Gondwanan sources (Table 3). The samples from the Permian basin have a dominant age distribution of 852–500 (mostly 685–500) Ma, as well as a lesser age distribution of 2203–1975 Ma (Fig. 10C), both distinctly from Gondwanan sources (Table 3). Most samples from the Permian basin have a secondary distribution with ages of 334–277 Ma similar to those in the Marathon and Anadarko samples (Fig. 10). The data lead to an interpretation of fluvial dispersal of detritus from the Ouachita-Marathon orogen and accreted Gondwanan terranes across the broad foreland and southern craton (Fig. 12E).

Arkoma Basin

The tuff beds in muddy turbidites of the Mississippian–Pennsylvanian Stanley Shale in the lower part of the proximal synorogenic clastic wedge in the Arkoma basin provide a clear link to a source in an arc system south of the foredeep (Niem, 1977), consistent with a continental-margin arc on the leading edge of the Sabine terrane (Fig. 12A), as well as a definitive age (328–320 Ma; Fig. 6) of arc volcanism (Shaulis et al., 2012). Detrital zircons with ages equal to the crystallization ages of the tuffs are lacking in the foreland detritus. Although dominated by synmagmatic grains, the tuffs contain zircon grains older than the crystallization age (Fig. 6), which have been interpreted to be detrital grains from the muddy turbidites (Shaulis et al., 2012), but which, alternatively, may be xenocrysts from the magma chamber in the Sabine terrane. Although the proportions differ somewhat, most of the age modes of the prevolcanic zircons in the tuffs of the Stanley Shale are similar to those of the Coahuila terrane, as well as those in the Marathon foreland and Fort Worth basin (cf. Figs. 6 and 10D, 10E, and 10I, respectively); however, the tuffs differ primarily in having a noticeably greater abundance of zircon grains in the age range of 1577–1283 Ma (Fig. 6). If the prevolcanic grains in the tuffs are detrital from Laurentian/Appalachian sources (Shaulis et al., 2012), the source of the 1577–1283 Ma grains is problematic, because grains of this age range are only secondary components of the Appalachian signature (cf. Figs. 6 and 10A). Detrital grains with ages of the Granite-Rhyolite province (1500–1320 Ma) of Laurentia are relatively abundant in the Ordovician–Silurian Ouachita passive-margin off-shelf

strata (Fig. 10F) and might have been available for recycling, but grains of those ages are rare in the Stanley Shale (Fig. 7). If the prevolcanic grains in the tuffs are xenocrystic, the composition of the basement of the Sabine terrane may differ from that of the Coahuila terrane in having a locally more substantial Rondonia–San Ignacio (1550–1300 Ma) component along with the Sunsás rocks, as suggested for northwestern Amazonia (e.g., Cardona et al., 2010), or, alternatively, the magma may have been contaminated by subducted sediment from the Ouachita margin. Future research may provide answers to these questions, as well as better resolution of the composition of the Sabine terrane.

A sandstone bed in the upper part of the proximal deposits of the Stanley Shale has a dominant group of detrital-zircon ages of 874–501 Ma (McGuire, 2017), corresponding in age to the Pan-African/Brasiliano assemblage of Gondwanan terranes (Fig. 7; Table 3). Another important age group of 1197–1018 Ma is equivalent in age to the Amazonian Sunsás and Laurentian Grenville provinces (Fig. 7; Table 3). A secondary age group of 2185–1953 Ma matches the distinctive Moroni-Itacaiúnas/Trans-Amazonian ages of Amazonia (Table 3). The overall distribution of detrital-zircon ages indicates a Gondwanan provenance (Fig. 12A), consistent with the composition of the Coahuila terrane and of the Sabine terrane as suggested by the prevolcanic age distributions in the tuff beds (Figs. 6, 7, and 10D; Table 3). In contrast, the Hot Springs Sandstone Member of the Stanley Shale has dominant age groups of 1195–994 Ma and 484–373 Ma (McGuire, 2017), respectively, corresponding to the Grenville and Taconic age groups in the Appalachians and overlapping with Gondwanan age groups (Fig. 7; Table 3). The Hot Springs sample, however, lacks distinctive Gondwanan components, thereby indicating a provenance different from the other sample from the Stanley Shale, most likely the Appalachians (Fig. 12A).

In the most distal shelf of the Arkoma basin in northern Arkansas, distribution patterns and paleocurrents of Mississippian sandstones (Batesville Sandstone and Wedington Sandstone Member of the Fayetteville Shale; Fig. 2, box B1; Figs. 5A and 12A) indicate southward prograding deltaic systems modified by marine reworking and interaction with carbonate deposition on the shallow-marine shelf (Garner, 1967; Ogren, 1968; Glick, 1979; Sutherland, *in* Johnson et al., 1988; Xie et al., 2016). The two most dominant detrital-zircon age groups have ages of 1210–937 Ma and of 496–339 Ma (Fig. 7). Ages are scattered between 1907 and 1210 Ma, and an older group has ages of 3036–2466 Ma. The age distributions have relatively few grains with distinctive Gondwanan ages of 2186–1945 Ma (Moroni-Itacaiúnas/Trans-Amazonian/Eburnian) or of 762–501 Ma (Pan-African/Brasiliano). The detrital-zircon age distributions (Fig. 7) of the Batesville and Wedington Sandstones, as well as of the Hot Springs Sandstone, are similar to the Appalachian signature (Fig. 10A). The Batesville, Wedington, and Hot Springs data, as well as data from coeval sandstones in the southern Illinois basin and in the Appalachian basin, are all close together in an MDS plot (Fig. 14A), indicating a similar provenance. Values of εHf_t from the Batesville Sandstone have a remarkably close match to those of Mississippian sandstones in the Appalachian foreland and in the southern Illinois basin (Fig. 15A) (Thomas et al., 2017, 2020). An ultimate source in the Appalachians with dispersal from the Appalachian basin through the southern part of the Illinois basin may have supplied the Batesville and Wedington deltaic sand to the cratonic fringe of the Arkoma basin, as well as the Hot Springs sand (within the muddy turbidites of the Stanley Shale) to the adjacent continental slope, during the Late Mississippian (Fig. 12A).

Pennsylvanian sandstones (Cane Hill Member of the Hale Formation, Bloyd Formation, and Savanna Sandstone; Figs. 2 and 5A) on the distal shelf of the Arkoma basin generally are interpreted to be fluvial to deltaic deposits with southward to westward directed sediment dispersal (Sutherland, *in* Johnson et al., 1988; Xie et al., 2018a). The detrital-zircon distributions are generally similar through the Upper Mississippian to Middle Pennsylvanian succession (Fig. 7), suggesting persistent sediment dispersal. The most prominent age groups of detrital zircons have ages of 1265–935 Ma and 495–374 Ma (Fig. 7). Ages are spread broadly from 1950 to 1265 Ma with a strong secondary mode between 1635 and 1618 Ma (Fig. 7). An older age group has modes between 2820 and 2569 Ma. The groups of ages in these samples generally match the Appalachian signature (Figs. 10A, 13, and 14B); however, these age groups are also available from Gondwanan terranes (Table 3). The sandstones (Fig. 7) have minor groups with ages of 2190–1950 Ma (Moroni-Itacaiúnas/Trans-Amazonian/Eburnian) and of 682–528 Ma (Pan-African/Brasiliano) that suggest a possible Gondwanan provenance; however, the sandstones in the Appalachian basin have similar minor groups of these ages (Thomas et al., 2017). Age data from the Corbin Sandstone in the Appalachian basin, the Caseyville Sandstone in the southern Illinois basin, and the Pennsylvanian sandstones in the northern shelf of the Arkoma basin are very close together in an MDS plot (Fig. 14B), indicating a common provenance and dispersal system. Distributions of εHf_t values from the Pennsylvanian Cane Hill and Savanna sandstones in the Arkoma basin are nearly identical to those from the Appalachian foreland and from the southern Illinois basin (Fig. 15B) (Thomas et al., 2017, 2020). The detrital-zircon U-Pb ages and εHf_t values strongly indicate an Appalachian source and dispersal through the southern part of the Illinois basin to the northern shelf of the Arkoma basin (Fig. 12C). One possible exception is the Savanna Sandstone, which has a somewhat greater proportion of grains with Pan-African/Brasiliano ages and a minor mode of 589 Ma (Fig. 7). The Pan-African/Brasiliano grains in the Savanna Sandstone, along with the chert pebbles in the stratigraphically higher Thurman Sandstone (Fig. 2, box C1) (Sutherland, *in* Johnson et al., 1988), show that some sediment spread from the Ouachita orogenic belt into the distal foreland to mix with the extrabasinal sediment (Fig. 12C).

To document the provenance of the synorogenic turbidites in the Ouachita foredeep, detrital zircons were analyzed from the Middle Pennsylvanian Atoka Formation in the Ouachita thrust belt from sample sites with northeast-directed, west-directed, and south-directed (Spiro) paleocurrents (Sharrah, 2006). All three sets of samples have a dominance of Mesoproterozoic (1205–933 Ma) zircons, a range of older zircons between 1947 and

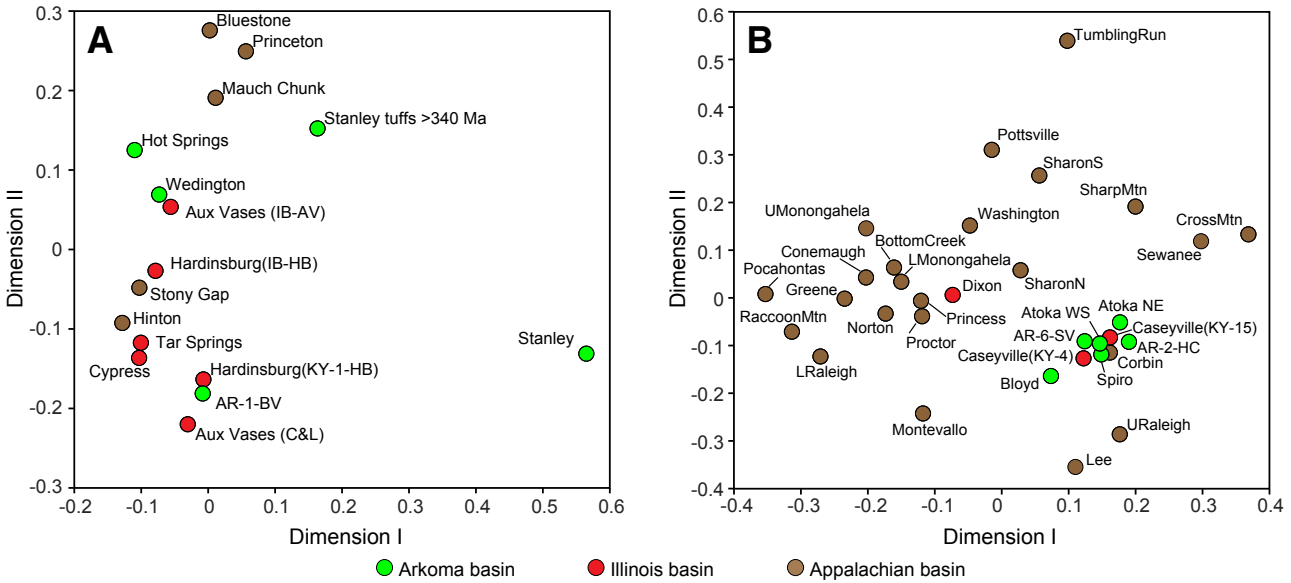

Figure 14. Two-dimensional multidimensional scaling (MDS) plots for detrital-zircon U-Pb age distributions for (A) Mississippian and (B) Pennsylvanian sandstones in the Arkoma basin in comparison with distributions in the southern Illinois basin and the Appalachian basin (B includes Lower Permian samples) along the inferred dispersal pathway from the Appalachians via the southern Illinois basin to the distal Arkoma basin. Data sources for panel A: Arkoma basin from original data herein and references cited in Figure 7; southern Illinois basin from Thomas et al. (2020) and sample Aux Vases (C&L) from Chapman and Laskowski (2019); Appalachian basin from Park et al. (2010) and Thomas et al. (2017). Data sources for panel B: Arkoma basin from original data herein and references cited in Figure 7; southern Illinois basin from Thomas et al. (2020); Appalachian basin from references cited for Figure 10A. Specifications for the MDS plots are described in the caption for Figure 13. See text for discussion of interpretations.

1210 Ma, and a scattering of zircons older than 2340 Ma, all of which have counterparts in both Amazonia/Gondwana and Laurentia (Fig. 7; Table 3). All of the samples have a group of younger zircons (492–336 Ma; Fig. 7), suggesting possible recycling from Appalachian sources (Sharrah, 2006); however, the same age range of zircons is available from the Coahuila terrane (Thomas et al., 2019) and may be from the Sabine terrane. The samples from sandstones with northeast-directed paleocurrents have a secondary group of 34 grains with ages of 799–505 Ma and a mode of 632 Ma, as well as 15 grains with ages of 2218–1962 Ma (Fig. 7), both distinctly Gondwanan (Table 3). The other two sets of Atoka samples have fewer grains in these age groups (Fig. 7). For these distinctive Gondwanan age groups in the northeast-dispersed Atoka sandstones (Table 3), the interpreted provenance is the west end of the accreted Sabine terrane, which is inferred to have collided with the Laurentian rift margin near the present location of the Waco uplift (Fig. 12B); the Atoka west-dispersed and south-dispersed (Spiro) sands are interpreted to be from Appalachian sources (Sharrah, 2006). An MDS plot shows that the northeast-dispersed, west-dispersed, and south-dispersed (Spiro) Atoka sandstones form a tight cluster that also includes a sample of the Corbin Sandstone from the Appalachian basin and two samples of Caseyville Sandstone from the southern Illinois basin (Fig. 14B), suggesting a common provenance for all of these sandstones. The Gondwanan grains in the northeast-dispersed sandstones suggest, however, that dispersal from the Sabine terrane was mixed with Appalachian detritus that prograded across the northern distal shelf into the distal side of the foredeep, similar to the dispersal of sand in the Spiro Sandstone (Fig. 12B).

In summary, some of the most proximal Mississippian–Pennsylvanian sediments in the Arkoma basin have detrital-zircon age distributions that are generally similar to those in the Fort Worth and Marathon foreland basins, suggesting the same or similar provenance within the accreted Gondwanan terranes of the Ouachita orogen (Fig. 12A). The orogenic source is compatible with longitudinal paleocurrents in the Ouachita foredeep. The Mississippian Hot Springs Sandstone, which lacks distinctive Gondwanan ages of detrital zircons, may represent southward dispersal across the northern distal shelf and down the cratonic side of the

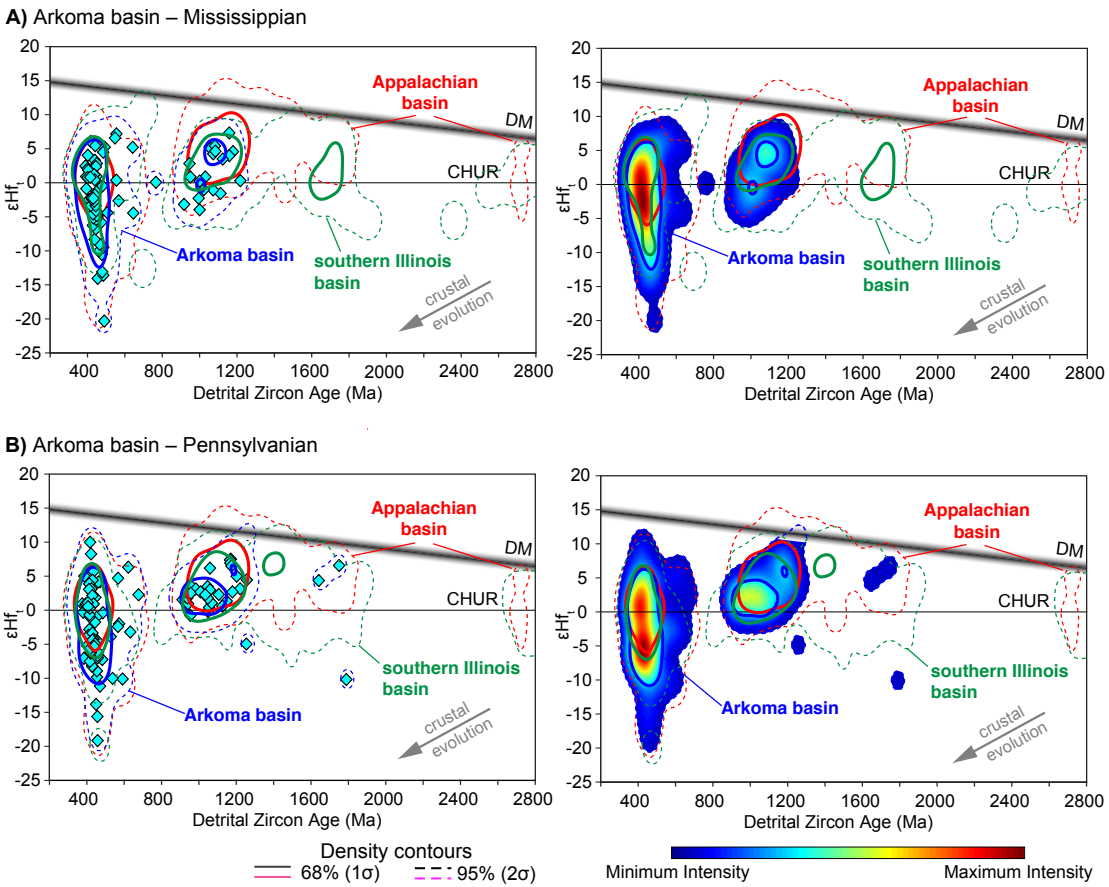

Figure 15. Comparisons of εHf$_t$ data from the Arkoma basin (Fig. 7) with respect to the southern Illinois basin and Appalachian basin (from Thomas et al., 2017, 2020): (A) Mississippian; (B) Pennsylvanian (Appalachian data include Lower Permian). CHUR—chondritic uniform reservoir; DM—depleted mantle. Specifications for the plots are described in the caption for Figure 11. See text for discussion of interpretations.

Ouachita foredeep, mixing with the synorogenic muddy turbidites (Fig. 12A). In the distal fringe of the Arkoma basin along the southern margin of the Laurentian craton, depositional systems indicate dominant sediment dispersal southward from the craton into the subsiding Arkoma foreland basin (Figs. 12B and 12C). Although all of the components of these sandstones could have come from the Sabine terrane, the paucity of truly distinctive Gondwanan components suggests a different source, most likely the Appalachians with dispersal through the southern part of the Illinois basin to the distal fringe of the Arkoma basin (Figs. 12B and 12C). The chert pebbles and some detrital zircons, however, indicate at least some mixing from Ouachita orogenic sources to the most distal foreland (Fig. 12C). In this regard, the Arkoma foreland basin differs from the Fort Worth basin, where even the most distal fringe has a distinctive detrital-zircon age distribution from accreted Gondwanan terranes. The Arkoma basin evidently marks the southwestward limit of dispersal through the Appalachian foreland, and the basins in the Ouachita-Marathon foreland farther southwest have distinct Gondwanan provenances in the accreted terranes (Fig. 12).

CONCLUSIONS

The age distributions of detrital zircons in Middle Pennsylvanian to Middle Permian sandstones in the Marathon foreland indicate a sediment supply from the accreted Coahuila (Gondwanan) terrane in the interior of the Marathon orogenic belt (Thomas et al., 2019). All of the ages of the Marathon detritus

could have been derived from the Coahuila terrane, requiring no other contribution from mixed sources such as the Appalachians. The documented composition of the Coahuila terrane may serve as a model for other probable, less-well-documented, accreted Gondwanan terranes, such as the Sabine terrane.

The age distributions of detrital zircons in Middle Pennsylvanian to Lower Permian sandstones in the Fort Worth basin in the Ouachita foreland are similar to those in the Marathon foreland, indicating the same source or another source with similar composition. The Sabine terrane along the interior part of the Ouachita orogen is the likely source for the foreland detritus in the Fort Worth basin. The stratigraphically highest and most distal sandstones in the Fort Worth basin have the Gondwanan detrital-zircon signature, consistent with progradation of synorogenic clastic sediment to the cratonic side of the basin throughout the history of basin filling as the basin became overfilled.

The age distributions of detrital zircons in Lower and Middle Permian sandstones in the Anadarko basin indicate dispersal of detritus onto the adjacent southern craton from the same sources that supplied the Marathon and Fort Worth foreland detritus. Published results from the intracratonic Permian basin have been interpreted similarly. Sediment dispersal from orogenic sources adjacent to either or both the Marathon and Fort Worth forelands spread onto the craton into intracratonic basins.

The age distributions of detrital zircons in Mississippian to Middle Pennsylvanian sandstones differ both laterally and vertically within the Arkoma basin. Some sandstones in the most proximal part of the basin have a Gondwanan signature; whereas those in the most distal basin generally do not have distinctive Gondwanan components, suggesting a provenance in the Appalachian orogen and sediment dispersal through the Appalachian foreland and southern Illinois basin to the cratonic side of the Arkoma foreland basin. Some sandstones indicate intermittent mixing from opposite sides of the basin.

The combined data from the Fort Worth and Arkoma foreland basins and from the Anadarko intracratonic basin suggest a broad pattern of sediment dispersal from the Ouachita-Marathon orogen (largely accreted Gondwanan terranes) onto the southern craton during the Late Mississippian through Early Permian and at least into the Middle Permian. Dispersal from the Appalachians via the Illinois basin brought sediment to the cratonic side of the Arkoma basin and distal foreland, and the Arkoma basin evidently marks the southwestern limit of dispersal of recognizable Appalachian detritus along the Ouachita-Marathon foreland.

ACKNOWLEDGMENTS

Sample collection and analyses were funded by National Science Foundation (NSF) award EAR-1304980 to Gehrels and Thomas. Thomas collected the samples with the assistance of Beth Welke. In the Anadarko basin, we were guided through the stratigraphy and depositional systems and to collecting sites by Neil Suneson, Jim Puckette, and Zach Poland. Majie Fan led us through the outcrops in the Fort Worth basin and also provided an instructive review of an early draft of the manuscript. In the Arkoma basin, Doy Zachry provided an overview of stratigraphy and locations for collecting; after our field season was frozen to an end by an ice storm, Doy along with Peggy Gucchione collected the sample from the Savanna Sandstone. All analyses were conducted at the Arizona LaserChron Center with the support of NSF awards EAR-1338583 and EAR-1649254. Tim Lawton and Ed Osborne provided helpful reviews and sharpened the discussion in a draft manuscript. We appreciate the efforts of reviewer Ryan Leary, an anonymous reviewer, Associate Editor Todd LaMaskin, and Editor David Fastovsky in seeing this article through the *Geosphere* review process.

REFERENCES CITED

Alsalem, O.B., Fan, M., Samora, J., Xie, X., and Griffin, W.R., 2018, Paleozoic sediment dispersal before and during the collision between Laurentia and Gondwana in the Fort Worth basin, USA: Geosphere, v. 14, p. 325–342, https://doi.org/10.1130/GES01480.1.

Amidon, W.H., Burbank, D.W., and Gehrels, G.E., 2005, U-Pb zircon ages as a sediment mixing tracer in the Nepal Himalaya: Earth and Planetary Science Letters, v. 235, no. 1–2, p. 244–260, https://doi.org/10.1016/j.epsl.2005.03.019.

Arbenz, J.K., 1989a, The Ouachita system, *in* Bally, A.W., and Palmer, A.R., eds., The Geology of North America—An Overview: Boulder, Colorado, Geological Society of America, The Geology of North America, v. A, p. 371–396, https://doi.org/10.1130/DNAG-GNA-A.371.

Arbenz, J.K., 1989b, Ouachita thrust belt and Arkoma basin, *in* Hatcher, R.D., Jr., Thomas, W.A., and Viele, G.W., eds., The Appalachian-Ouachita Orogen in the United States: Boulder, Colorado, Geological Society of America, The Geology of North America, v. F-2, p. 621–634, https://doi.org/10.1130/DNAG-GNA-F2.621.

Arbenz, J.K., 2008, Structural Framework of the Ouachita Mountains: Oklahoma Geological Survey Circular 112A, 40 p.

Arbenz, J.K., Muehlberger, W.R., Nicholas, R.L., Tauvers, P.R., and Viele, G.W., 1989, Ouachita system—cross sections, *in* Hatcher, R.D., Jr., Thomas, W.A., and Viele, G.W., eds., The Appalachian-Ouachita Orogen in the United States: Boulder, Colorado, Geological Society of America, The Geology of North America, v. F-2, Plate 12.

Becker, T.P., Thomas, W.A., Samson, S.D., and Gehrels, G.E., 2005, Detrital zircon evidence of Laurentian crustal dominance in the lower Pennsylvanian deposits of the Alleghanian clastic wedge in eastern North America: Sedimentary Geology, v. 182, p. 59–86, https://doi.org/10.1016/j.sedgeo.2005.07.014.

Becker, T.P., Thomas, W.A., and Gehrels, G.E., 2006, Linking late Paleozoic sedimentary provenance in the Appalachian basin to the history of Alleghanian deformation: American Journal of Science, v. 306, p. 777–798, https://doi.org/10.2475/10.2006.01.

Bouvier, A., Vervoort, J.D., and Patchett, J.D., 2008, The Lu-Hf and Sm-Nd isotopic composition of CHUR: Constraints from unequilibrated chondrites and implications for the bulk composition of terrestrial planets: Earth and Planetary Science Letters, v. 273, p. 48–57, https://doi.org/10.1016/j.epsl.2008.06.010.

Bowring, S., 1984, U-Pb zircon ages of granitic boulders in the Ordovician Blakely Sandstone, Arkansas, and implications for their provenance, *in* Stone, C.G., and Haley, B.R., eds., A Guidebook to the Geology of the Central and Southern Ouachita Mountains, Arkansas: Arkansas Geological Commission Guidebook 84–2, p. 123.

Brown, L.F., Jr., Cleaves, A.W., II, and Erxleben, A.W., 1973, Pennsylvanian Depositional Systems in North-Central Texas: Texas Bureau of Economic Geology Guidebook 14, 122 p.

Cameron, K.L., López, R., Ortega-Gutiérrez, F., Solari, L.A., Keppie, J.D., and Schulze, C., 2004, U-Pb geochronology and Pb isotope compositions of leached feldspars: Constraints on the origin and evolution of Grenvillian rocks from eastern and southern Mexico, *in* Tollo, R.P., Corriveau, L., McLelland, J., and Bartholomew, M.J., eds., Proterozoic Tectonic Evolution of the Grenville Orogen in North America: Geological Society of America Memoir 197, p. 755–769, https://doi.org/10.1130/0-8137-1197-5.755.

Cardona, A., Chew, D., Valencia, V.A., Bayona, G., Miskovic, A., and Ibañez-Mejía, M., 2010, Grenvillian remnants in the Northern Andes: Rodinian and Phanerozoic paleogeographic perspectives: Journal of South American Earth Sciences, v. 29, p. 92–104, https://doi.org/10.1016/j.jsames.2009.07.011.

Cecil, R., Gehrels, G., Patchett, J., and Ducea, M., 2011, U-Pb-Hf characterization of the central Coast Mountains batholith: Implications for petrogenesis and crustal architecture: Lithosphere, v. 3, p. 247–260, https://doi.org/10.1130/L134.1.

Centeno-García, E., 2005, Review of Upper Paleozoic and Lower Mesozoic stratigraphy and depositional environments of central and west Mexico: Constraints on terrane analysis and paleogeography, *in* Anderson, T.H., Nourse, J.A., McKee, J.W., and Steiner, M.B., eds., The Mojave-Sonora Megashear Hypothesis: Development, Assessment, and Alternatives: Geological Society of America Special Paper 393, p. 233–258, https://doi.org/10.1130/0-8137-2393-0.233.

Chapman, A.D., and Laskowski, A.K., 2019, Detrital zircon U-Pb data reveal a Mississippian sediment dispersal network

originating in the Appalachian orogen, traversing North America along its southern shelf, and reaching as far as the southwest United States: Lithosphere, v. 11, p. 581–587, https://doi.org/10.1130/L1068.1.

Clift, P.D., Heinrich, P., Dunn, D., Jacobus, A., and Blusztajn, J., 2018, The Sabine block, Gulf of Mexico: Promontory on the North American margin?: Geology, v. 46, p. 15–18, https://doi.org/10.1130/G39592.1.

Cohen, K.M., Finney, S.C., Gibbard, P.L., and Fan, J.-X., 2013, updated, The ICS [International Commission on Stratigraphy] International Chronostratigraphic Chart: Episodes, v. 36, p. 199–204, https://doi.org/10.18814/epiiugs/2013/v36i3/002.

Cordani, U.G., and Teixeira, W., 2007, Proterozoic accretionary belts in the Amazonian craton, *in* Hatcher, R.D., Jr., Carlson, M.P., McBride, J.H., and Martínez Catalán, J.R., eds., 4-D Framework of Continental Crust: Geological Society of America Memoir 200, p. 297–320, https://doi.org/10.1130/2007.1200(14).

Crosby, E.J., and Mapel, W.J., 1975, Central and west Texas, *in* McKee, E.D., and Crosby, E.J., coordinators, Paleotectonic Investigations of the Pennsylvanian System in the United States, Part I. Introduction and Regional Analyses of the Pennsylvanian System: U.S. Geological Survey Professional Paper 853, p. 197–232.

Culotta, R., Latham, T., Sydow, M., Oliver, J., Brown, L., and Kaufman, S., 1992, Deep structure of the Texas Gulf passive margin and its Ouachita-Precambrian basement: Results of the COCORP San Marcos arch survey: American Association of Petroleum Geologists Bulletin, v. 76, p. 270–283.

Denison, R.E., 1982, Geologic Cross Section from the Arbuckle Mountains to the Muenster Arch, Southern Oklahoma and Texas: Geological Society of America Map and Chart Series MC-28R, 8 p.

Denison, R.E., 1989, Foreland structure adjacent to the Ouachita foldbelt, *in* Hatcher, R.D., Jr., Thomas, W.A., and Viele, G.W., eds., The Appalachian-Ouachita Orogen in the United States: Boulder, Colorado, Geological Society of America, The Geology of North America, v. F-2, p. 681–688, https://doi.org/10.1130/DNAG-GNA-F2.681.

Dickinson, W.R., and Lawton, T.F., 2001, Carboniferous to Cretaceous assembly and fragmentation of Mexico: Geological Society of America Bulletin, v. 113, p. 1142–1160, https://doi.org/10.1130/0016-7606(2001)113<1142:CTCAAF>2.0.CO;2.

Dodson, S.A., 2008, Petrographic and Geochronologic Provenance Analysis of Upper Pennsylvanian Fluvial Sandstones of the Conemaugh and Monongahela Groups, Athens County, Ohio [M.S. thesis]: Athens, Ohio, Ohio University, 86 p.

Dunn, D.P., 2009, Arkansas crustal xenoliths: Implications for basement rocks of the northern Gulf Coast, USA: Lithosphere, v. 1, p. 60–64, https://doi.org/10.1130/L10.1.

Eriksson, K.A., Campbell, I.H., Palin, J.M., Allen, C.M., and Bock, B., 2004, Evidence for multiple recycling in Neoproterozoic through Pennsylvanian sedimentary rocks of the central Appalachian basin: The Journal of Geology, v. 112, p. 261–276, https://doi.org/10.1086/382758.

Flawn, P.T., Goldstein, A., Jr., King, P.B., and Weaver, C.E., 1961, The Ouachita System: University of Texas, Bureau of Economic Geology Publication 6120, 401 p.

Galloway, W.E., and Brown, L.F., Jr., 1973, Depositional systems and shelf-slope relations on cratonic basin margin, uppermost Pennsylvanian of north-central Texas: American Association of Petroleum Geologists Bulletin, v. 57, p. 1185–1218.

Garner, H.F., 1967, Moorefield–Batesville stratigraphy and sedimentation in Arkansas: Geological Society of America Bulletin, v. 78, p. 1233–1245, https://doi.org/10.1130/0016-7606(1967)78[1233:MSASIA]2.0.CO;2.

Gehrels, G.E., 2000, Introduction to detrital zircon studies of Paleozoic and Triassic strata in western Nevada and northern California, *in* Soreghan, M.J., and Gehrels, G.E., eds., Paleozoic and Triassic Paleogeography and Tectonics of Western Nevada and Northern California: Geological Society of America Special Paper 347, p. 1–17, https://doi.org/10.1130/0-8137-2347-7.1.

Gehrels, G.E., and Pecha, M.E., 2014, Detrital zircon U-Pb geochronology and Hf isotope geochemistry of Paleozoic and Triassic passive margin strata of western North America: Geosphere, v. 10, p. 49–65, https://doi.org/10.1130/GES00889.1.

Gehrels, G.E., Valencia, V., and Ruiz, J., 2008, Enhanced precision, accuracy, efficiency, and spatial resolution of U-Pb ages by laser ablation–multicollector–inductively coupled plasma–mass spectrometry: Geochemistry Geophysics Geosystems, v. 9, Q03017, https://doi.org/10.1029/2007GC001805.

Gleason, J.D., Finney, S.C., and Gehrels, G.E., 2002, Paleotectonic implications of a Mid- to Late-Ordovician provenance shift, as recorded in sedimentary strata of the Ouachita and southern Appalachian Mountains: The Journal of Geology, v. 110, p. 291–304, https://doi.org/10.1086/339533.

Gleason, J.D., Gehrels, G.E., Dickinson, W.R., Patchett, P.J., and Kring, D.A., 2007, Sources of detrital zircon grains in turbidite and deltaic sandstones of the Lower to Middle Pennsylvanian Haymond Formation, Marathon assemblage, Texas: Journal of Sedimentary Research, v. 77, p. 888–900, https://doi.org/10.2110/jsr.2007.084.

Glick, E.E., 1979, Arkansas, *in* Craig, L.C., and Connor, C.W., coordinators, Paleotectonic Investigations of the Mississippian System in the United States; Part I. Introduction and Regional Analyses of the Mississippian System: U.S. Geological Survey Professional Paper 1010, p. 125–145.

Gradstein, F.M., Ogg, J.G., and Smith, A.G., 2004, A Geologic Time Scale 2004: Cambridge, UK, Cambridge University Press, 589 p., https://doi.org/10.4095/215638.

Graham, S.A., Ingersoll, R.V., and Dickinson, W.R., 1976, Common provenance for lithic grains in Carboniferous sandstones from Ouachita Mountains and Black Warrior basin: Journal of Sedimentary Petrology, v. 46, p. 620–632.

Gray, M.B., and Zeitler, P.K., 1997, Comparison of clastic wedge provenance in the Appalachian foreland using U/Pb ages of detrital zircons: Tectonics, v. 16, p. 151–160, https://doi.org/10.1029/96TC02911.

Grimm, R.P., Eriksson, K., and Carbaugh, J., 2013, Tectono-sedimentary evolution of Early Pennsylvanian alluvial systems at the onset of the Alleghanian orogeny, Pocahontas basin, Virginia: Basin Research, v. 25, p. 450–470, https://doi.org/10.1111/bre.12008.

Handford, C.R., 1986, Facies and bedding sequences in shelf-storm–deposited carbonates—Fayetteville Shale and Pitkin Limestone (Mississippian), Arkansas: Journal of Sedimentary Petrology, v. 56, p. 123–137, https://doi.org/10.1306/212F88A0-2B24-11D7-8648000102C1865D.

Handford, C.R., 1995, Baselap patterns and the recognition of lowstand exposure and drowning—A Mississippian-ramp example and its seismic signature: Journal of Sedimentary Research, v. B65, p. 323–337.

Hanson, R.E., Puckett, R.E., Jr., Keller, G.R., Brueseke, M.E., Bulen, C.L., Mertzman, S.A., Finegan, S.A., and McCleery, D.A., 2013, Intraplate magmatism related to opening of the southern Iapetus Ocean: Cambrian Wichita igneous province in the Southern Oklahoma rift zone: Lithos, v. 174, p. 57–70, https://doi.org/10.1016/j.lithos.2012.06.003.

Harry, D.L., Londono, J., and Huerta, A., 2003, Early Paleozoic transform-margin structure beneath the Mississippi coastal plain, southeast United States: Geology, v. 31, p. 969–972, https://doi.org/10.1130/G19787.1.

Hatcher, R.D., Jr., 2010, The Appalachian orogen: A brief summary, *in* Tollo, R.P., Bartholomew, M.J., Hibbard, J.P., and Karabinos, P.M., eds., From Rodinia to Pangea: The Lithotectonic Record of the Appalachian Region: Geological Society of America Memoir 206, p. 1–19, https://doi.org/10.1130/2010.1206(01).

Hibbard, J.P., van Staal, C.R., and Miller, B.V., 2007, Links among Carolinia, Avalonia, and Ganderia in the Appalachian peri-Gondwanan realm, *in* Sears, J.W., Harms, T.A., and Evenchick, C.A., eds., Whence the Mountains? Inquiries into the Evolution of Orogenic Systems: A Volume in Honor of Raymond A. Price: Geological Society of America Special Paper 433, p. 291–311, https://doi.org/10.1130/2007.2433(14).

Hogan, J.P., and Gilbert, M.C., 1998, The Southern Oklahoma aulacogen: A Cambrian analog for mid-Proterozoic AMCG (anorthosite-mangerite-charnockite-granite) complexes?, *in* Hogan, J.P., and Gilbert, M.C., eds., Central North America and Other Regions: Proceedings of the Twelfth International Conference on Basement Tectonics: Dordrecht, Netherlands, Kluwer, p. 39–78.

Houseknecht, D.W., 1986, Evolution from passive margin to foreland basin: The Atoka Formation of the Arkoma basin, south-central U.S.A., *in* Allen, P.A., and Homewood, P., eds., Foreland Basins: International Association of Sedimentologists Special Publication 8, p. 327–345.

Johnson, K.S., Amsden, T.W., Denison, R.E., Dutton, S.P., Goldstein, A.G., Rascoe, B., Jr., Sutherland, P.K., and Thompson, D.M., 1988, Southern Midcontinent region, *in* Sloss, L.L., ed., Sedimentary Cover—North American Craton: U.S.: Boulder, Colorado, Geological Society of America, The Geology of North America, v. D-2, p. 307–359, https://doi.org/10.1130/DNAG-GNA-D2.307.

Jusczuk, S.J., 2002, How Do the Structures of the Late Paleozoic Ouachita Thrust Belt Relate to the Structures of the Southern Oklahoma Aulacogen [Ph.D. dissertation]: Lexington, Kentucky, University of Kentucky, 339 p.

Keller, G.R., Braile, L.W., McMechan, G.A., Thomas, W.A., Harder, S.H., Chang, W.-F., and Jardine, W.G., 1989, Paleozoic continent-ocean transition in the Ouachita Mountains imaged from PASSCAL wide-angle seismic reflection-refraction data: Geology, v. 17, p. 119–122, https://doi.org/10.1130/0091-7613(1989)017<0119:PCOTIT>2.3.CO;2.

Kier, R.S., Brown, L.F., Jr., and McBride, E.F., 1979, The Mississippian and Pennsylvanian (Carboniferous) Systems in the United States—Texas: U.S. Geological Survey Professional Paper 1110-S, p. S1–S45.

Kissock, J.K., Finzel, E.S., Malone, D.H., and Craddock, J.P., 2018, Lower–Middle Pennsylvanian strata in the North American midcontinent record the interplay between erosional unroofing of the Appalachians and eustatic sea-level

rise: Geosphere, v. 14, p. 141–161, https://doi.org/10.1130/GES01512.1.
Konstantinou, A., Wirth, K.R., Vervoort, J.D., Malone, D.H., Davidson, C., and Craddock, J.P., 2014, Provenance of quartz arenites of the early Paleozoic midcontinent region, USA: The Journal of Geology, v. 122, p. 201–216, https://doi.org/10.1086/675327.
Krogh, T.E., Kamo, S.L., Sharpton, V.L., Marin, L.E., and Hildebrand, A.R., 1993, U-Pb ages of single shocked zircons linking distal K/T ejecta to the Chicxulub crater: Nature, v. 366, p. 731–734, https://doi.org/10.1038/366731a0.
Lawlor, P.J., Ortega-Gutierrez, F., Cameron, K.L., Ochoa-Camarillo, H., Lopez, R., and Sampson, D.E., 1999, U-Pb geochronology, geochemistry, and provenance of the Grenvillian Huiznopala Gneiss of eastern Mexico: Precambrian Research, v. 94, p. 73–99, https://doi.org/10.1016/S0301-9268(98)00108-9.
Lawton, T.F., and Molina-Garza, R.S., 2014, U-Pb geochronology of the type Nazas Formation and superjacent strata, northeastern Durango, Mexico: Implications of a Jurassic age for continental-arc magmatism in north-central Mexico: Geological Society of America Bulletin, v. 126, p. 1181–1199, https://doi.org/10.1130/B30827.1.
Lillie, R.J., Nelson, K.D., de Voogd, B., Brewer, J.A., Oliver, J.E., Brown, L.D., Kaufman, S., and Viele, G.W., 1983, Crustal structure of Ouachita Mountains, Arkansas: A model based on integration of COCORP reflection profiles and regional geophysical data: American Association of Petroleum Geologists Bulletin, v. 67, p. 907–931.
Liu, L., and Stockli, D.F., 2019, U-Pb ages of detrital zircons in lower Permian sandstone and siltstone of the Permian Basin, west Texas, USA: Evidence of dominant Gondwanan and peri-Gondwanan sediment input to Laurentia: Geological Society of America Bulletin, v. 132, p. 245–262, https://doi.org/10.1130/B35119.1.
Loomis, J., Weaver, B., and Blatt, H., 1994, Geochemistry of Mississippian tuffs from the Ouachita Mountains, and implications for the tectonics of the Ouachita orogen, Oklahoma and Arkansas: Geological Society of America Bulletin, v. 106, p. 1158–1171, https://doi.org/10.1130/0016-7606(1994)106<1158:GOMTFT>2.3.CO;2.
Lopez, R., 1997, High-Mg Andesites from the Gila Bend Mountains, Southwestern Arizona: Evidence for Hydrous Melting of Lithosphere during Miocene Extension and the Pre-Jurassic Geotectonic Evolution of the Coahuila Terrane, Northwestern Mexico: Grenville Basement, a Late Paleozoic Arc, Triassic Plutonism, and the Events South of the Ouachita Suture [Ph.D. thesis]: Santa Cruz, California, University of California–Santa Cruz, 147 p.
Lopez, R., Cameron, K.L., and Jones, N.W., 2001, Evidence for Paleoproterozoic, Grenvillian, and Pan-African age Gondwanan crust beneath northeastern Mexico: Precambrian Research, v. 107, p. 195–214, https://doi.org/10.1016/S0301-9268(00)00140-6.
Mack, G.H., Thomas, W.A., and Horsey, C.A., 1983, Composition of Carboniferous sandstones and tectonic framework of southern Appalachian-Ouachita orogen: Journal of Sedimentary Petrology, v. 53, p. 931–946.
Mapel, W.J., Johnson, R.B., Bachman, G.O., and Varnes, K.L., 1979, Southern Midcontinent and Southern Rocky Mountains Region: Paleotectonic Investigations of the Mississippian System in the United States: U.S. Geological Survey Professional Paper 1010-J, p. 161–187.
Martens, U., Weber, B., and Valencia, V.A., 2010, U/Pb geochronology of Devonian and older Paleozoic beds in the southeastern Maya block, Central America: Its affinity with peri-Gondwanan terranes: Geological Society of America Bulletin, v. 122, p. 815–829, https://doi.org/10.1130/B26405.1.
McGuire, P.R., 2017, U-Pb Detrital Zircon Signature of the Ouachita Orogenic Belt [M.S. thesis]: Fort Worth, Texas, Texas Christian University, 78 p.
Mickus, K.L., and Keller, G.R., 1992, Lithospheric structure of the south-central United States: Geology, v. 20, p. 335–338, https://doi.org/10.1130/0091-7613(1992)020<0335:LSOTSC>2.3.CO;2.
Morris, E.M., and Stone, C.G., 1986, A preliminary report on the metagabbros of the Ouachita core, *in* Stone, C.G., Howard, J.M., and Haley, B.R., eds., Sedimentary and Igneous Rocks of the Ouachita Mountains of Arkansas, Part 1: Arkansas Geological Commission Guidebook 86–3, p. 87–90.
Morris, R.C., 1989, Stratigraphy and sedimentary history of post–Arkansas Novaculite Carboniferous rocks of the Ouachita Mountains, *in* Hatcher, R.D., Jr., Thomas, W.A., and Viele, G.W., eds., The Appalachian-Ouachita Orogen in the United States: Boulder, Colorado, Geological Society of America, The Geology of North America, v. F-2, p. 591–602, https://doi.org/10.1130/DNAG-GNA-F2.591.
Mueller, P.A., Heatherington, A.L., Foster, D.A., Thomas, W.A., and Wooden, J.L., 2014, The Suwannee suture: Significance for Gondwana-Laurentia terrane transfer and formation of Pangaea: Gondwana Research, v. 26, p. 365–373, https://doi.org/10.1016/j.gr.2013.06.018.
Nelson, K.D., Lillie, R.J., de Voogd, B., Brewer, J.A., Oliver, J.E., Kaufman, S., Brown, L.D., and Viele, G.W., 1982, COCORP seismic reflection profiling in the Ouachita Mountains of western Arkansas: Geometry and geologic interpretation: Tectonics, v. 1, p. 413–430, https://doi.org/10.1029/TC001i005p00413.
Nicholas, R.L., and Rozendal, R.A., 1975, Subsurface positive elements within Ouachita foldbelt in Texas and their relation to Paleozoic cratonic margin: American Association of Petroleum Geologists Bulletin, v. 59, p. 193–216.
Nicholas, R.L., and Waddell, D.E., 1989, The Ouachita system in the subsurface of Texas, Arkansas, and Louisiana, *in* Hatcher, R.D., Jr., Thomas, W.A., and Viele, G.W., eds., The Appalachian-Ouachita Orogen in the United States: Boulder, Colorado, Geological Society of America, The Geology of North America, v. F-2, p. 661–672, https://doi.org/10.1130/DNAG-GNA-F2.661.
Nielsen, K.C., Viele, G.W., and Zimmerman, J., 1989, Structural setting of the Benton-Broken Bow uplifts, *in* Hatcher, R.D., Jr., Thomas, W.A., and Viele, G.W., eds., The Appalachian-Ouachita Orogen in the United States: Boulder, Colorado, Geological Society of America, The Geology of North America, v. F-2, p. 635–660, https://doi.org/10.1130/DNAG-GNA-F2.635.
Niem, A.R., 1977, Mississippian pyroclastic flow and ash-fall deposits in the deep-marine Ouachita flysch basin, Oklahoma and Arkansas: Geological Society of America Bulletin, v. 88, p. 49–61, https://doi.org/10.1130/0016-7606(1977)88<49:MPFAAD>2.0.CO;2.
Ogren, D.E., 1968, Stratigraphy of Upper Mississippian rocks of northern Arkansas: American Association of Petroleum Geologists Bulletin, v. 52, p. 282–294.
Ortega-Gutierrez, F., Ruiz, J., and Centeno-Garcia, E., 1995, Oaxaquia, a Proterozoic microcontinent accreted to North America during the late Paleozoic: Geology, v. 23, p. 1127–1130, https://doi.org/10.1130/0091-7613(1995)023<1127:OAPMAT>2.3.CO;2.
Park, H., Barbeau, D.L., Jr., Rickenbaker, A., Bachmann-Krug, D., and Gehrels, G., 2010, Application of foreland basin detrital-zircon geochronology to the reconstruction of the southern and central Appalachian orogen: The Journal of Geology, v. 118, p. 23–44, https://doi.org/10.1086/648400.
Perry, W.J., Jr., 1989, Tectonic Evolution of the Anadarko Basin Region, Oklahoma: U.S. Geological Survey Bulletin 1866A, 19 p.
Pickell, J.M., 2012, Detrital Zircon Geochronology of Middle Ordovician Siliciclastic Sediment on the Southern Laurentian Shelf [M.S. thesis]: College Station, Texas, Texas A&M University, 120 p.
Pindell, J.L., and Kennan, L., 2009, Tectonic evolution of the Gulf of Mexico, Caribbean and northern South America in the mantle reference frame: An update, *in* James, K.H., Lorente, M.A., and Pindell, J.L., eds., The Origin and Evolution of the Caribbean Plate: Geological Society [London] Special Publication 328, p. 1–55, https://doi.org/10.1144/SP328.1.
Poland, Z.A., and Simms, A.R., 2012, Sedimentology of an erg to an erg-margin depositional system, the Rush Springs Sandstone of western Oklahoma, U.S.A.: Implications for paleowinds across northwestern Pangea during the Guadalupian (Middle Permian): Journal of Sedimentary Research, v. 82, p. 345–363, https://doi.org/10.2110/jsr.2012.32.
Poole, F.G., Perry, W.J., Jr., Madrid, R.J., and Amaya-Martínez, R., 2005, Tectonic synthesis of the Ouachita-Marathon-Sonora orogenic margin of southern Laurentia: Stratigraphic and structural implications for timing of deformational events and plate-tectonic model, *in* Anderson, T.H., Nourse, J.A., McKee, J.W., and Steiner, M.B., eds., The Mohave-Sonora Megashear Hypothesis: Development, Assessment, and Alternatives: Geological Society of America Special Paper 393, p. 543–596, https://doi.org/10.1130/0-8137-2393-0.543.
Ross, C.A., 1986, Paleozoic evolution of southern margin of Permian basin: Geological Society of America Bulletin, v. 97, p. 536–554, https://doi.org/10.1130/0016-7606(1986)97<536:PEOSMO>2.0.CO;2.
Rozendal, R.A., and Erskine, W.S., 1971, Deep test in the Ouachita structural belt of central Texas: American Association of Petroleum Geologists Bulletin, v. 55, p. 2008–2017.
Saylor, J.E., Jordan, J.C., Sundell, K.E., Wang, X., Wang, S., and Deng, T., 2018, Topographic growth of the Jishi Shan and its impact on basin and hydrology evolution, NE Tibetan Plateau: Basin Research, v. 30, no. 3, p. 544–563, https://doi.org/10.1111/bre.12264.
Schuchert, C., 1923, Sites and nature of the North American geosynclines [1922 Geological Society of America Presidential Address]: Geological Society of America Bulletin, v. 34, p. 151–229, https://doi.org/10.1130/GSAB-34-151.
Sharrah, K.L., 2006, Comparative Study of the Sedimentology and Provenance of the Atoka Formation in the Frontal Ouachita Thrust Belt, Oklahoma [Ph.D. thesis]: Tulsa, Oklahoma, University of Tulsa, 252 p.
Shaulis, B.J., Lapen, T.J., Casey, J.F., and Reid, D.R., 2012, Timing and rates of flysch sedimentation in the Stanley Group, Ouachita Mountains, Oklahoma and Arkansas, U.S.A.: Constraints from U-Pb zircon ages of subaqueous ash-flow tuffs: Journal of Sedimentary Research, v. 82, p. 833–840, https://doi.org/10.2110/jsr.2012.68.

Silverman, B.W., 1986, Density Estimation for Statistics and Data Analysis: London, Chapman and Hall, 175 p., https://doi.org/10.1007/978-1-4899-3324-9.

Soreghan, G.S., and Soreghan, M.J., 2013, Tracing clastic delivery to the Permian Delaware basin, U.S.A.: Implications for paleogeography and circulation in westernmost equatorial Pangea: Journal of Sedimentary Research, v. 83, p. 786–802, https://doi.org/10.2110/jsr.2013.63.

Steiner, M.B., and Walker, J.D., 1996, Late Silurian plutons in Yucatan: Journal of Geophysical Research, v. 101, p. 17727–17735, https://doi.org/10.1029/96JB00174.

Stewart, J.H., Blodgett, R.B., Boucot, A.J., Carter, J.L., and Lopez, R., 1999, Exotic Paleozoic strata of Gondwanan provenance near Ciudad Victoria, Tamaulipas, Mexico, *in* Ramos, V.A., and Keppie, J.D., eds., Laurentia–Gondwana Connections before Pangea: Geological Society of America Special Paper 336, p. 227–252, https://doi.org/10.1130/0-8137-2336-1.227.

Stone, C.G., and Haley, B.R., 1977, The occurrence and origin of the granite–meta-arkose erratics in the Ordovician Blakely Sandstone, Arkansas, *in* Stone, C.G., ed., Symposium on the Geology of the Ouachita Mountains, Stratigraphy, Sedimentology, Petrography, Tectonics, and Paleontology: Little Rock, Arkansas, Arkansas Geological Commission, v. 1, p. 107–111.

Sundell, K., Saylor, J.E., and Pecha, M., 2019, Provenance and recycling of detrital zircons from Cenozoic Altiplano strata and the crustal evolution of western South America from combined U-Pb and Lu-Hf isotopic analysis, *in* Horton, B., and Folguera, A., eds., Andean Tectonics: Amsterdam, Netherlands, Elsevier, p. 363–397, https://doi.org/10.1016/B978-0-12-816009-1.00014-9.

Sutherland, P.K., 1988, Late Mississippian and Pennsylvanian depositional history in the Arkoma basin area, Oklahoma and Arkansas: Geological Society of America Bulletin, v. 100, p. 1787–1802, https://doi.org/10.1130/0016-7606(1988)100<1787:LMAPDH>2.3.CO;2.

Thomas, W.A., 1977, Evolution of Appalachian-Ouachita salients and recesses from reentrants and promontories in the continental margin: American Journal of Science, v. 277, p. 1233–1278, https://doi.org/10.2475/ajs.277.10.1233.

Thomas, W.A., 1989, The Appalachian-Ouachita orogen beneath the Gulf Coastal Plain between the outcrops in the Appalachian and Ouachita Mountains, *in* Hatcher, R.D., Jr., Thomas, W.A., and Viele, G.W., eds., The Appalachian-Ouachita Orogen in the United States: Boulder, Colorado, Geological Society of America, The Geology of North America, v. F-2, p. 537–553, https://doi.org/10.1130/DNAG-GNA-F2.537.

Thomas, W.A., 2006, Tectonic inheritance at a continental margin [2005 Geological Society of America Presidential Address]: GSA Today, v. 16, no. 2, p. 4–11, https://doi.org/10.1130/1052-5173(2006)016[4:TIAACM]2.0.CO;2.

Thomas, W.A., 2011, The lapetan rifted margin of southern Laurentia: Geosphere, v. 7, p. 97–120, https://doi.org/10.1130/GES00574.1.

Thomas, W.A., 2014, A mechanism for tectonic inheritance at transform faults of the lapetan margin of Laurentia: Geoscience Canada, v. 41, p. 321–344, https://doi.org/10.12789/geocanj.2014.41.048.

Thomas, W.A., 2019, Tectonic inheritance at multiple scales during more than two complete Wilson cycles recorded in eastern North America, *in* Wilson, R.W., Houseman, G.A., McCaffrey, K.J.W., Doré, A.G., and Buiter, S.J.H., eds., Fifty Years of the Wilson Cycle Concept in Plate Tectonics: Geological Society [London] Special Publication 470, p. 337–352, https://doi.org/10.1144/SP470.4.

Thomas, W.A., and Astini, R.A., 1996, The Argentine Precordillera: A traveler from the Ouachita embayment of North American Laurentia: Science, v. 273, p. 752–757, https://doi.org/10.1126/science.273.5276.752.

Thomas, W.A., and Astini, R.A., 1999, Simple-shear conjugate rift margins of the Argentine Precordillera and the Ouachita embayment of Laurentia: Geological Society of America Bulletin, v. 111, p. 1069–1079, https://doi.org/10.1130/0016-7606(1999)111<1069:SSCRMO>2.3.CO;2.

Thomas, W.A., Viele, G.W., Arbenz, J.K., Nicholas, R.L., Denison, R.E., Muehlberger, W.R., and Tauvers, P.R., 1989, Tectonic map of the Ouachita orogen, *in* Hatcher, R.D., Jr., Thomas, W.A., and Viele, G.W., eds., The Appalachian-Ouachita Orogen in the United States: Boulder, Colorado, Geological Society of America, The Geology of North America, v. F-2, Plate 9.

Thomas, W.A., Becker, T.P., Samson, S.D., and Hamilton, M.A., 2004, Detrital zircon evidence of a recycled orogenic foreland provenance for Alleghanian clastic-wedge sandstones: The Journal of Geology, v. 112, p. 23–37, https://doi.org/10.1086/379690.

Thomas, W.A., Tucker, R.D., Astini, R.A., and Denison, R.E., 2012, Ages of pre-rift basement and synrift rocks along the conjugate rift and transform margins of the Argentine Precordillera and Laurentia: Geosphere, v. 8, p. 1366–1383, https://doi.org/10.1130/GES00800.1.

Thomas, W.A., Gehrels, G.E., and Romero, M.C., 2016, Detrital zircons from crystalline rocks along the Southern Oklahoma fault system, Wichita and Arbuckle Mountains, USA: Geosphere, v. 12, p. 1224–1234, https://doi.org/10.1130/GES01316.1.

Thomas, W.A., Gehrels, G.E., Greb, S.F., Nadon, G.C., Satkoski, A.M., and Romero, M.C., 2017, Detrital zircons and sediment dispersal in the Appalachian foreland: Geosphere, v. 13, p. 2206–2230, https://doi.org/10.1130/GES01525.1.

Thomas, W.A., Gehrels, G.E., Lawton, T.F., Satterfield, J.I., Romero, M.C., and Sundell, K.E., 2019, Detrital zircons and sediment dispersal from the Coahuila terrane of northern Mexico into the Marathon foreland of the southern Midcontinent: Geosphere, v. 15, p. 1102–1127, https://doi.org/10.1130/GES02033.1.

Thomas, W.A., Gehrels, G.E., Sundell, K.E., Greb, S.F., Finzel, E.S., Clark, R.J., Malone, D.H., Hampton, B.A., and Romero, M.C., 2020, Detrital zircons and sediment dispersal in the eastern Midcontinent of North America: Geosphere, v. 16, p. 817–843, https://doi.org/10.1130/GES02152.1.

Thompson, D.M., 1982, The Atoka Group (Lower-Middle Pennsylvanian), Northern Fort Worth Basin, Texas; Terrigenous Depositional Systems, Diagenesis, Reservoir Distribution, and Quality: University of Texas at Austin, Bureau of Economic Geology Report of Investigations 125, 62 p.

Van Avendonk, H.J.A., and Dalziel, I.W.D., 2018, Comment: The Sabine block, Gulf of Mexico: Promontory on the North American margin?: Geology, v. 46, p. e440, https://doi.org/10.1130/G40053C.1.

Van Schmus, W.R., et al., 1993, Transcontinental Proterozoic provinces, *in* Reed, J.C., Jr., Bickford, M.E., Houston, R.S., Link, P.K., Rankin, D.W., Sims, P.K., and Van Schmus, W.R., eds., Precambrian: Conterminous U.S.: Boulder, Colorado, Geological Society of America, The Geology of North America, v. C-2, p. 171–334, https://doi.org/10.1130/DNAG-GNA-C2.171.

Vermeesch, P., 2013, Multi-sample comparison of detrital age distributions: Chemical Geology, v. 341, p. 140–146, https://doi.org/10.1016/j.chemgeo.2013.01.010.

Vervoort, J.D., and Patchett, P.J., 1996, Behavior of hafnium and neodymium isotopes in the crust: Constraints from crustally derived granites: Geochimica et Cosmochimica Acta, v. 60, no. 19, p. 3717–3733, https://doi.org/10.1016/0016-7037(96)00201-3.

Vervoort, J.D., Patchett, P.J., Blichert-Toft, J., and Albarede, F., 1999, Relationships between Lu-Hf and Sm-Nd isotopic systems in the global sedimentary system: Earth and Planetary Science Letters, v. 168, p. 79–99, https://doi.org/10.1016/S0012-821X(99)00047-3.

Viele, G.W., and Thomas, W.A., 1989, Tectonic synthesis of the Ouachita orogenic belt, *in* Hatcher, R.D., Jr., Thomas, W.A., and Viele, G.W., eds., The Appalachian-Ouachita Orogen in the United States: Boulder, Colorado, Geological Society of America, The Geology of North America, v. F-2, p. 695–728, https://doi.org/10.1130/DNAG-GNA-F2.695.

Wright, J.E., Hogan, J.P., and Gilbert, M.C., 1996, The Southern Oklahoma aulacogen: Not just another B.L.I.P.: Eos (Washington, D.C.), v. 77, no. 46, p. F845.

Xie, X., Cains, W., and Manger, W.L., 2016, U-Pb detrital zircon evidence of transcontinental sediment dispersal: Provenance of Late Mississippian Wedington Sandstone member, NW Arkansas: International Geology Review, v. 58, no. 15, p. 1951–1966, https://doi.org/10.1080/00206814.2016.1193775.

Xie, X., Buratowski, G., Manger, W.L., and Zachry, D., 2018a, U-Pb detrital-zircon geochronology of the middle Bloyd sandstone (Morrowan) of northern Arkansas (U.S.A.): Implications for Early Pennsylvanian sediment dispersal in the Laurentian foreland: Journal of Sedimentary Research, v. 88, p. 795–810, https://doi.org/10.2110/jsr.2018.47.

Xie, X., Anthony, J.M., and Busbey, A.B., 2018b, Provenance of Permian Delaware Mountain Group, central and southern Delaware basin, and implications of sediment dispersal pathway near the southwestern terminus of Pangea: International Geology Review, v. 61, no. 3, p. 361–380, https://doi.org/10.1080/00206814.2018.1425925.